HALOGEN CATIONS

HALOGEN CATIONS

By

MICHAEL J. MORTON, M.A.

A Thesis

Submitted to the Faculty of Graduate Studies

in Partial Fulfillment of the Requirements

for the Degree

Doctor of Philosophy

McMaster University

September 1969

DOCTOR OF PHILOSOPHY (1969)
(Chemistry)

McMASTER UNIVERSITY
Hamilton, Ontario

TITLE: Halogen Cations

AUTHOR: Michael John Morton, M.A. (Cambridge University)

SUPERVISOR: Dr. R. J. Gillespie

NUMBER OF PAGES: ix, 137

SCOPE AND CONTENTS:

In an investigation on the formation of halogen cations, the I_4^{2+}, Br_3^+, Br_2^+ and Cl_3^+ cations have been identified by conductivity, cryoscopy, ultraviolet and visible spectrophotometry, Raman spectroscopy and magnetic susceptibility measurements in strong acids. Bromine trifluorosulphate has been shown to ionise in the $SbF_5:3SO_3/HSO_3F$ system to give the $Br(SO_3F)_2^+$ ion, and Raman bands of bromine fluorosulphates, $ClSO_3F$ and $S_2O_6F_2$ have been listed. No evidence has been found for the Cl_2^+ or ClF^+ ions in solution, and the assignment of observed ESR spectra to these cations is criticised.

Raman spectra of the adducts AsF_5 2ClF and BF_3 2ClF have shown that they contain the $ClClF^+$ cation and not the $ClFCl^+$ cation. The bending frequency of the ClF_2^+ cation has been reassigned, and force constants have been calculated for the ClF_2^+ and Cl_3^+ cations.

Resonance Raman spectra of the I_2^+ and Br_2^+ cations have been observed, and, as few examples of this effect are known, the variation in fundamental and overtone intensities with exciting wavelength have been investigated.

ACKNOWLEDGMENTS

The author would like to express his sincere gratitude for the advice and encouragement given throughout this work by his research director, Professor R. J. Gillespie. He would also like to thank the members of the Department of Chemistry for lively discussions, entertainment and assistance; particular thanks are due to Dr. J. Barr for his cooperation and advice in the preparation of various materials, Mr. J. Bacon for assistance with the NMR spectrometer and Dr. G. Pez for his help and advice in Raman spectroscopy.

The financial assistance which made this work possible is gratefully acknowledged. The Department of University Affairs, Province of Ontario, provided an Ontario Graduate Fellowship, and McMaster University provided an Assistantship and a Travel Grant.

Finally, the author would like to thank Mrs. Michelle McLean, who typed this thesis.

TABLE OF CONTENTS

LIST OF TABLES

LIST OF FIGURES

CHAPTER 1.

Introduction.

1. Halogen Cations.

(a) Introduction.

In a review on halogen cations, Arotsky and Symons pointed out that since an early stage in chemical history, confusion has arisen in the literature over the terms 'positive halogen' and 'halogen cation', and that this has resulted in frequent reference to Cl^+, Br^+ and I^+ in chemically improbably systems (1). Here, the term 'halogen cations' will be used only to describe simple or polymeric cations containing only one of the halogens, and will be distinguished from interhalogen and halogen oxy-cations.

Two trends have long been noted in the Periodic Table. One is the increase in electropositive character on descending a group, which has lead to the expectation that I^+ should be the most readily formed monopositive cation of the common halogens. The second trend is the decreasing positive character on crossing a period in the Table, from which it is expected that the Te^+ cation will be formed more easily than the I^+ cation. At this time, however, the Te^+ cation has not been identified as a stable species, and nor is there any experimental evidence left standing for the I^+ cation. Recently a trend towards the formation of polymeric cations on crossing the Periodic Table has been becoming apparent. Bismuth in group V forms the cluster cations Bi_5^{3+} and Bi_9^{5+} in addition to the Bi^+ cation (2,3). In group VI salts of O_2^+

are well characterised (4,5) and Gillespie et al. have identified the cations S_8^{2+}, S_{16}^{2+}, Se_8^{2+}, Se_4^{2+}, Te_4^{2+} and Te_4^{4+} (6 - 9). Sulphur also gives paramagnetic cations (10), which may be reversibly produced by heating solutions of S_{16}^{2+} and S_8^{2+} in strong acid solvents; these may be S_8^+, S_4^+ and S_2^+. This trend away from monatomic cations towards polymeric cations is expected to continue to the halogens, making the formation of I^+ rather than I_2^{2+} for the iodine (+1) cation unlikely, except perhaps at elevated temperatures.

(b) Iodine Cations.

In 1938 Masson (11) observed that the brown solutions formed when iodine is added to iodosyl sulphate in concentrated sulphuric acid solutions reacted with chlorobenzene to form both iodo and iodoso derivatives. He postulated the presence of I_3^+ and I_5^+ to explain the stoichiometry of these reactions, and showed that univalent positive iodine was largely disproportionated to I_3^+, I_5^+ and IO^+. Arotsky, Mishra and Symons (12) have given conductimetric evidence for I_3^+ formed from iodic acid and iodine in 100% sulphuric acid, and have suggested that I_5^+ may be formed on the basis of changes in the visible and ultraviolet spectra when iodine is added to I_3^+ solutions.

Gillespie and co-workers have confirmed the existence of I_3^+ and I_5^+ in 100% sulphuric acid by detailed conductimetric and cryoscopic measurements, and have shown that solutions which correspond stoichiometrically to univalent positive iodine are largely disproportionated (13). Gillespie and Milne have characterised I_3^+ and I_5^+ in fluorosulphuric acid solutions (23). The structure of these ions are not known, but I_3^+ presumably has an angular structure like $IC\ell_2^+$ (14).

In 1932 Carlsohn prepared the salts $I^+(py)_2X^-$ and $I^+(py)Y^-$ where X is nitrate or perchlorate, and Y is nitrate, a benzoate or acetate. These compounds were regarded as salts of the I^+ cation stabilised by ligands such as pyridine or β-picoline. Perhaps it would be less misleading to regard them as being analogous to I_3^+ and I_2^+ respectively as the pyridine is acting as a strong donor in each case. The iodine cation has also been loosely referred to in postulating self ionisations in iodine, iodine monobromide and iodine monochloride (16a).

eg $$2\ ICl \rightleftharpoons I^+ + ICl_2^-$$

In this case the cation is probably I_2Cl^+, which may disproportionate to I_3^+ and ICl_2^+. Bell and Gelles, on thermodynamic grounds, have argued strongly against the postulate the I^+ could exist in aqueous media (17).

It has been known for a long time that iodine forms deep blue solutions of a cationic species in 65% oleum (18). It had been claimed by Symons et al. that such solutions contained the I^+ cation (1, 12, 18, 19, 20). The conclusion that iodine was oxidised to the +1 state by 65% oleum was based on:

1. Spectrophotometric determination of the SO_2 produced on oxidation of iodine by 65% oleum.
2. The conductivity of I_2 and ICl in 65% oleum, and conductiometric titration with boric acid.
3. Analysis. On diluting the oleum solutions to 100% sulphuric acid, 80% of the iodine was recovered, as expected for the disproportionation of I^+ to iodine and pentavalent iodine.

Magnetic susceptibility measurement gave +1.44 BM per iodine atom, and the three visible absorptions were assigned to p - p transitions due to the ligand field in the I^+ cation (1). Aynsley et al. interpreted their observations on IF_5 solutions of the blue species in terms of I^+ (21).

In 1965 Gillespie and Milne showed by careful conductimetric, spectrophotometric and magnetic susceptibility measurements in fluorosulphuric acid, that the blue iodine species is I_2^+ and not I^+ (23). Solutions of iodine in fluorosulphuric acid were oxidised with peroxydisulphuryl difluoride, and the concentration of the blue iodine cation reached a maximum at the 2:1 ratio

$$1.\quad 2\ I_2 + S_2O_6F_2 \longrightarrow 2\ I_2^+ + 2\ SO_3F^-.$$

An equilibrium constant of 2.0 $kg^{3/4}\ mole^{-3/4}$ was calculated for the disproportionation of the I_2^+ cation to I_3^+ and trivalent iodine trifluorosulphate, according to the equation:

$$2.\quad 8\ I_2^+ + 8\ SO_3F^- \rightleftharpoons I(SO_3F)_3 + 5\ I_3^+ + 5\ SO_3F^-.$$

Where iodine trifluorosulphate acts as a weak acid, with an equilibrium constant of 10 $mol^{-1} kg$ (24).

$$3.\quad I(SO_3F)_3 + SO_3F^- \rightleftharpoons I(SO_3F)_4^-.$$

The magnetic moment of the I_2^+ cation was found to be 2.0 ± 0.1 BM, in agreement with the expected value.

The solutions of the blue iodine cation in oleums have been reinvestigated by conductimetric, spectrophotometric and cryoscopic methods,

and these show that the I_2^+ cation is formed (25). There appears to have been a systematic computational error in the original work (26). The analysis in which 80% of the iodine was recovered on diluting the 65% oleum solution to 100% sulphuric acid also supports the formation of I_2^+, as this is the result expected for disproportionation to iodine and trivalent iodine, which is stable in 100% sulphuric acid (23). Kemmitt et al. have prepared blue crystalline solids of iodine with antimony pentafluoride and tantalum pentafluoride, which they formulated as $I_2^+Sb_2F_{11}^-$ and $I_2^+Ta_2F_{11}^-$ respectively. They studied the blue solution of the iodine cation both in antimony pentafluoride, and with the Lewis acids SbF_5, TaF_5, NbF_5, AsF_5 and PF_5 in iodine pentafluoride, and have interpreted their results in terms of the I_2^+ cation. No ESR spectrum was obtained, in accordance with the expectation that the large spin-orbit coupling would broaden the spectrum beyond detection. Attempts to observe the Raman spectrum of the I_2^+ cation in solution were unsuccessful (26).

(c) Bromine Cations.

Symons et al. have failed to prepare solution of the Br_3^+ cation in oleums, but have stated that 'when solutions of bromine in 65% oleum are oxidised, they give tervalent derivatives via the Br_3^+ cation' (1).

McRae (27) has investigated the compound SbF_5Br, first reported by Ruff in 1906 (28). A vapour pressure - mole fraction diagram for the SbF_5-Br_2 system showed a rise in the vapour pressure when the mole fraction of bromine reached 0.3, and the brown colour of the solution, λ_{max} = 375 mμ, migrated to the cathode on electrolysis. No solids of definite composition were isolated from the diamagnetic mixture, which

presumably contained SbF_3, but it was suggested that bromine is oxidised by SbF_5 to the Br_3^+ cation.

Edwards et al. have prepared the scarlet salt (λ_{max} 510 mμ) $Br_2^+Sb_3F_{16}^-$ from bromine pentafluoride and antimony pentafluoride (29). The two bromine atoms are 2.13A apart, and a Raman spectrum of the solid gave a strong peak at 368 cm^{-1}. This communication appeared at the same time as our communication on the Br_2^+ and Br_3^+ cations in super acid solutions (30).

(d) Chlorine Cations.

The Cl_3^+ cation has not been reported. Recently Olah and Comisarow have claimed the identification of the Cl_2^+ and ClF^+ cations by means of ESR spectra obtained from solutions of ClF, ClF_3 and ClF_5 in super acid solvents (31,32). Bartlett, in private communications (eg in Ref 26) dated 1967 has reported the preparation of the complex Cl_2IrF_6 by reaction between iridium hexafluoride and chlorine and has suggested that it may contain the Cl_2^+ cation. However no data has been published on this compound.

2. Interhalogen Cations.

Of the possible interhalogen cations, crystal structures have been determined only for salts of ICl_2^+ (14) and BrF_2^+ (33). These gave bond angles of 92.5 and 95° respectively and indicated substantial halogen bridging between cation and anion leading to the conclusion that the fully ionic formulation is not justified.

Adducts between halogen fluorides and strong Lewis acids have been prepared and have been formulated as salts of the following cations:

IF_2^+ (34) BrF_2^+ (37) ClF_2^+ (36) FCl_2^+ (39).

IF_4^+ (35) BrF_4^+ (38) ClF_4^+ (38)

IF_6^+ (36)

Christe et al. have published vibrational data and force constant calculations on ClF_2^+ (40), IF_6^+ (41), ClF and FCl_2^+ (39). They have reported that similar data was to be published on IF_4^+, BrF_4^+ and ClF_4^+ (38). No vibrational data has been published on the IF_2^+ or BrF_2^+ cations, although Sharp et al. have reported the infrared spectrum of the adduct $GeF_4.2BrF_3$, which they conclude is not ionic (40).

Interhalogen cations analogous to I_5^+ have not been suggested, and of the cations analogous to I_3^+, such as I_2Br^+, I_2Cl^+, IBr_2^+, $BrICl^+$, Br_2Cl^+, $BrCl_2^+$ and ICl_2^+, only ICl_2^+ has been identified. No spectroscopic studies have been made of any of these species. Gillespie et al. have suggested that I_2Br^+ and I_2Cl^+ may exist in sulphuric acid solutions on the basis of conductivity measurements (41), but the data is also consistent with complete disproportionation to I_3^+ and ICl_2^+ or IBr_2^+ respectively. Fialkov and co-workers (42,43) have prepared the complexes $SbCl_5.2ICl$ and $SbCl_5.3ICl$ and have shown that the iodine migrates to the cathode on electrolysis. These compounds were formulated as $I^+(SbCl_6^-)$. n.ICl, but again could contain the I_2Cl^+ cation.

3. The Fluorosulphuric Acid Solvent System.

As halogen cations are highly electrophilic species, we can expect their formation only in media of very low basicity. Thus it is that the blue iodine cation has been observed only in solvents such as fluorosulphuric acid, disulphuric acid, antimony pentafluoride and iodine

pentafluoride (1), in which the most basic species present is the solvent anion*. Furthermore, as all these media have a high dielectric constant, we can imagine that the charge density at the cation and anion is spread out to some extent over a solvation sphere, resulting in a lower Lewis acidity and basicity for the cation and anion respectively.

Although the blue iodine cation has been known for some time, it was identified as I_2^+ only in 1965 (22). This identification, first made in fluorosulphuric acid, and later confirmed in disulphuric acid (25), rested on a detailed understanding of the properties of the solvent systems that enabled conductivity and cryoscopic data to be unambiguously interpreted.

The first serious study on fluorosulphuric acid as a non-aqueous solvent system was performed by Woolf in 1955 (44). He found the specific conductance of the acid doubly distilled in glass at 163±0.5°C, to be 2.20×10^{-4} ohm^{-1} cm^{-1} and postulated the self-ionisation reaction

$$4.\qquad 2HSO_3F \rightleftharpoons H_2SO_3F^+ + SO_3F^-.$$

Woolf suggested that conduction took place by a proton-transfer mechanism, and investigated several fluorides for acid-base character by conductimetric titrations. Bases ionise to give the characteristic anion of the solvent,

---

*In the absence of strong Lewis acids, the iodine cation is produced in iodine pentafluoride only in the presence of traces of moisture; this suggests that the stable anion $IO_2F_2^-$ is formed rather than IF_6^- as suggested by Aynsley et al. (21). The IF_6^- ion is derived from a very weak Lewis acid, and in consequence is strongly basic.

5. $KSO_3F \longrightarrow K^+ + SO_3F^-$

6. $B + HSO_3F \longrightarrow BH^+ + SO_3F^-$

Antimony pentafluoride is an acid, giving the acidium cation and an anion which was later shown to be the antimony pentafluoro-fluorosulphate anion (48), and not the hexafluoroantimonate proposed by Woolf.

7. $SbF_5 + 2HSO_3F \longrightarrow H_2SO_3F^+ + SbF_5SO_3F^-$

A detailed study of the fluorosulphuric acid solvent system has been made by Gillespie and co-workers (24, 47-50) and recently reviewed (51). Table I summarises some of the physical properties of fluorosulphuric acid.

Peroxidydisulphuryl-difluoride is a particularly convenient oxidising agent in fluorosulphuric acid as it is reduced to fluorosulphate anions

8. $S_2O_6F_2 + 2e^- \longrightarrow 2SO_3F^-$

Thus the oxidation of iodine with varying ratios of iodine to $S_2O_6F_2$ was followed, and it was established that I_5^+, I_3^+, I_2^+ and $I(SO_3F)_3$ are successively formed.

The conductivity of these solutions can be interpreted by defining a value γ as the number of moles of SO_3F^- ion produced per mole of solute. Since the conductivity is due predominantly to the fluorosulphate ion (Table I), the value γ for any solute is given, to a good approximation, by the ratios of the concentrations of that potassium fluorosulphate solution (γ=1) which gives the same conductivity as the solute solution.

Similarly the total number of particles in solution produced per mole of solute defined as ν can be measured by comparison of the freezing points depressions with those of standard solutes, such as $S_2O_6F_2$ and KSO_3F for which $\nu = 1$ and 2 respectively. For dilute solutions these give a cryoscopic constant of 3.93. In the presence of excess sulphur trioxide in the solvent, the initial slope of the freezing-point depression against concentration curve for basic solutes is decreased due to the formation of the $S_2O_6F^-$ ion at low temperatures

9. $$SO_3F^- + SO_3 \longrightarrow S_2O_6F^-$$

As an example of these techniques, Gillespie and Milne found that when iodine was oxidised with $S_2O_6F_2$ in solution, peaks at 480 and 305 mμ reached a maximum at the 3:1 ratio. The values $\gamma = 0.67$ and $\nu = 1.33$ observed immediately confirmed the formation of the I_3^+ cation according to the equation

10. $$I_2 + 1/3\ S_2O_6F_2 \longrightarrow 2/3\ I_3^+ + 2/3\ SO_3F^-$$

The acidity of fluorosulphuric acid can be increased by addition of the weak acid of the system, SbF_5. On adding sulphur trioxide to these solutions, the acidity increases still further until the SbF_5:SO_3 ratio of 1:3 is reached. This corresponds to the formation of the strong acid $SbF_2(SO_3F)_3$

11. $$SbF_2(SO_3F)_3 + 2HSO_3F \longrightarrow H_2SO_3F^+ + SbF_2(SO_3F)_4^-$$

A small excess of sulphur trioxide is necessary to ensure complete

conversion of SbF_5 to $SbF_2(SO_3F)_3$ (48). These solutions are highly conducting due to the high concentrations of the $H_2SO_3F^+$ ion. However the conductivity curve gradient decreases with concentration due to a dimerization equilibrium

$$12.\quad 2SbF_2(SO_3F)_4^- + H_2SO_3F^+ \rightleftharpoons [SbF_2(SO_3F)_3]_2SO_3F^- + 2HSO_3F$$

By conductimetric titrations with KSO_3F, Gillespie et al. found that the equilibrium constant K has a value 250 ± 13 over the range 0.02 to 0.12 molal, where

$$K = \frac{[SbF_2(SO_3F)_3]_2[SO_3F^-]}{[SbF_2(SO_3F)_4^-]^2[H_2SO_3F^+]}$$

NMR studies at higher concentrations showed that $S_2O_5F_2$ is slowly formed in these solutions due to the elimination of two fluorosulphates, giving antimony oxy-fluoride-fluorosulphate polymers (48).

This super acid solvent system has not been exploited previously in the study of halogen cations. Except perhaps for cryoscopy, we can utilize similar techniques in this medium as were used in fluorosulphuric acid. Bases may be titrated conductimetrically with the acidium cation to give a γ value defined as before, by comparison with a similar titration with potassium fluorosulphate.

4. Purpose of this Work.

During the course of previous investigations in which the I_5^+, I_3^+ and I_2^+ cations were characterised, evidence was found for the formation of another iodine cation in solutions of I_2^+ in fluorosulphuric acid at

low temperatures. The purpose of this work was to identify this species and to extend the investigation by studying the possible formation and range of stabilities of corresponding bromine and chlorine cations.

TABLE 1

Properties of Fluorosulphuric Acid (51).

Boiling point ^{o}C	162.7
Freezing point ^{o}C	-88.98
Density at $25^{o}C$ g cc^{-1}	1.726
Viscosity at $25^{o}C$ cp	1.56
Cryoscopic constant ^{o}C $mol^{-1}kg$	3.93
Specific Conductivity $25^{o}C$ ohm^{-1} cm^{-1}	1.085×10^{-4}

Molar Ionic Conductivities at Infinite Dilution

SO_3F^-	135.
$H_2SO_3F^+$	185.
K^+	17.
NH_4^+	21.

CHAPTER II.

Experimental.

1. Preparation and Purification of Materials.

Dry Air

Compressed air was passed through a drying train consisting of a Dreschel bottle containing sulphuric acid, two 12" drying towers containing granular silica gel and molecular sieves, and a three foot tube packed with phosphorous pentoxide supported on glass wool.

Fluorosulphuric Acid

Technical fluorosulphuric acid (Baker and Adamson) was purified by double distillation in a two stage glass still, as described by Barr (45). The still was rigorously dried by flaming out, and by passing a slow stream of dry air through it overnight. Passage of dry air through the receiver was continued during distillation.

Occasionally the initial fluorosulphuric acid contained a large excess of sulphur trioxide, which was not effectively separated by distillation. In these cases the crude acid, contained in the first stage of the still, was cooled in a dry-ice bucket and pellets of sodium bifluoride were added. The bulk of the acid then distilled over in the required range of 162 to 164°C. The purity of a portion of the final product was checked cryoscopically, and any excess of sulphur trioxide was titrated with hydrogen fluoride until the freezing point rose to -89.000°C. Additions of a 20% w/w solution of hydrogen fluoride in

fluorosulphuric acid were made using an all teflon-syringe fitted with a platinum needle (Hamilton Syringe Co. Inc.) and closed with a cap made from 1 mm Kel-F tubing. A calculated quantity of the hydrogen fluoride solution was then added to the bulk stock of the solvent.

Peroxydisulphuryl Difluoride

Peroxydisulphuryl difluoride was prepared by the method of Dudley and Cady (52), by reaction of fluorine and sulphur trioxide at 130°C over a silver catalyst. The catalyst was supported on copper mesh which had been coated in a silver cyanide complex bath. The flow rates of each reactant, diluted with nitrogen, were monitored with fluorolube oil bubblers. A small excess of fluorine was achieved by adjusting flow rates until solid sulphur trioxide ceased to form at the top of the collection trap, which was cooled in dry ice.

The product was shaken with 100% sulphuric acid to remove sulphur trioxide, and distilled at -76°C into storage traps fitted with teflon-glass valves (Fischer and Porter). Prior to use the compound was doubly distilled from dry ice on a pyrex vacuum line fitted with teflon taps.

Potassium Fluorosulphate

Potassium fluorosulphate was prepared as described by Barr (45). Equivalent quantities of fluorosulphuric acid and concentrated potassium hydroxide were added dropwise onto finely crushed ice. The cooled solution was filtered and the crude product was recrystallised from water, washed with acetone and ether, and stored over phosphorous pentoxide in a desiccator.

Sulphur trioxide

Sulphur trioxide was distilled from Baker and Adamson 'Sulphan' in a still protected from moisture by a magnesium perchlorate drying tube.

Hydrogen fluoride

Anhydrous hydrogen fluoride (Harshaw Chemical Co.) was used directly.

Iodine

Shawinigan reagent grade iodine was used directly.

Bromine

Shawinigan reagent grade bromine was dried over phosphorous pentoxide and distilled from potassium bromide.

Chlorine

Chlorine (Matheson Co. Inc.) was purified by literature methods (53). It was passed successively through potassium permanganate solution, sulphuric acid and phosphorous pentoxide and then distilled from a trap cooled in dry ice.

Antimony Pentafluoride

Antimony pentafluoride (Ozark Mahoning Inc.) was doubly distilled in a pyrex glass still in an atmosphere of dry air. The fraction boiling between 142° and 143°C was collected and subsequently distilled at 25°C under vacuum on a grease free pyrex and teflon vacuum line.

Arsenic Pentafluoride

Arsenic pentafluoride (Ozark Mahoning Inc.) was condensed on the monel vacuum line into a Kel-F trap cooled in a dry-ice acetone slush bath. It was then distilled twice from dry ice to liquid nitrogen temperatures, and each time a first fraction containing phosphorous pentafluoride was pumped off.

Boron trifluoride

Boron trifluoride (Matheson Co. Inc.) was condensed into a trap at liquid nitrogen temperature, and distilled from the liquid on allowing the trap to warm up.

Chlorine trifluoride

Chlorine trifluoride (Matheson Co. Inc.) was doubly distilled on the monel vacuum line from Kel-F traps cooled in dry-ice acetone slush bath. The middle fraction was collected.

Chlorine monofluoride

Chlorine monofluoride (Ozark Mahoning Inc.) was distilled from the liquid contained in a Kel-F trap cooled in an allyl alcohol slush bath ($-129^{o}C$) on the monel line. This was repeated at least four times to remove chlorine and fluorocarbons.

2. Manipulation of materials.

Rigorous precautions were taken to exclude moisture in this work. Glassware was stored in large desiccators over phosphorous pentoxide, and all manual operations were performed in a dry box.

For quantitative work, a dry box containing a Mettler H.6. balance was used. This dry box (S. Blickman Inc.) had an evacuable port which was refilled with extra-dry nitrogen. The atmosphere was circulated through an external circuit in which any moisture or acid vapour was removed in liquid nitrogen traps. A second smaller dry box was fitted with a similar circulating system, and had a port which was slowly flushed with extra-dry nitrogen for fifteen minutes before entry.

Solutions in fluorosulphuric acid were handled using smooth-glass syringes fitted with teflon plungers, and platinum needles with Kel-F hubs (Hamilton Syringe Co.). The ends of the needles could be closed off with Kel-F tubing and the syringes could be conveniently weighed before and after additions. Conductivity cells and flasks containing solutions were introduced through the vacuum port of the 'large dry box' using a steel box fitted with a 1/2" thick perspex lid which was screwed down onto a rubber 'O' ring to give a vacuum tight seal; the box was purged with extra-dry nitrogen.

Vacuum line operations were performed either with a pyrex or with a monel vacuum line, both of which were set up inside fume hoods. The pyrex line was fitted with 4 mm Fischer and Porter teflon-glass valves, and alterations were made to suit the experiment. Attachments were made either with 1/4" teflon Swagelok connectors or with B10 joints using Kel-F grease (3 M.s.).

The monel vacuum line was fitted with Whitey valves with Kel-F seats, and with a monel Bourdon gauge (Taylor Instrument Co. Serial 62KF138). Kel-F traps, supplied by the Argonne National Laboratory, could be connected with a teflon Swagelok to one of four outlets. Gas cylinders or the 10 cm monel infrared cell could be swageloked via 1/4" teflon tubing to a fifth outlet. Before use the line was flamed out under vacuum and thoroughly aged with chlorine trifluoride.

3. Conductivity Measurements.

Conductivity measurements at 25°C were made as described by Milne (22). The cells used had a capacity of 100 ml and three platinum electrodes gave a choice of cell constants of approximately 3 or 30 cm^{-1}.

The cells were cleaned with aqua regia and the electrodes were plated with platinum black by electrolysing a 0.3% solution of chloroplatinic acid in dilute hydrochloric acid containing lead acetate (54). A current of ten m amp was automatically reversed every ten seconds, and was passed for ten minutes.

The cell constants were found by measuring the conductance of a standard 0.01 D solution of potassium chloride (55) made up in distilled water from an ion-exchange column. This solution has a specific conductance of 0.0014088 ohm^{-1} cm^{-1} at 25°C.

Low temperature conductivity measurements were made by plunging the cell in a trichlorethylene slush bath at -86.4°C, and allowing fifteen minutes for the cell to reach the temperature of the thick sludge: the temperature was measured with a platinum resistance thermometer, and was reproducible to ± 0.05°C. The cell was allowed to warm to ambient temperature before making the next addition of solute. All additions of concentrated solutions were made in the dry box using weighed syringes. Weighed quantities of the solution could also be extracted from the conductivity cell using the teflon-glass syringes.

The conductance of solutions was measured with a Wayne-Kerr Universal Bridge operating at 1 KHz. The reading was repeated after agitation of the cell in the constant temperature bath, to ensure that the steady value had been reached.

4. Cryoscopy.

The apparatus and technique for making cryoscopic measurements in fluorosulphuric acid has been described in detail by Gillespie, Milne

and Thompson (49). The cryoscope, containing approximately 120 g solution, was cooled in a liquid nitrogen bath, and the pressure within its vacuum jacket was adjusted to give a cooling rate of between 0.3 and 0.4°C per minute; a tap to a mercury diffusion pump was opened for a few seconds at a time while the solution was still some twenty degrees above the freezing point, and the cooling rate was measured a minute later with a stop watch. The temperature was measured to 0.001°C with a Leeds Northrup platinum resistance thermometer used in conjunction with a Mueller resistance bridge. The thermometer calibration was checked periodically by determining its resistance at the triple point of water using a Trans-Sonics Inc. 'Equiphase cell', and a computer programme was written to calculate and print out the resistance at temperature intervals of 0.01°C.

Resistance readings were recorded at thirty second intervals starting when the solution had reached the estimated freezing point. When the solution had supercooled by approximately 2°C, freezing was initiated by dropping in a small piece of platinum cooled in liquid nitrogen. The temperature rose rapidly, after which a cooling curve was plotted with readings at one minute intervals for fifteen minutes, with occasional reversal of the 1 m amp thermometer current. The cooling curve was extrapolated back to the freezing point, which was estimated to be accurate to ±0.005°C.

Additions were made using teflon-glass syringes through a B 14 joint at the top of the cryoscope. At other times this joint was capped with an 'anhydrone' guard tube which served as the exit for the slow stream of dry air continually sweeping the top of the cryoscope.

5. UV and Visible Absorption Spectra.

Absorption spectra were taken on a Bausch and Lomb Spectronic 505 or 600, or on a Cary 14 spectrophotometer. One centimeter path length silica cuvettes with inserts to vary the path length down to 0.05 mm facilitated study of solutions of halogen cations at concentrations comparable to those used in conductance and magnetic susceptibility measurements. Path lengths were calibrated with alkaline solutions of potassium chromate (56). At later stages in this work, custom made quartz cells (Hellma Ltd.) in which all four sides were optically clear were used. These cells gave two different path lengths when used with the quartz inserts (Applied Physics Inc.).

The cells and inserts were rigorously dried by washing with acetone and ether, followed by vacuum desiccation over phosphorous pentoxide. They were filled from syringes in a dry box, and teflon covers were clamped on and bound with teflon tape.

Low temperature spectra were taken in a quartz Dewar with quartz windows. The Dewar was cooled by passing cold nitrogen from a liquid nitrogen boiler through a cork bung closing the top, and the temperature was measured with a thermocouple. The temperature could be controlled within $1^{o}C$ by manually changing the flow of coolant with a variac.

6. Magnetic Susceptibility Measurements.

Magnetic susceptibility measurements were made by the Gouy method using an Alpha Scientific Laboratory Model AL 7500 electromagnet and a Sartorius Vacuum Electrono microbalance. The variable-temperature experimental arrangement was built after a design of Earnshaw (57) and

Newport Instruments Limited. The sample, which consisted of ten cm of solution sealed in a fifteen cm long 5 mm od quartz tube, was suspended by a copper link chain inside a copper block with an internal diameter of 6.5 mm. The copper block was non-inductively wound with heating wire and platinum control wire, and was mounted within a triple Dewar so that it could be cooled with liquid nitrogen through a vacuum. The electronic temperature control unit was designed and built by Mr. Claus Schonfeld and has been described in Guest's thesis (58). The temperature was measured with a copper-constantan thermocouple cemented into a groove down the inside of the copper block, and the thermocouple was calibrated with a platinum resistance thermometer. The sample was suspended in an atmosphere of dry nitrogen, and the microbalance could be read to one µg. However, between about -70° and room temperature the reading fluctuated over a range of 5 µg due to the more severe heating and cooling cycle than at lower temperatures. The quartz tube constants were calibrated using conductivity water and checked with dilute nickel chloride solutions (59).

7. Raman Spectra.

The Raman spectrometer consisted of a Spex Industries model 1400 double monochromator with an I.T.T. FW 130 phototube detector, dc amplification and a strip chart recorder. The model 1400 spectrometer is a 3/4 meter Czerny-Turner scanning spectrometer with 1,200 g/mm gratings blazed at 7500 A giving a dispersion of 5.5 A per mm.

The exciting radiation at 6328.2 A was produced from a Spectra Physics model 125 He/Ne laser which usually operated at 50 mw, but was

capable of giving up to 80 mw at peak performance. The laser beam was reflected through 90° by a dielectric mirror and passed vertically up the Spex 1430 sample illuminator consisting of a 20 A half-width spike filter, a half wave plate, an iris diaphragm and a fully adjustible condensing lens to focus the beam on the sample.

Standard samples, both solids and liquids were sealed in 2 mm od glass capillary tubes and mounted horizontally in a brass holder. Light scattered at right angles to the beam and to the axis of the tube was focused on the entrance slit of the monochromator to give a sharp image, having passed through a polarisation scrambler. This method of mounting samples was due to Dr. G. Pez, and the advantages of this technique have been summarised in detail by Freeman and Landon (60), who showed that excellent Raman spectra and depolarisation ratios could be obtained in capillary tubes on sample sizes down to 0.008 ml.

The Raman spectra of hydrogen fluoride solutions and corrosive solids were obtained using 5 mm od thin wall Kel-F tubes which were heat sealed on the vacuum line. The image of the Kel-F walls fell well outside the limits of the entrance slit. Solutions of strong acids which had been in contact with Kel-F often fluoresced badly, but this could be quenched by small quantities of a strong oxidising agent such as ClF, which appears to oxidise the impurities responsible for the fluorescence.

For low-temperature spectra the sample tubes were mounted in a quartz tube with an evacuated jacket, silvered except for a one cm band around the centre. Nitrogen was boiled off at a variable rate from a Dewar and passed through the tube, and the temperature was recorded with a thermocouple.

During this work, a Spectra Physics model 140 argon-ion laser was acquired for resonance Raman studies. This gave up to 1,000 mw at 5145 A or 4880 A, and lased at lower power output at several other frequencies in the blue and green regions. The argon-ion laser was mounted parallel to the helium-neon laser and the beam was reflected through 90^{o} in a horizontal plane by an adjustable dielectric mirror before entering the bottom of the sample illuminator which was rotated by 90^{o} for the argon-ion laser. With this configuration the plane of polarisation of the beam was at right angles to the direction of observed Raman scattering, as required, without the use of half wave plates.

CHAPTER III.

Formation of the I_4^{2+} cation in Fluorosulphuric Acid.

1. Introduction.

On cooling solutions of the blue iodine cation, I_2^+, in fluorosulphuric acid, there is a dramatic colour change from blue to red near the freezing point. Milne (22) recorded the changes in the UV and visible spectra of a 0.0186 m 1/1 $I_2/S_2O_6F_2$ solution. He found that the optical density of the 640 mμ I_2^+ peak increased slightly down to -20°C, and then decreased until, at -92°C, its intensity was approximately one-third of that at 25°C. At low temperatures an intense new peak at 357 mμ appeared, together with peaks at 290 and 470 mμ which were similar to those of I_3^+. Milne also measured the conductivity of 1/1 solutions at -78.52°C and compared them to that of potassium fluorosulphate solutions at that temperature. He found that the γ values at low temperature had decreased to 0.52 - 0.43 in the concentration range 0.005 - 0.025 m, and therefore suggested increased disproportionation according to the equations:

13. $8\ I_2^+ + 8\ SO_3F^- \rightleftharpoons I(SO_3F)_3 + 5\ I_3^+ + 5\ SO_3F^-$

14. $I(SO_3F)_3 + SO_3F^- \rightleftharpoons I(SO_3F)_4^-$.

He suggested that the absorption at 357 mμ may be due to the $I(SO_3F)_4^-$ ion and that further association to form $I_3I(SO_3F)_4$ may occur. His observed freezing points of $\nu = 1.20$ for 1/1 solutions and $\nu = 1.56$ for 2/1 solutions were consistent with these qualitative suggestions. Gillespie and Milne (23) pointed out that it was not possible to come to any more quantitative conclusions until conductimetric, spectroscopic and magnetic susceptibility measurements had been carried out at low temperatures.

2. UV and Visible Absorption Spectra.

Figures 1 and 2 show that a dramatic change occurs in the absorption spectrum of a solution containing I_2^+ as the temperature is lowered. This change is rapid and reversible; it occurs in all solutions containing I_2^+ and is easily observed visually as the colour of the solutions change from an intense blue to a deep red-brown near the freezing point. As the temperature is lowered, the optical density of all peaks at first increase slowly, presumably because the peaks become sharper and also because the density of the solution increases. Thus the molal extinction coefficient of the I_2^+ ion increases from 4500 at 25° to 5300 at -60° and, assuming that this linear increase continues to lower temperatures, to 5650 at -86°C (Fig 2). At around -50° to -60°, however, depending on the concentration and composition of the solution, the 640 mμ peak due to the I_2^+ ion begins to decrease in intensity with increasing rapidity, and new peaks appear at 470, 357 and 290 mμ. Since I_3^+ has peaks at 470 and 305 mμ (23), the additional peak at 357 mμ shows either that the new species it not I_3^+, or that a new species is produced in addition to I_3^+.

The quantitative relationship between the optical density of the 640 mμ I_2^+ absorption, and that of the new species, was studied in a series of experiments in which the concentration of I_2^+ and the relative concentrations of other species varied over a wide range. The results at two temperatures, -70° and -86.5°, at which there is a reasonable equilibrium concentration of the new species, are listed in Table II. In these experiments quartz inserts were used to reduce the path length and give observed optical densities in the range 0 - 2. At very short path lengths, such as 0.005 cm the problem of adsorbed water was particularly severe due to the large surface to volume ratio in the cells and the extreme sensitivity of iodine cations to hydrolysis.

Any such hydrolysis, however, does not affect the equilibrium relationship between the optical densities of the I_2^+ peak and that of the unknown. Therefore a plot of the log of the optical density of the 640 mμ peak against the log of the optical density of the 357 mμ peak was made, and shown in Fig 3. A least-squares fit gave a straight line of slope 2.0 at -70^o and 1.9 at $-86{\cdot}5^o$, showing that there is an equilibrium between 2 mol of I_2^+ and 1 mol of the species giving rise to the 357 mμ peak. The simplest interpretation of this result is that the new species is I_4^{2+}

15. $$2\ I_2^+ \rightleftharpoons I_4^{2+}\ .$$

On changing the temperature, the change in optical density at 290 and 470 mμ was proportional to that at 357 mμ in all experiments, and it is reasonable therefore also to attribute these peaks to the I_4^{2+} ion. Reaction of I_2^+ with some other species in solution, eg I_3^+, $I(SO_3F)_3$, or $I(SO_3F)_4^-$, can be ruled out as all of the points in Fig 3 lie very close to the two straight lines irrespective of the other species in the solutions studied.

The only other reasonable possibilities are the equilibria

16. $$2\ I_2^+ \rightleftharpoons I_3^+ + I^+$$

17. $$2\ I_2^+ \rightleftharpoons I_2^{2+} + I_2$$

Although I_3^+ has characteristic peaks at 470 and 305 mμ, the latter of which could be shifted to 290 mμ, this equilibrium is unlikely for two reasons. (1) It was found that increased concentrations of I_3^+ did not shift the equilibrium. (2) Taking the extinction coefficient of the 305

mμ I_3^+ peak to be 11,000 at -86.5° (23), the optical density at -86.5° indicated the impossible result that approximately 2 mol of I_3^+ are formed from 2 mol of I_2^+.

Equilibrium 17 giving I_2^{2+} and molecular iodine is also very unlikely for at least two reasons. (1) Iodine would react with I_3^+ in solutions containing this ion to give I_5^+ which has its own characteristic spectrum (23), and this was not observed: such a reaction would also affect the equilibrium. (2) I_2^{2+} would be expected to be paramagnetic (cf. O_2) and the solutions became diamagnetic at the freezing point.

Assuming that I_2^+ dimerizes to I_4^{2+} with decreasing temperature, we may use the absorption spectra data to obtain the extinction coefficients of the characteristic peaks of I_4^{2+} and also to obtain values for the equilibrium constant for the dimerization equilibrium $K_d = [I_4^{2+}]/[I_2^+]^2$. Table III gives the results of these experiments on dilute solutions having $I_2/S_2O_6F_2$ ratios of 1.33:1 or 1:1 and therefore containing sufficient $I(SO_3F)_3$ to repress completely the disproportionation of the I_2^+ (equations 13,14). The I_2^+ concentration can therefore be obtained from the intensity of the I_2^+ peak at 640 mμ, and the decrease in the I_2^+ concentration with decreasing temperature can be attributed to its dimerization of I_4^{2+}. Hence the concentration of I_4^{2+} and the extinction coefficients for the 357, 470 and 290 mμ peaks may be obtained. Small approximate corrections were made for the I_2^+ absorption underlying the 470 mμ peaks and the $I(SO_3F)_3$ absorption underlying the 290 mμ peak. The results gave mean values for the extinction coefficients of 46,000 for the 357 mμ peak, 25,000 for the 290 mμ peak, and

11,000 for the 470 mμ peak. In view of the experimental difficulties in making these measurements, these values may be in error by as much as 10%. From the data in Figure 3 it was then possible to obtain mean values of the dimerization constant K_d of 23±2 mol^{-1} kg at -70°C and 170±20 mol^{-1} kg at -86.5°C. Finally we have $\Delta H = -RT^2\Delta$ (Ln K/T) = -10±2 kcal.

3. Magnetic Measurements.

The magnetic susceptibility of 0.07 m solution of I_2^+ was measured from room temperature down to 140°C (frozen solution). This represented the minimum concentration at which the change in magnetic susceptibility could be studied, and the maximum concentration at which the optical density of the 640 mμ could be recorded for comparison. The concentration of I_2^+ was calculated from the magnetic susceptibility by assuming that the magnetic moment of I_2^+ is 2.0 BM (Table IV). The absorption spectrum of the same solution was measured between room temperature and -90° and the concentration of I_2^+ was again calculated from the extinction coefficient of the 640 mμ peak of the I_2^+ ion corrected for the temperature change according to the data in Table IV. Figure 4 shows that both sets of data agree, within an estimated experimental error of ±10% in each method, with the curve calculated from ΔH for the dimerization, assuming ΔH does not vary significantly with the temperature. This confirms that the species formed at low temperature is diamagnetic and that the magnetic moment of the I_2^+ ion is indeed 2.0 BM. The ion I_4^{2+} contains an even number of electrons and would be expected to be diamagnetic.

4. Cryoscopy.

Freezing point depression measurements were made on both the 1:1 and 2:1 solutions. The results are given in Table V. They agree well with those obtained previously, and they show that the value of ν is 1.45 - 1.25 for the 1:1 solutions and 1.6 - 1.5 for the 2:1 solutions in the concentration ranges studied. (An allowance has been made for the interaction of the small excess SO_3 present in the solvent, with the fluorosulphate ion: $SO_3F^- + SO_3 \longrightarrow S_2O_6F^-$ (23). The values of ν are in reasonable agreement with values calculated from K_d=300 for the dimerization at the freezing point, ie 1.64 - 1.57 over the range 0.02 - 0.08 m in the 2:1 solution. At higher concentration limiting values of ν = 1.2 and 1.5 for the 1:1 and 2:1 solutions are expected according to the equations

18. $I_2 + S_2O_6F_2 \longrightarrow 0.4 I_4^{2+} + 0.4\ I(SO_3F)_4^- + 0.4\ SO_3F^-$

19. $2I_2 + S_2O_6F_2 \longrightarrow I_4^{2+} + 2SO_3F^-$

In equation 18 it is assumed that equilibrium 14 lies extensively to the right hand side. It was shown previously (24) that the equilibrium constant for this reaction is 10 mol^{-1} kg at 25°C, and the conductivity results given later show that it has a value of 50 at -86.4°C. A still larger value is predicted at the freezing point of the solutions, and hence this accounts qualitatively for the decrease from ν = 1.45 to 1.25 in dilute 1:1 solutions.

5. Conductivity Measurements.

The equilibrium $2I_2^+ \rightleftharpoons I_4^{2+}$ does not directly affect the conductivities of solutions in fluorosulphuric acid, which are due largely to the fluorosulphate ion. However, in any solutions containing $I(SO_3F)_3$, equilibrium 14 does affect the conductivity. Hence it was necessary to determine the

equilibrium constant $K_a = [I(SO_3F)_4^-] / [I(SO_3F)_3][SO_3F^-]$ at -86.4°C in order to interpret the conductivity results at this temperature of any solution containing $I(SO_3F)_3$.

Table VI gives the results of a conductivity study at 25°C and -86.4°C in which additions of potassium fluorosulphate were made to a 0.0687 m solution of $I(SO_3F)_3$. At 25° the results were in excellent agreement with those obtained previously, giving K_a = 10 mol^{-1} kg, and at -86.4° they agreed well with a curve calculated on the basis of K_a = 50 mol^{-1} kg and $K_b = 2 \times 10^{-4}$ mol kg^{-1} (Figure 5,Appendix). The γ values at low temperature were calculated by comparing the conductivity to that of potassium fluorosulphate at -86.4°C (7). This was done by calculating the ratio of the conductances of potassium fluorosulphate at the same concentration, rather than the ratio of molalities giving the same conductance which allows for the self ionisation of the solvent. At low temperatures the self ionisation of the solvent is negligible, but the solution becomes very non-ideal with increasing ionic strength, as shown by the curvature of the conductance of potassium fluorosulphate plotted against concentration. Hence, to obtain consistant values of K_a, it was necessary to calculate γ values by comparisons of conductance at the same ionic strength; this is not affected by reaction 14.

The conductivities of 1:1 $I_2/S_2O_6F_2$ solutions are given in Figure 6 and Table VII. They are in excellent agreement with the conductivity expected for the equations

$$I_2 + S_2O_6F_2 \longrightarrow 0.4I_4^{2+} + 0.4\ I(SO_3F)_3 + 0.8\ SO_3F^-$$

$$I(SO_3F)_3 + SO_3F^- \rightleftharpoons I(SO_3F)_4^-.$$

for which γ = 0.8 - 0.4 depending on the extent of formation of $I(SO_3F)_4^-$. The observed values of 0.75 to 0.72 at room temperature agree well with those obtained previously (23) for the same concentration range, and the values of 0.70 - 0.63 at -86.4°C show the expected decrease with the increasing formation of $I(SO_3F)_4^-$ and are, in fact, in excellent agreement with conductivities calculated on the basis of K_a = 50 mol^{-1} kg (Figure 5 and Appendix).

The conductivity of 2:1 $I_2/S_2O_6F_2$ solutions, given in Table VII and Figure 7 were again in excellent agreement with those obtained previously at 25°C. The γ values at -86.4°C were calculated by comparison with the conductivity of o-phenylene diamine at -86.4°C (61). This compound gives a doubly charged cation in fluorosulphuric acid of similar size to the I_4^{2+} ion. The γ value of 0.9 at -86.4°C is close to that of 1.0 expected from the equation

$$2I_2 + S_2O_6F_2 \longrightarrow I_4^{2+} + 2SO_3F^-$$

and the difference is smaller than that observed at 25°C, indicating less disproportionation of I_2^+ to I_3^+ and trifluorosulphates (equations 13, 14) at -86.4°C. In contrast, the γ values for 1:1 solutions obtained by Milne at -78.52°C were much lower than those at room temperature, or those obtained here at -86.4°C. This indicates that disproportionation of I_2^+ is more extensive at low temperatures, but that the trend is reversed by the rapid increase of K_d between -78.52°C and the freezing point, resulting in a greatly diminished concentration of I_2^+ which reverses the disproportionation equilibrium.

6. Conclusions

The above spectroscopic, magnetic, cryoscopic and conductivity data establish clearly that the I_2^+ ion dimerises extensively at low temperatures to give the I_4^{2+} ion. This new species is diamagnetic and has absorption bands at 470, 357 and 290 mμ.

The structure of the ion is not known, but a tetrahedral structure, a square planar structure, or an acyclic chain structure might appear reasonable. A simple qualitative molecular orbital treatment of tetra-atomic molecules based on s and p orbitals only leads to the conclusion that a stable tetrahedral molecule can contain a maximum of 20 valence electrons, while a square-planar molecule can contain a maximum of 22 valence electrons. Since I_4^{2+} has 26 valence electrons, it would appear that the only possibility would be an acyclic chain, ie

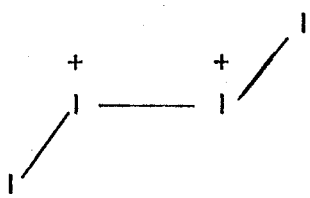

However if d orbitals make an appreciable contribution to bonding, this conclusion is no longer necessarily valid. For a tetrahedral molecule the bonding orbitals are a_1, e and t_2, accomodating 12 electrons, and in addition there are 4 lone-pair orbitals a_1 and t_2. The next lowest set of orbitals are probably the antibonding t_1 set, and, if these are stabilised by d orbital contribution, then the tetrahedron could accomodate another six electrons, and the 26 electron system would represent a stable closed shell configuration. Thus if d orbitals make a significant contribution to the bonding, it is possible that I_4^{2+} has a tetrahedral structure.

TABLE 11

Photometric Data

$10^2 m_{I_2}$	$I_2/S_2O_6F_2$	Optical Density* 640mμ 25	640mμ -70	640mμ -86.5	357 mμ -70	357 mμ -86.5°C
0.27	1.33/1	9.6	11.4	8.6	4.5	14.6
0.58	1.33/1	19.5	20	13.9	16	40 †
1.435	1/1	52	43.5	25	85	166
0.563	1/1	29.5	29.7	18.7	28	70
0.20	2/1	5.8	6.75	5.6	1.2	7.2
9.50	2/1	260	94	50	300	540 †
9.50	1.67/1	340	-	64	-	1,000 †
0.87	1/3	4	6.9	4.5	2.6	8
0.72	2.4/1	16	16	10	10	30

* Optical densities per unit path length

† Estimated from 470 mμ peak height

TABLE III

Extinction Coefficients for the I_4^{2+} Absorptions

	$10^3 m_{I_2}$		
	2.7	5.625	14.35
$I_2:S_2O_6F_2$	1.33:1	1.1	1.1
OD* (640 mμ) (25°)	9.6	29.5	52.0
(-86.5°)	8.6	18.7	25.0
$10^3 m_{I_2}$ + (25°)	2.13	6.55	11.6
(-86.5°)	1.52	3.36	4.42
$10^3 m_{I_4^{2+}}$ (-86.5°)	0.30	1.59	3.59
OD(I_4^{2+}) (357 mμ)	14.6	70	166
(470 mμ)†	3.3	17	43
(290 mμ)#	7	41	95
ε(I_4^{2+}) (357 mμ)	48,000	44,000	46,000
(470 mμ)	11,000	11,000	12,000
(290 mμ)	23,000	26,000	26,000

* All optical densities are given per cm of path length.

† Corrected for I_2^+ absorption at 470 mμ.

Corrected for $I(SO_3F)_2$ shoulder.

TABLE IV

Magnetic Susceptibility and Visible Spectrum of a 0.108 m, 0.74:1 $I_2/S_2O_6F_2$ Solution

Magnetic data*				Visible data†			
Temp, °C	-Δw, μg	10^6 g	$10^2 ml_2^+$ #	Temp, °C	OD (640 mμ)	ε 640 mμ	$10^2 ml_2^+$
22	835	116	7.6	22	1.50	4500	6.67
3	835	116	7.1	0	1.50	4750	6.32
-25	830	124	6.9	-35	1.19	5100	4.66
-50	865	57	2.8	-44	1.06	5200	4.08
-69	880	41	1.9	-48	0.96	5250	3.76
-87	905	0	0.0	-75	0.43	5550	1.55
-100	905	0	0.0	-86	0.24	5650	0.85
-143	900	5	0.2	-100	0.07	5750	0.24

* Quartz tube constant, 1.86; diamagnetic correction, 683 μg; solvent correction, 221 μg.

† Path length, 0.005 cm.

\# Calculated assuming $\mu I_2^+ = 2.00$ BM.

TABLE V

Freezing Point Data

2:1 $I_2/S_2O_6F_2$		1:1 $I_2/S_2O_6F_2$	
$10^2 m I_2$	θ, °C	$10^2 m I_2$	θ, °C
1.86	0.125	0.981	0.045
3.53	0.24	2.04	0.089
4.43	0.25	2.98	0.131
5.33	0.31	3.47	0.159
6.27	0.36		
7.11	0.41		
7.82	0.44		

θ = freezing point depression.

TABLE VI

Conductivities of $I(SO_3F)_3/KSO_3F$ Solutions

	10^5K, $ohm^{-1}cm^{-1}$		γ	
$m(KSO_3F)$	25°	-86.4°	25°	-86.4°
...	97.7	2.89	...	...
0.0081	202.5	6.61	...	0.4
0.0242	408.8	14.83	0.66	0.35
0.0440	691.8	29.00	0.64	0.40
0.0899	1420	68.89	0.68	0.51
0.1317	2075	106.2	0.71	0.60
0.1681	2621	135.4	0.75	0.65

m $I(SO_3F)_3$ = 0.0687.

TABLE VII

Conductivities of $I_2/S_2O_6F_2$ Solutions

$10^2 ml_2$	10^4K ohm^{-1} cm^{-1} 25°	10^4K ohm^{-1} cm^{-1} -86.4°	γ 25°	γ -86.4°
		2:1 Solutions		
...	1.11	0.007	...	...
0.031	8.96	0.588	0.85	1.0
0.063	15.95	1.078	0.85	1.0
3.31	70.68	4.75	0.87	0.92
3.95	83.42	5.67	0.87	0.92
4.96	103.3	6.99	0.87	0.90
6.46	131.6	8.82	0.87	0.90
9.52	185.7	12.23	0.87	0.91
		1:1 Solutions		
0.0	1.14	0.007	...	...
0.518	10.28	0.599	0.75	0.70
0.926	18.11	1.100	0.74	0.66
1.435	27.10	1.649	0.73	0.65
1.930	35.20	2.135	0.72	0.63

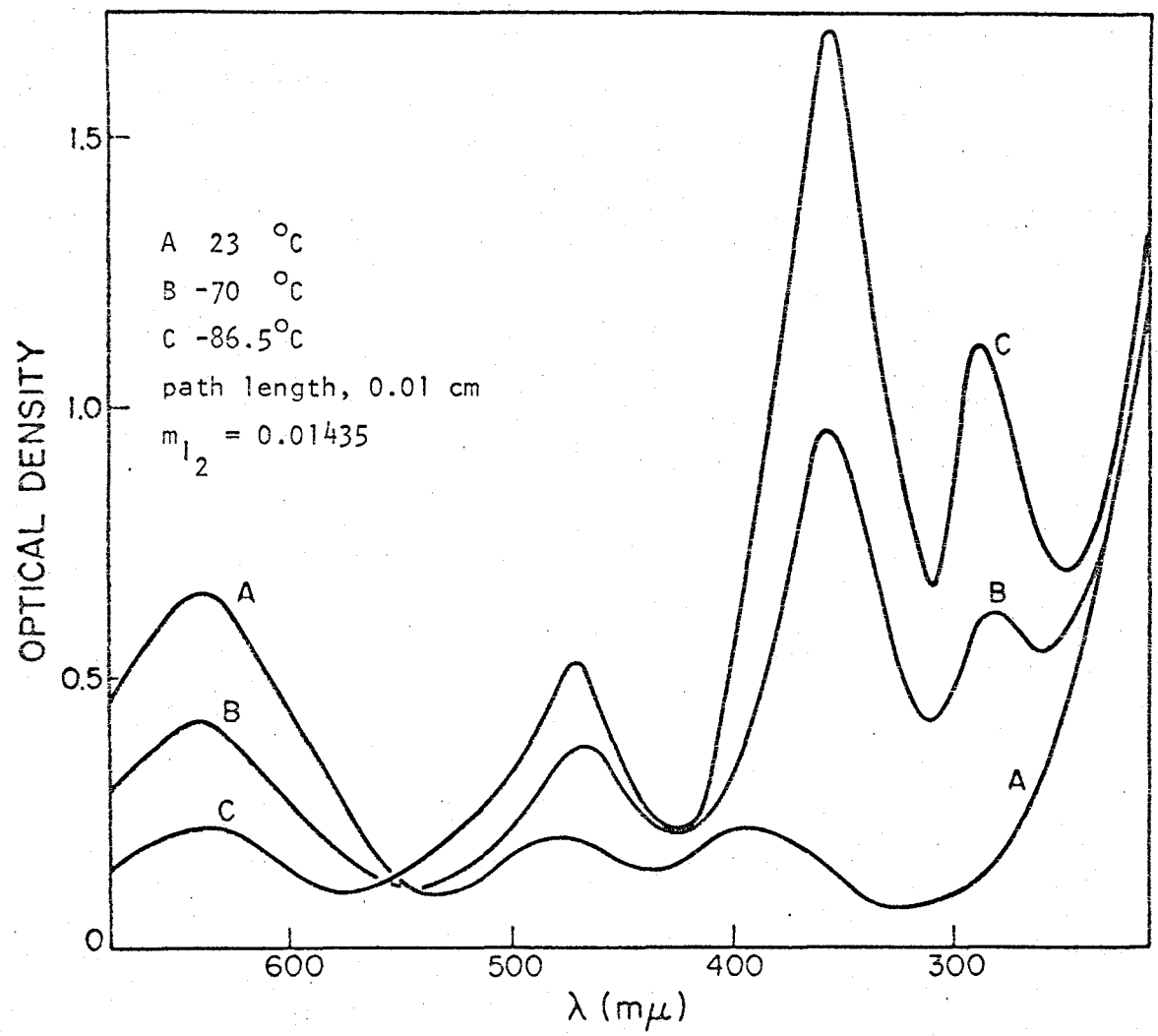

Figure 1. UV and visible spectrum of a 1:1 $I_2/S_2O_6F_2$ solution.

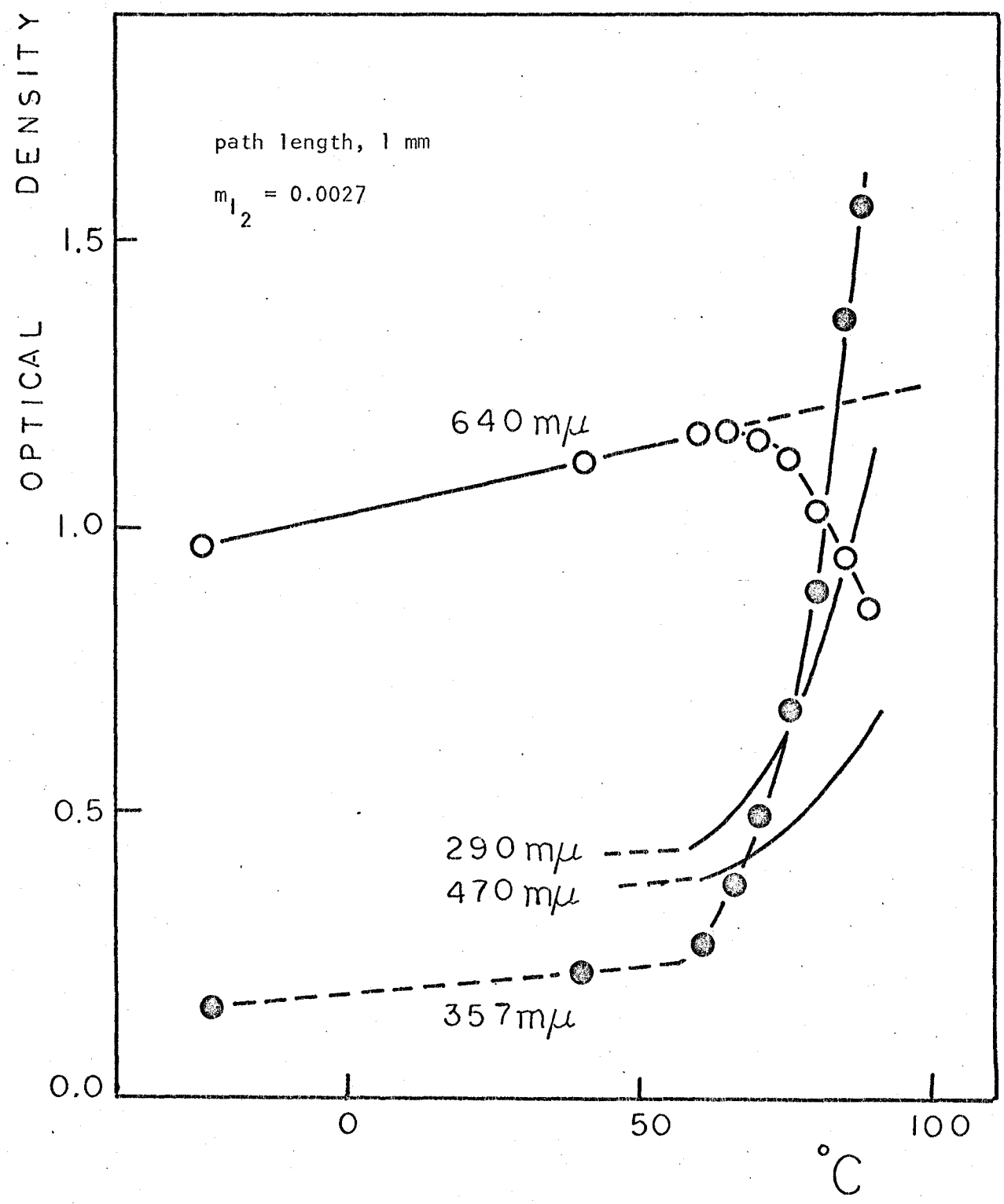

Figure 2. Temperature dependence of the spectrum of a 1.33:1 $I_2/S_2O_6F_2$ solution.

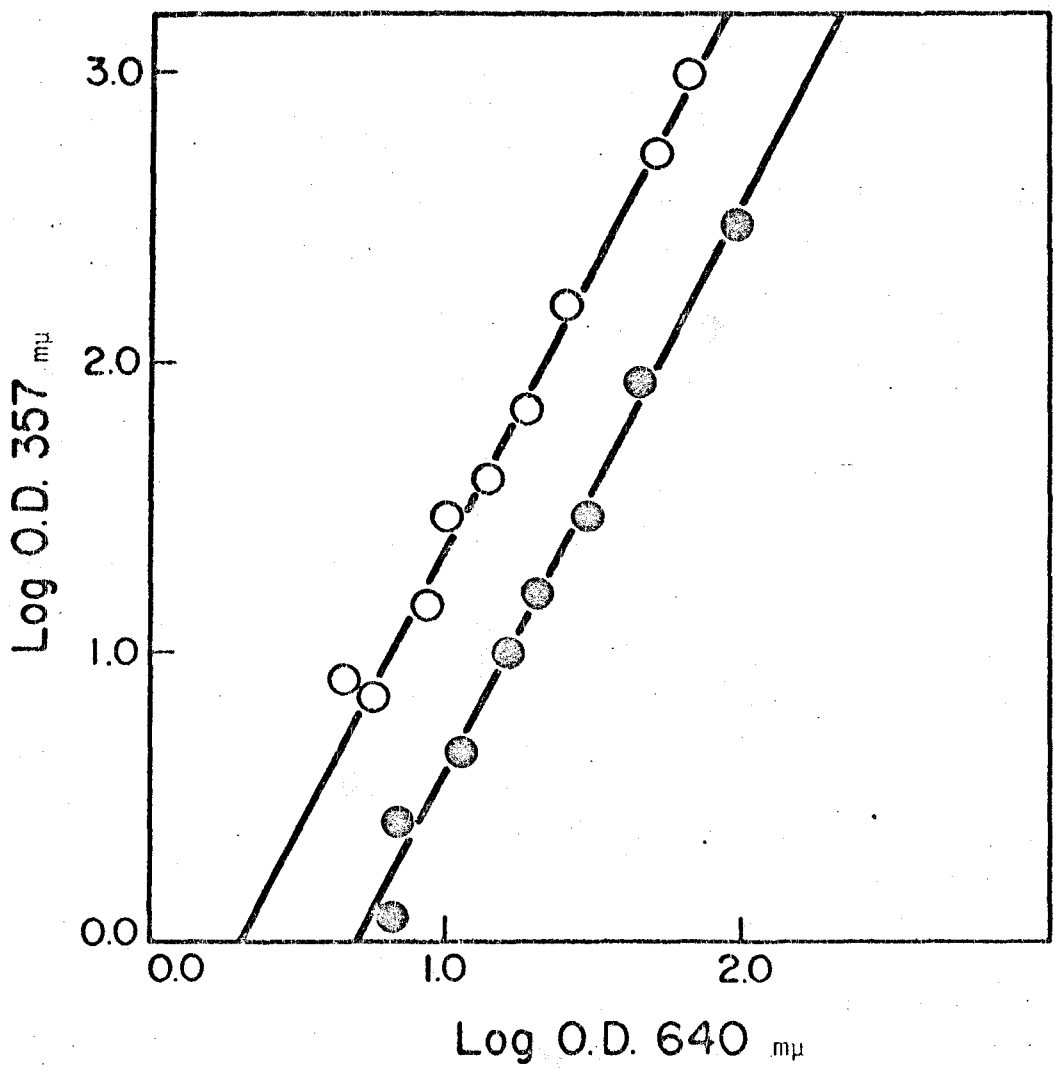

Figure 3. Photometric plot: ● , -70°C; ○ , -86.5°C.

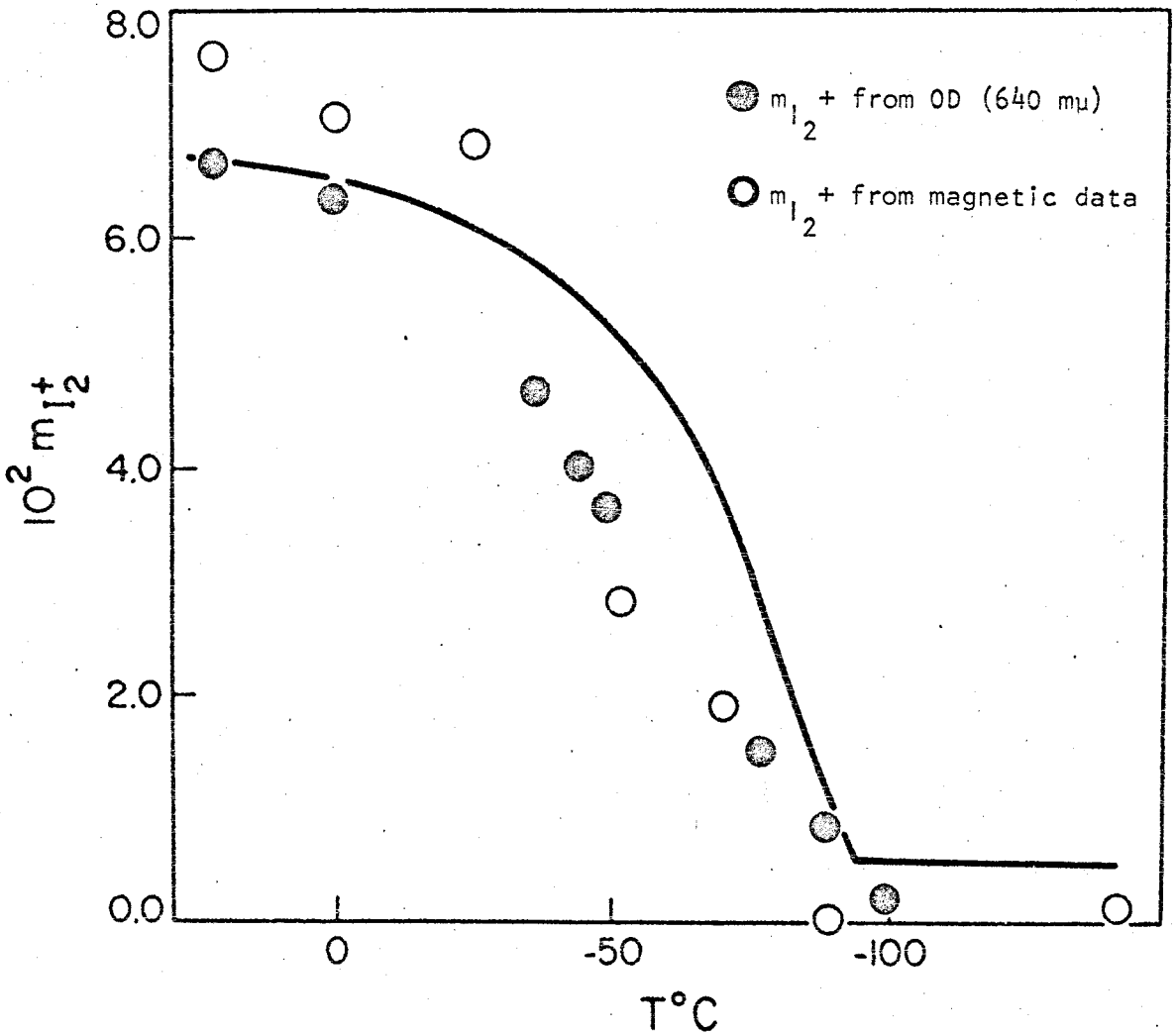

Figure 4. Variation of I_2^+ concentration with temperature.

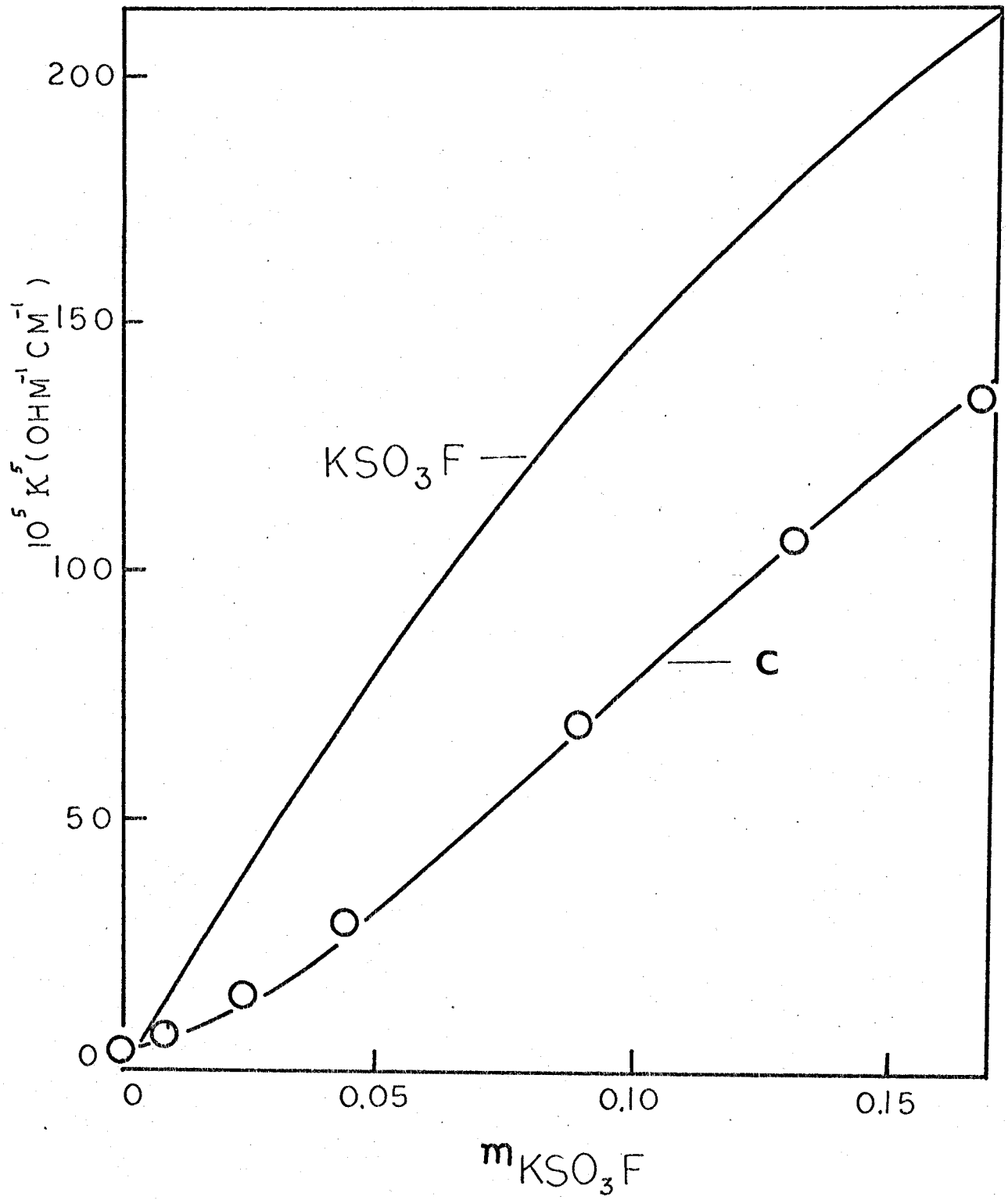

Figure 5. Conductivities at -86.4°C for addition of KSO_3F to .0687m $I(SO_3F)_3$: **C** , calculated curve for $K_a = 50$ and $K_b = 2 \times 10^{-4}$.

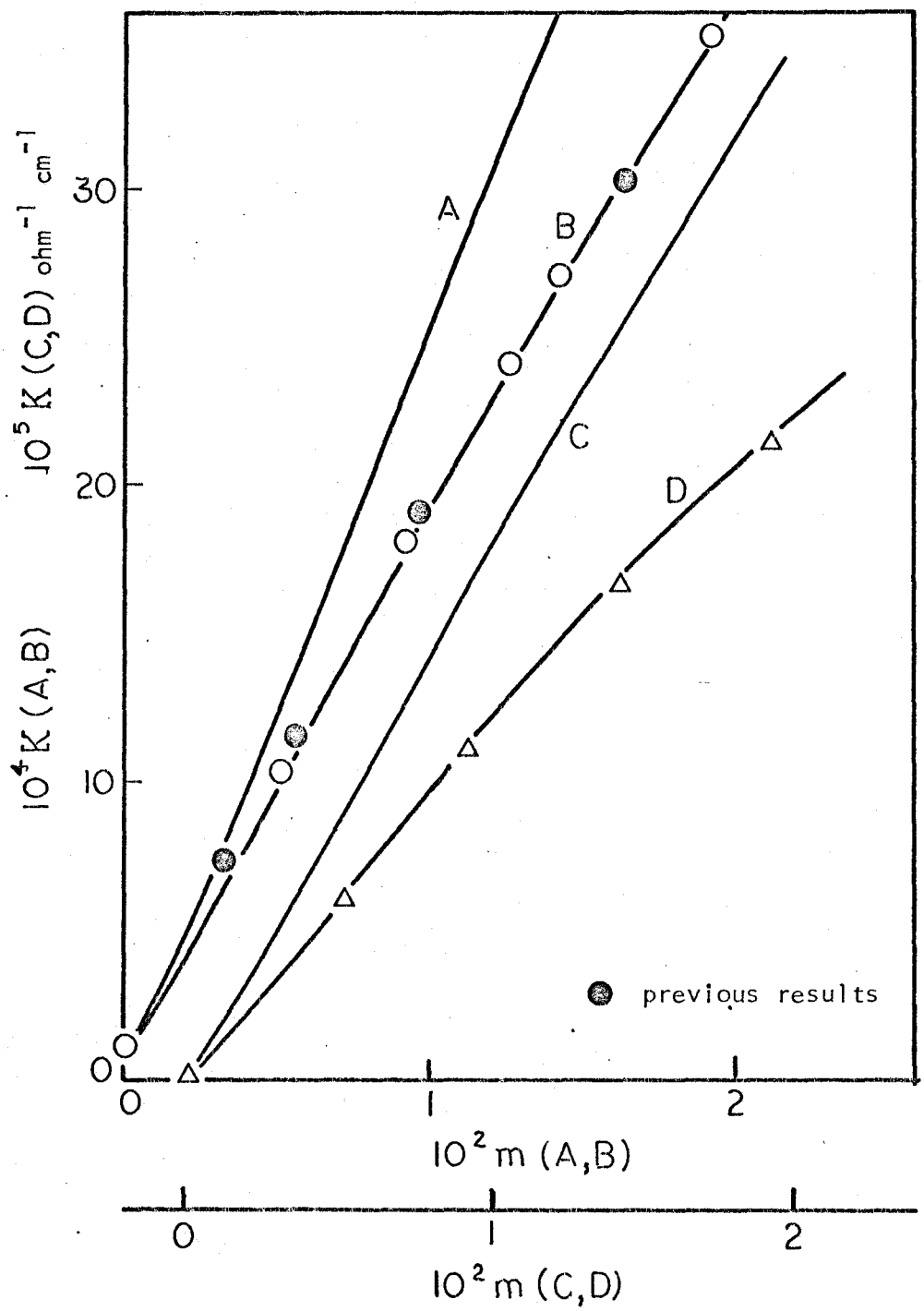

Figure 6. Conductivities of 1:1 $I_2/S_2O_6F_2$ solutions: A, KSO_3F (25°); B, 1:1 solutions (25°); C, KSO_3F (-86.4°); D, 1:1 solutions (-86.4°).

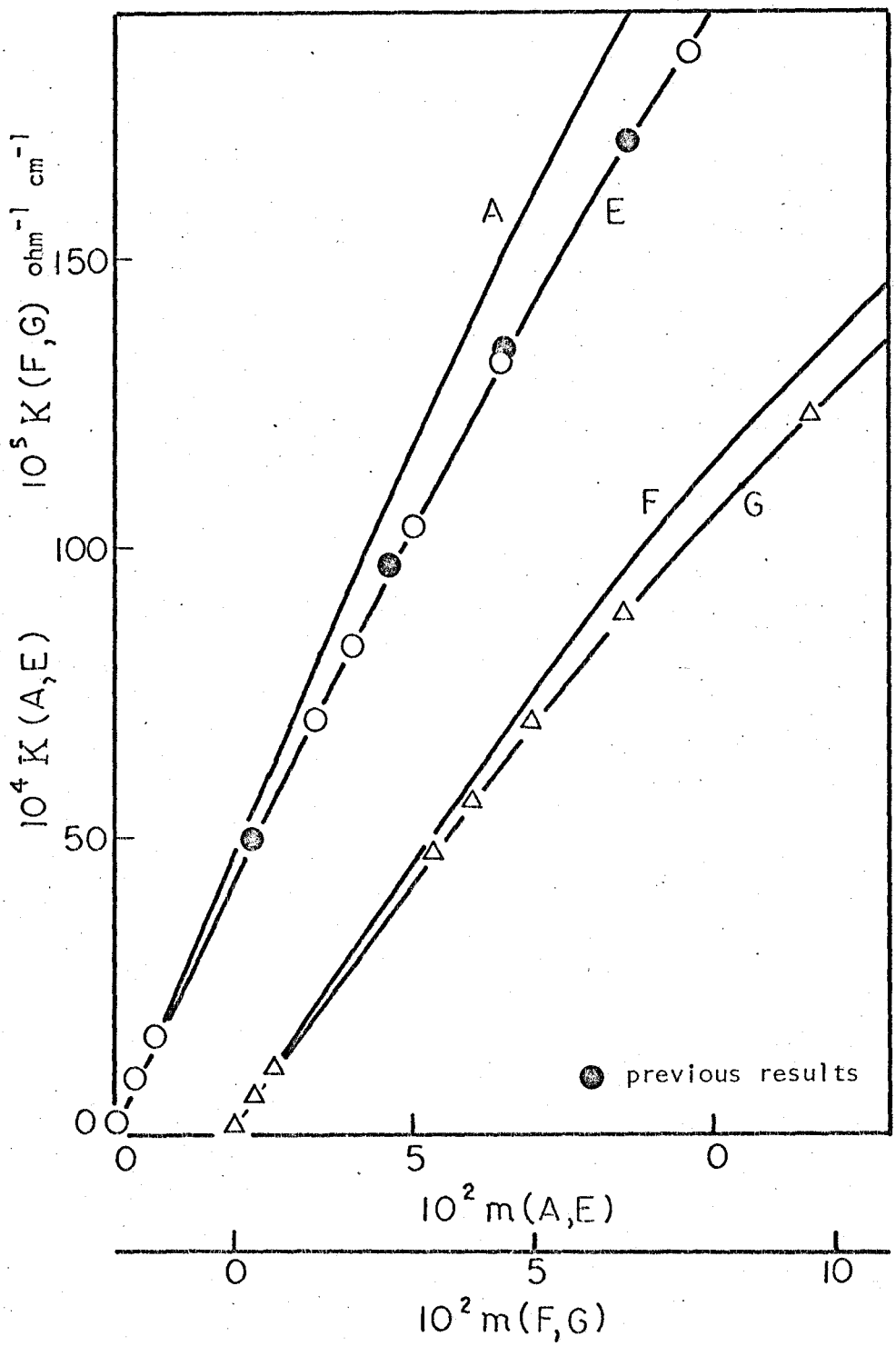

Figure 7. Conductivities of 2:1 $I_2/S_2O_6F_2$ solutions: A, KSO_3F (25°); E, 2:1 solutions (25°); F, o-phenylenediamine/2 (-86.4°); G, 2:1 solutions (-86.4°).

APPENDIX

Theoretical conductivity curves for solutions obtained by adding KSO_3F to $I(SO_3F)_3$ were plotted from the expression

$$m_{KSO_3F} = \frac{\alpha\left[K_a\beta - (K_b/\beta)\right] + K_a\beta^2 + \beta + K_b}{1 + K_a\beta + (K_b/\beta)}$$

Where α is the initial molality of $I(SO_3F)_3$, β is the molality of SO_3F^- in solution, and K_a and K_b are the acid and base equilibrium constants for $I(SO_3F)_3$.

For 1:1 $I_2/S_2O_6F_2$ solutions at -86.4°C, with K_a = 50 mol^{-1} kg

$$m_{I_2} = \frac{\beta(50\beta + 1)}{0.8 + 20\beta}$$

CHAPTER IV

Bromine Cations in the Super Acid $SbF_5:3SO_3/HSO_3F$.

1. Introduction.

Although the I_3^+ cation is stabilised by the acidity of sulphuric acid, the I_2^+ cation is almost completely disproportionated in this solvent, and it needs the greater acidity of fluorosulphuric acid to enable it to exist in sufficient concentration for identification by its intense visible peak at 640 mμ, which is shifted to the red from that of iodine. Even so, the I_2^+ cation can be detected in 100% sulphuric acid by its intense resonance Raman spectrum (Chapter VI). Accordingly it was anticipated that it might be possible to prepare the Br_2^+ cation in the highly acidic $SbF_5:3SO_3/HSO_3F$ system, and that, if so, identifications would be possible even at very low concentrations by a resonance Raman spectrum. By analogy with I_2^+, a strong visible absorption was expected shifted to the red from that of bromine (410 mμ).

When bromine monofluorosulphate (61) was distilled into a cold 0.178 m $SbF_5:3SO_3$ solution in fluorosulphuric acid, the red brown compound dissolved on warming to give an intense cherry-red coloured solution, (ε_{max} 510 mμ, Figure 8). Similar solutions could be obtained by oxidising bromine with $S_2O_6F_2$ in this solvent. An intense Raman peak at 360 cm^{-1} was observed with an intensity proportional to that of the 510 mμ peak responsible for the red colour.

2. Raman Spectra

Figure 9 shows the Raman spectrum of a 0.399 m solution of $BrSO_3F$ in the 0.178 m super acid. The most intense peak is at 360 cm^{-1} and there are progressively weaker and broader overtones at 710 and 1060 mμ: these peaks are due to the resonance Raman spectrum of the Br_2^+ cation, which will be discussed in Chapter VI. In order to identify the other weak peaks which appear in addition to the solvent peaks, the Raman spectra of $S_2O_6F_2$, $^{\circ}BrSO_3F$, $Br(SO_3F)_3$ in HSO_3F, $Br(SO_3F)_3$ in the super acid, and a $Br_2/S_2O_6F_2$ solution in the ratio 3:1 in the super acid were run. The results, listed in Table 8 enable peaks at 177, 318, 466, 657 and 1210 cm^{-1} from the exciting radiation to be assigned to $BrSO_3F$. The $Br(SO_3F)_2^+$ cation in the solution is identified by the peak at 745 mμ and the broad peak at 290 mμ can be assigned to the Br_3^+ cation. The formation of these species can be accounted for by the following equilibria;

20. $5\ BrSO_3F + 2H_2SO_3F^+ \rightleftharpoons 2Br_2^+ + Br(SO_3F)_3 + 4HSO_3F$

21. $4\ BrSO_3F + H_2SO_3F^+ \rightleftharpoons Br_3^+ + Br(SO_3F)_3 + 2HSO_3F$

22. $Br(SO_3F)_3 + H_2SO_3F^+ \rightleftharpoons Br(SO_3F)_2^+ + 2HSO_3F.$

Raman spectra of the 3:1 bromine solutions in the super acid gave a broad peak at 290 mμ, probably due to the symmetric and antisymmetric stretches of the Br_3^+ cation. These appear at a lower frequency than that of bromine in fluorosulphuric acid (320 cm^{-1}). The bending frequency was not observed, as it was probably obscured in the solvent peaks below 200 cm^{-1}. A similar result was obtained for the Cl_3^+ cation which gave

a peak in solution at 500 cm^{-1} whereas that of chlorine in fluorosulphuric acid is at 555 cm^{-1} (Chapter V).

3. Conductivity Measurements.

Table IX and Figure 10 give the conductivities of solutions of $Br_2/S_2O_6F_2$ in the ratio 2.31:1 in the 0.176 m super acid. The initial conductivity of the super acid was in excellent agreement with the value calculated from the results of Gillespie et al. (61). The γ values for this conductivity titration of the solvent acidium cation with the bromine solution which were calculated by comparison with the slope for potassium fluorosulphate (61), showed a decrease with concentration as expected from equations 20, 21 and 22. In a second experiment this solution was oxidised with a solution of $S_2O_6F_2$ in the super acid, until at the 1:3 ratio the solution had turned from red to a very pale yellow, corresponding to complete oxidation to trivalent bromine fluorosulphates. The γ values, listed in Table X, were plotted against the oxidation state of the bromine in Figure 11. The expected slopes for the formation of Br_3^+, unionised $BrSO_3F$ and $Br(SO_3F)_2^+$ only are also shown in Figure 11. Although the experimental γ value reached a minimum at the 1:1 ratio, corresponding to a maximum concentration of unionised $BrSO_3F$, the γ value of 1.51 indicates 75% ionisation of bromine trifluorosulphate at this acidity to form the $Br(SO_3F)_2^+$ cation. Thus we can calculate an equilibrium constant for equation 22 by first calculating the molal concentration of acidium cation in the solution.

Using the values $\lambda^* = 320$ for $H_2SO_3F^+$, and $\lambda^* = 13$ for complex antimony anions, as given by Gillespie et al., where λ^* is defined by the equation,

23. $$\lambda^* = 1{,}000\ K_{ion}/m$$

where K_{ion} is the specific conductance (ohm^{-1} cm^{-1}) of an individual ion at a concentration m (mol kg^{-1}), the conductance of the initial super acid of 354.5×10^{-4} ohm^{-1} cm^{-1} gives an initial concentration of $H_2SO_3F^+$ of 0.106 molal from the equation;

$$\text{Conductance} \quad K = 10^{-3} \ \Sigma_n \lambda^*_n m_n = 354.5 \times 10^{-4}$$

In the 1:3 solution, the concentration of ionic bromine cations is given by $m_{Br_2} \cdot \gamma$, and assuming a value of λ^* of 15 (61) for these cations, the conductance of 186.5×10^{-4} ohm^{-1} cm^{-1} gives an acidium ion concentration of 0.050 molal. Hence the equilibrium constant K_b for equation 22 given by

25. $$K_b = \frac{[Br(SO_3F)_2^+]}{[Br(SO_3F)_3]\ [H_2SO_3F^+]}$$

has a value of 60 ± 10 mol^{-1} kg.

The conductivity of solutions at the $Br_2/S_2O_6F_2$ ratio of 2.31:1 gave γ values of 0.63 - 0.56 over the concentration range studied (Table IX). At this ratio we expect a γ value between 0.567 for the formation of Br_3^+ and $BrSO_3F$ only, according to the equation;

26. $Br_2 + 0.433\ S_2O_6F_2 \longrightarrow 0.567\ Br_3^+ + 0.299\ BrSO_3F + 0.567\ SO_3F^-$

and 0.868 for complete formation of Br_2^+ and Br_3^+;

27. $Br_2 + 0.433\ S_2O_6F_2 \longrightarrow 0.268\ Br_3^+ + 0.598\ Br_2^+ + 0.868\ SO_3F^-$.

Due to the complexity of the system, the absolute value of a γ value is at best accurate to $\pm$ 5%, so that these conductivity values cannot be used to calculate the concentration of Br_2^+ with any accuracy, but they are consistent with equation 26, with partial oxidation of Br_3^+ to Br_2^+ by $BrSO_3F$ according to equation 27. At the 1:1 ratio, the γ value of 0.43 may be attributed to disproportionation of $BrSO_3F$ according to equations 20, 21 and 22. We may note from equation 20, that for every

mole of Br_2^+ produced, 0.5 moles of $Br(SO_3F)_3$ are formed. The $Br(SO_3F)_3$ is 80% ionised at this acidium ion concentration using the value of K_b from equation 25 so that a total of 1.4 moles of acidium cation are consumed for every mole of Br_2^+ produced. Thus we can put an upper limit of $\gamma/1.4$, which equals 0.31, on the ratio of the number of moles of Br_2^+ formed per mole of bromine in solutions by assuming that no Br_3^+ is formed at the 1:1 ratio. However we may also note, from equations 21 and 22, that for every mole of Br_3^+ formed, 1.8 moles of the acidium cation are consumed, so that in the other extreme 0.23 moles of Br_3^+ would give this γvalue. In either case some 60% of the bromine remains as an unionised $BrSO_3F$ at this acidity.

4. UV and Visible Spectra.

Figure 12 shows the changes observed in the visible spectrum of a 1.422 x 10^{-2} molal solution of bromine in fluorosulphuric acid on oxidation with a concentrated solution of $S_2O_6F_2$ to the approximate ratios of 1:0.33, 1:1, 1:3 and 1:5. On oxidation the extinction coefficient at 375 mμ increased until at the 1:0.33 ratio the curve B was obtained. Above this ratio the shoulder at 375 mμ, attributed to the Br_3^+ cation decreased, but a shoulder at 310 mμ increased, until at the 1:3 ratio there was no further change, corresponding to complete oxidation to bromine trifluorosulphate. On repeating the experiment in 0.03 m $SbF_5:3SO_3$ in HSO_3F, a peak at 510 mμ was observed between the ratios of 2:1 and 1:2 with an estimated optical density of ∿ 120 per cm per mole of bromine in solution above the underlying absorptions (Table XI). The optical density at the 3:1 ratio in .03 m super acid gave a molal extinction coefficient of 1,600 for the Br_3^+

cation at 375 mμ (Table XI).

Table XII lists the optical densities at various wavelengths per mole of bromine in solution of various solutions extracted from the conductivity cells with weighed teflon-glass syringes. Although the conductivity K of these solutions from which the acidium ion concentration can be calculated, the concentration of bromine, and the oxidation ratio of the bromine in the bulk solution were accurately known, the results of the visible spectra are probably not accurate to more than ten per cent. This is due to the very large surface to volume ratios in the short path length cells and the consequent problem of adsorbed water even after the most careful desiccation.

Quantitative interpretation of the results is further complicated by the sensitivity of the disproportionation of $BrSO_3F$ to the acidity (which can be estimated from the conductance) and to the overlapping absorptions of Br_2^+, Br_3^+ and $BrSO_3F$ at 375 mμ. In Table XII the extinction coefficients at 510 375 and 300 mμ are listed, expressed per mole of bromine in solution. Thus at 510 mμ, if all the bromine in solution appeared as the Br_2^+ cation, the extinction coefficient listed would be that of Br_2^+. The results show that the concentration of the Br_2^+ cation per mole of bromine in solution reaches a maximum at the 1:1 ratio, and that the optical density at 375 mμ decreases on oxidation.

Using the extinction coefficient of 1,600 for Br_3^+ at 375 mμ gives approximately 0.4 moles Br_3^+ per mole Br_2 in solution at the 2.31/1 ratio. The γ value of 0.57 at .0585 m_{Br_2} therefore gives ~0.17 moles Br_2^+ per mole of bromine in solution, and hence a molal extinction coefficient of $\sim 1.3(5) \times 10^3$

for the Br_2^+ cation. At the 1/1 ratio the γ value is given by the equation (section 3)

28. $$\gamma = 1.4\ m'_{Br_2^+} + 1.8\ m'_{Br_3^+}$$

where m'_X is the moles of X formed per mole of bromine. In section 3 of this chapter, an upper limit of 0.31 for $m'_{Br_2^+}$ was calculated assuming that $m'_{Br_3^+}$ equals zero. This gives a lower limit of 1,400 for the extinction coefficient of Br_2^+ at 510 mμ, using the data in Table XII. This would require the optical density at 375 mμ to be entirely due to absorptions of $BrSO_3F$ and Br_2^+ rather than to the Br_3^+ cation. However spectra of 1:1 solutions show a very weak shoulder at 375, and the Raman spectrum of the concentrated 1:1 solution showed a weak peak at 290 cm^{-1} due to Br_3^+ present at this ratio. The contribution due to the Br_2^+ cation to the optical density per mole of bromine was estimated to be at most 80, giving a value of 0.05 for $m'_{Br_3^+}$, and hence an extinction coefficient of 1,800 for Br_2^+ as a probable upper limit from equation 28. It is concluded from these two results that the molal extinction of the Br_2^+ ion is 1,600 ± 300. On cooling 1:1 solutions, the optical density at 510 mμ decreased until at -80°C no shoulder at 510 mμ was visible. However as no new peaks were observed, there is no evidence for the formation of the Br_4^{2+} cation and the simplest explanation is that the degree of disproportionation of $BrSO_3F$, as in equation 20, to the Br_2^+ cation decreases with temperature.

5. Magnetic Measurements.

Table XIII gives the result of magnetic measurements on a very concentrated solution of $BrSO_3F$ in 1.38 molal super acid. The solution was less diamagnetic than the solvent alone, showing that paramagnetic species are formed. Assuming

a value of 2.0 B M for the Br_2^+ cation, as observed for the I_2^+ cation (23), gives a concentration of 0.06 moles Br_2^+ per g of solution. As the density was 2.0, this gives 0.12 moles Br_2^+ per litre at 37°C. The paramagnetism decreased sharply with temperature. The visible spectrum of the same solution gave an optical density of 117 per cm at a path length of .0068 cm and using a molar extinction coefficient of 1,600/1.8, where 1.8 is the density of the 0.176 m super acid, gives a Br_2^+ concentration of 0.13 ± .02 molar at 28°C in good agreement with the magnetic results.

6. Conductivities in Fluorosulphuric Acid.

Table XIV gives the conductivities of a 3:1 solution of $Br_2/S_2O_6F_2$ in fluorosulphuric acid, which gives a γ value of 0.37, indicating ~50% ionisation to Br_3^+.

eg 29. $Br_2 + BrSO_3F \rightleftharpoons Br_3^+ + SO_3F^-$.

or 30. $Br_3SO_3F \rightleftharpoons Br_3^+ + SO_3F^-$.

By analogy with iodine, the Br_5^+ cation could also be formed by the equilibrium,

31. $Br_3^+ + Br_2 \rightleftharpoons Br_5^+$

However this is probably present only in trace quantities in fluorosulphuric acid as even at the 3:1 ratio bromine could be pumped off the concentrated solutions quite readily. This shows that the Br_3^+ cation is unstable according to equation 29, as indicated by the conductivity results and presumably the Br_5^+ ion is still less stable.

7. ESR and NMR Spectra.

No ESR spectra were obtained from solutions of the paramagnetic Br_2^+

cation down to -100°C. The ground state of this cation should be the $^2\Pi_{3/2}g$ state in which strong spin orbit coupling would probably broaden any ESR spectrum beyond detection. In NMR spectra of solutions of the Br_2^+ cation in the super acid, no significant broadening of the fluorosulphuric acid peak was observed. In contrast solutions of the paramagnetic I_2^+ cation caused a dramatic broadening of the solvent peak to a half height width of over 50 cycles per second at similar concentrations. This indicates that the relaxation rate of the unpaired electron spin in the Br_2^+ cation is very short on the NMR time-scale, unlike that of the I_2^+ cation. A recent study of the photoelectron spectra of the halogens in the gas phase (61) showed that the $^2\Pi_{3/2}g$ - $^2\Pi_{3/2}g$ separation of the gaseous I_2^+ cation is 0.63 electron volts, while that for gaseous Br_2^+ is only 0.39 electron volts making relaxation of the electron-spin easier for the bromine cation. Also the smaller Br_2^+ cation would be more solvated compared to the I_2^+ cation, so that any relaxation arising from coupling of the electron spin with solvent molecules would be more effective for the Br_2^+ cation.

8. Conclusions.

It has been shown that in the super acid system $SbF_5:3SO_3/HSO_3F$ stable solutions of the Br_2^+ and Br_3^+ cation can be obtained, whereas in fluorosulphuric acid only the Br_3^+ cation in equilibrium with Br_2 and $BrSO_3$ is formed. Bromine trifluorosulphate was shown to be a weak base in the super acid. In contrast to ISO_3F which is completely disproportionated in fluorosulphuric acid (23), $BrSO_3F$ does not disproportionate in fluorosulphuric acid (61), but is somewhat disproportionated in the super acid where it is in equilibrium with the bromine cations and

trivalent bromine fluorosulphates. On cooling solutions of the Br_2^+ cation, which was characterised by its paramagnetic susceptibility, Raman spectrum and visible absorption at 510 mμ, the concentration of Br_2^+ decreased, probably due to disproportionation to $BrSO_3F$ and Br_3^+. No evidence for the Br_4^{2+} cation was obtained, as no new ultraviolet peaks were observed.

TABLE VIII

Raman Spectra of Bromine Fluorosulphates and $S_2O_6F_2$ (cm^{-1}).

$S_2O_6F_2$	$BrSO_3F$	$Br(SO_3F)_3$ in HSO_3F.
190 m	177 m	178 m
209 m	280 sh	294 sh
307 ms	318 s	318 s
389 w	400 w	464 m
483 w	466 m	659 ms
528 w	540 w	737 m
598 w	573 w	1267 m
798 s	613 w	
824 ms	658 s	
881 m	832 w	$Br(SO_3F)_2^+$ in Super Acid
1249 s	890 w	308 s
1496 w	1206 m	462 m
		746 m
		1242 m

Br_2^+ in Super Acid	360, 710, 1070	cm^{-1}
Br_2 in HSO_3F	320	cm^{-1}
Br_3^+ in Super Acid	290	cm^{-1}

TABLE IX

Conductivities at 25°C of a 2.31:1 $Br_2/S_2O_6F_2$ Solution in 0.178 m Super Acid

Composition of Super Acid:	211. 96	g	HSO_3F
	8.983	g	SO_3
	8.105	g	SbF_5
Composition of Concentrated Solution:			
	0.4684	g	Br_2
	0.8073	g	$BrSO_3F$
	13.24	g	Super Acid

Wt Super Acid in Cell = 47.28 g

$10^2 m_{Br_2}$	$10^4 K$	γ
0	354.5	-
1.108	338.9	0.63
2.555	321.1	0.59
4.239	300.5	0.58
5.854	281.1	0.57
7.841	258.2	0.56

TABLE X

Conductivities of solutions formed by oxidation of 2.31:1 $Br_2/S_2O_6F_2$ in 0.176 m super acid with $S_2O_6F_2$ solution

Composition of $S_2O_6F_2$ Solutions: 24.357 g 0.176 m super acid

1.6033 g $S_2O_6F_2$

Contents of Cell: 7.841×10^{-2} m Br_2 solution (2.31:1) in 47.39 g 0.176 m super acid.

$10^2 m_{Br_2}$	Ratio $Br_2:S_2O_6F_2$	$10^4 K$	γ
7.841	1 : 0.433	258	0.56
7.46	0.67	273	0.50
7.33	0.87	282.5	0.45
7.00	1.10	283.5	0.46
6.77	1.30	274.5	0.54
6.34	1.64	255	0.71
5.97	1.99	234	0.92
5.66	2.35	217	1.10
5.32	2.78	193	1.39
5.09	3.10	186.5	1.51

TABLE XI

UV and Visible Spectra of Bromine Solutions in .03 m Super Acid, oxidised with $S_2O_6F_2$

Ratio $Br_2 : S_2O_6F_2$	Optical Densities 510 mμ	375 mμ	310 mμ
3 : 1	0.08	1.23	1.54
2 : 1	0.20	0.70	0.86
1 : 1	0.22(5)	0.63	1.60
1 : 2	0.21	0.47	>2

Path Length = 1.00 mm

Bromine Concentration= 1.18×10^{-2} m

TABLE XII

UV and Visible Spectra of Bromine/$S_2O_6F_2$ Solutions in 0.176 m Super Acid

Ratio I:X	$10^2 m_{Br_2}$	$10^4 K$	Path	Molal Extinction Coefficients per Br_2*		
$Br_2:S_2O_6F_2$		$ohm^{-1}cm^{-1}$	mm	510 mμ	375 mμ	300 mμ
0.433	4.239	300.5	0.506	230	650	-
0.433	5.845	281	0.506	230	670	-
0.67	7.46	273	0.211	375	375	730
1.00	5.573	293	0.144	450	450	800
1.00	5.573	293	0.506	450	450	-
1.00	18.38	-	0.144	210	235	585
1.30	6.77	274.5	0.506	236	220	-
2.10	4.80	220	0.144	65	110	1000
2.35	5.66	217	0.211	11	63	450
2.78	5.32	193	10.00	2	27	-

*Optical densities per cm divided by molality of bromine in solution.

TABLE XIII

Magnetic Susceptibility and Visible Spectra of $BrSO_3F$ in Super Acid

Composition of Solution Wt Br_2 = 1.3438 g

Wt SbF_5 = 5.8500 g

Wt SO_3 = 7.3586 g

Wt $S_2O_6F_2$ = 1.4185 g

Wt HSO_3F = 19.50 g

Ratio Br_2: $S_2O_6F_2$ = 1 : 1.06

Molality SbF_5:3.4.SO_3 = 1.38

Tube Constant = 2.08 Wt Sample contents = 2.62 g

T °C	Solvent Δw µg	Sample Δw µg	∂(Δw)µg (±10µg)
+37°C.	660	535	125
-20°C.	660	640	20
-70°	660	650	10

Visible Spectrum of this solution. Path Length .0068 cm.

T°C	Optical Density 510 mµ.
28	0.80
-20	0.41
-80	0.00

TABLE XIV

Conductivities of 3:1 $Br_2/S_2O_6F_2$ solutions in HSO_3F

Composition of Concentrated Solution

8.5312 g	Br_2
3.5163 g	$S_2O_6F_2$
42.5964 g	HSO_3F

Ratio = 3.01 : 1.

$10^2\ m_{Br_2}$	$10^4 K$ ohm^{-1} cm^{-1}
-	14.60
2.291	35.46
4.392	52.99
6.519	70.66
8.696	91.65
10.760	110.44
13.504	133.21

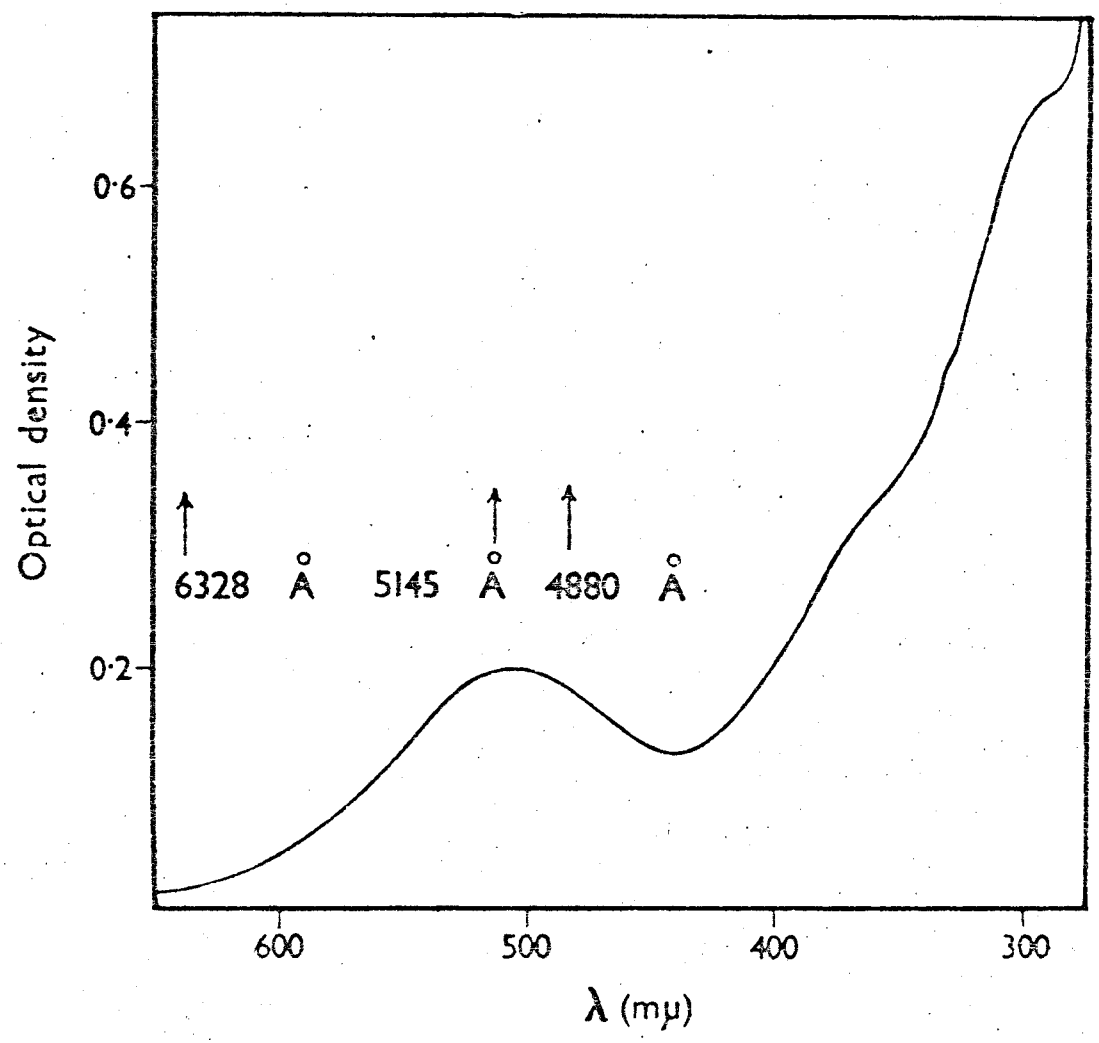

Figure 8. UV and visible spectrum of 0.069 m $BrSO_3F$ in 0.176 m super acid. Path length 0.144 mm.

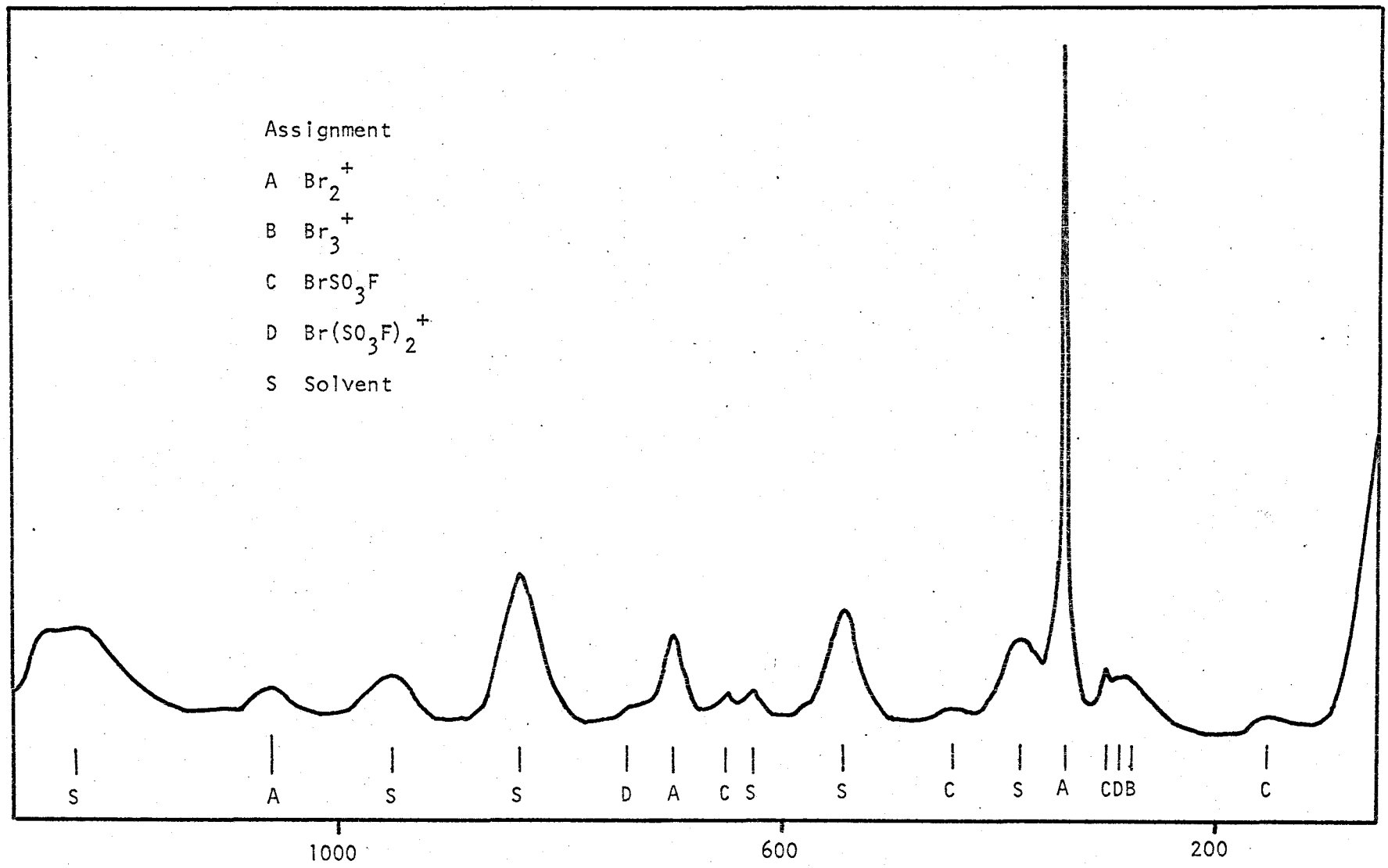

Figure 9. Raman spectrum of 0.399 m $BrSO_3F$ in 0.176 m super acid.

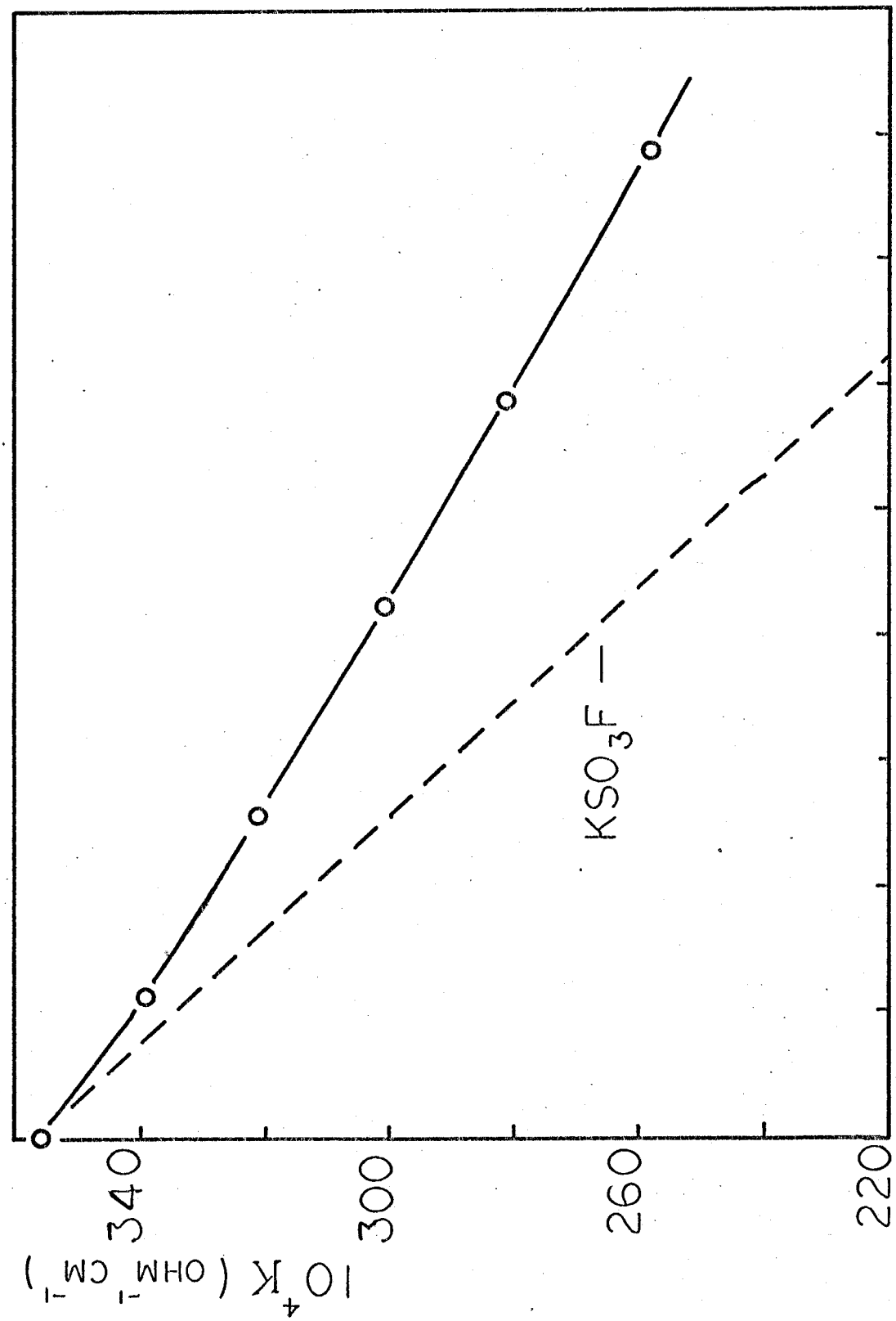

Figure 10. Conductivities at 25°C: 2.31:1 $Br_2/S_2O_6F_2$ solutions in 0.176 m super acid.

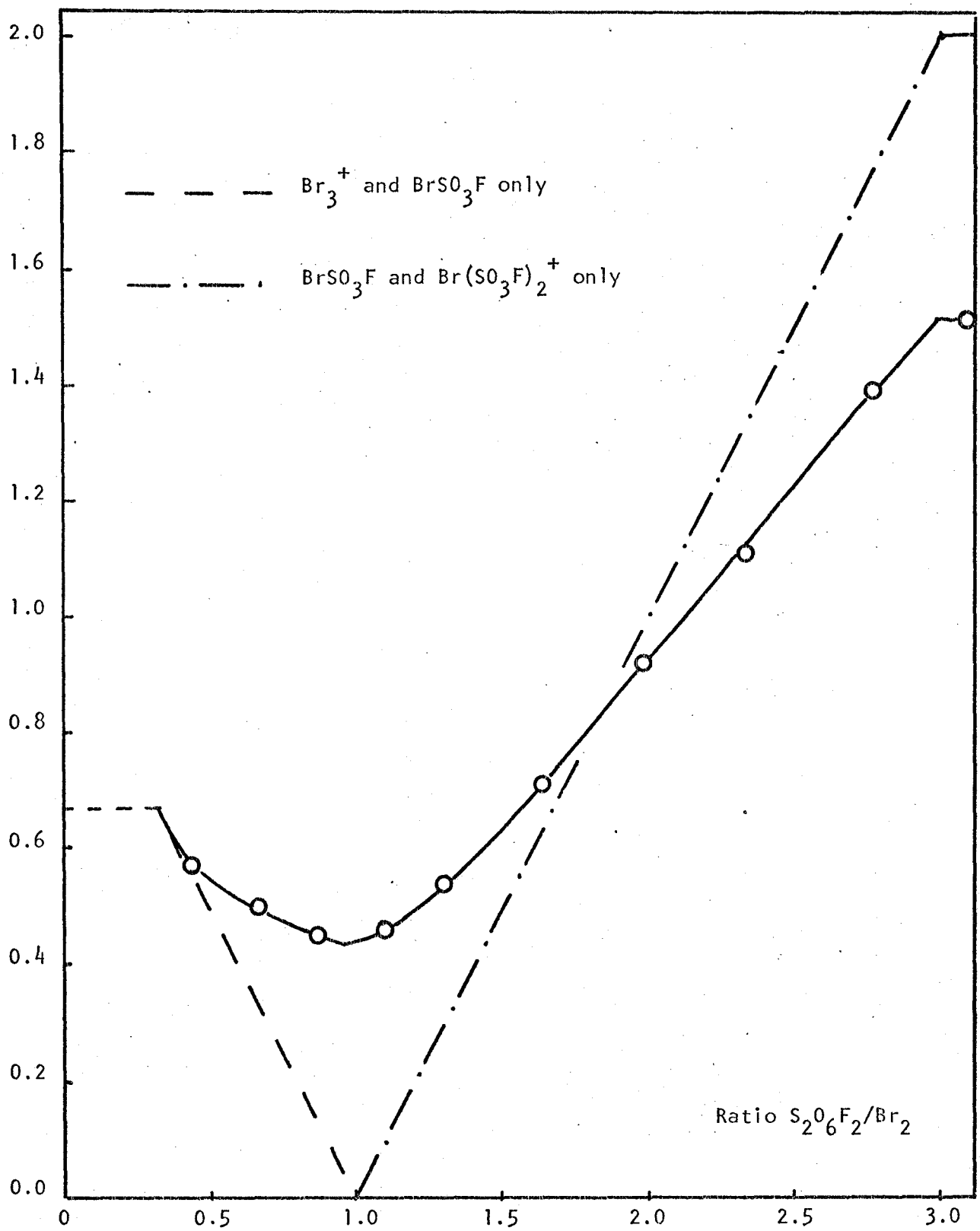

Figure 11. Conductivities at 25°C. Oxidation of bromine with $S_2O_6F_2$ in 0.176 m super acid.

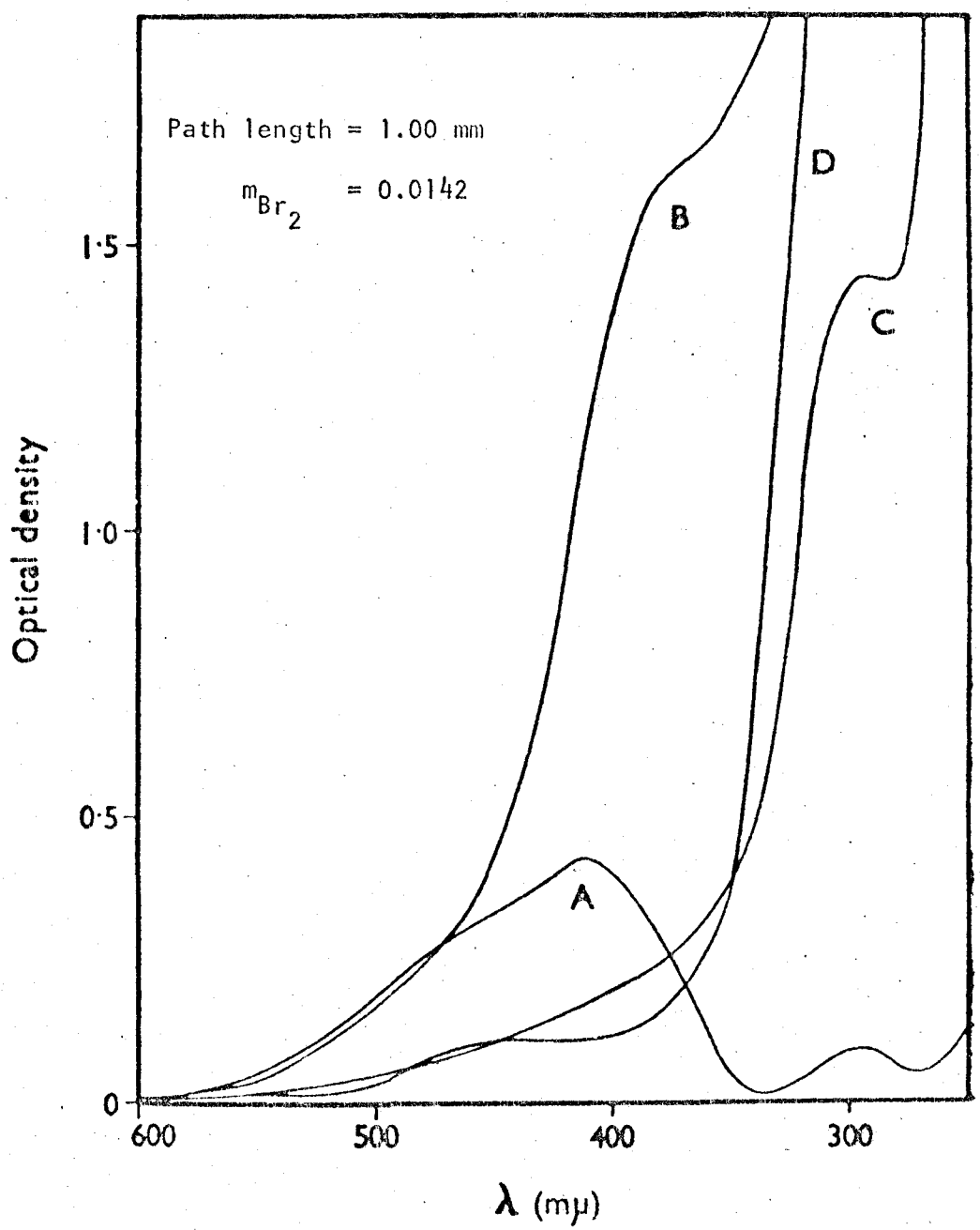

Figure 12. UV and visible spectra in HSO_3F. Ratio $Br_2/S_2O_6F_2$: A, 1:0; B, 1:0.33; C, 1:1; D, 1:3 and 1:5.

CHAPTER V

Chlorine and Fluoro-chlorine Cations.

1. The Vibrational Spectrum of the ClF_2^+ cation.

In a recent paper (63) Christe and Sawodny have reported the infrared spectra of $ClF_2^+AsF_6^-$ and $ClF_2^+BF_4^-$ and the Raman spectrum of $ClF_2^+AsF_6^-$ and have given a reinterpretation of earlier infrared data on these compounds (64). The Raman spectra of $ClF_2^+SbF_6^-$, $ClF_2^+AsF_6^-$ and $ClF_2^+BF_4^-$ were investigated here, and on the basis of these results a reassignment of one of the fundamental frequencies of the ClF_2^+ and new values for the force constants are proposed.

The compounds were prepared by literature methods (64), by reaction of chlorine trifluoride with the Lewis acids in 4 mm thin wall Kel-F tubes, which were attached to the monel vacuum line. The excess ClF_3 was pumped off at 25°C for the SbF_6^- and AsF_6^- salts, and at -76°C for the BF_4^- salt, and the Kel-F tube was subsequently heat sealed under vacuum, and used for Raman studies as described in Chapter II.

The Raman spectra of the three compounds are shown in Figure 13 and the frequencies of the bands are listed in Tables XV - XVII together with the assignments. These assignments can be made very reasonably on the basis of ionic structures, Ie $ClF_2^+MF_6^-(MF_4^-)$ for these compounds

using previously published assignments for SbF_6^-, AsF_6^- and BF_4^- (65,68). The assignment made here for ClF_2^+ differs from that of Christe and Sawodny in that ν_2 is assigned at 384 cm^{-1} rather than 544 cm^{-1}. Bands are observed in the 520-540 cm^{-1} region for each of the compounds but in each case they are best assigned to the anion, and it is only a coincidence that all three compounds have a band in this region. A band is observed in all three compounds close to 380 cm^{-1} (actually split into a doublet at 373 and 396 cm^{-1} in ClF_2BF_4) which cannot reasonably be attributed to the anion in any of these compounds and which is therefore assigned as ν_2 of ClF_2^+. Further evidence against the former assignment for ν_2 is provided by the fact that on dissolving the compound $ClF_2^+SbF_6^-$ in excess SbF_5 the doublet at 532-543 cm^{-1} disappears and is replaced by bands at 578 and 710 cm^{-1} as a consequence of the conversion of SbF_6^- to $Sb_2F_{11}^-$ or some higher polymers of the form $Sb_nF_{5n+1}^-$ (45), while the bands attributed to ClF_2^+ remain unchanged. Finally we note that ClO_2^- which is isoelectronic with ClF_2^+ has frequencies of 786, 402 and 804 cm^{-1} for ν_1,ν_2, ν_3 respectively (68) which are very close to the frequencies of 808,384 and 821 cm^{-1} that are proposed here for the ClF_2^+ cation in $ClF_2^+AsF_6^-$. The slight increase in the stretching frequencies from ClO_2^- to ClF_2^+ indicates that the Cl-F bond strength in ClF_2^+ is greater than the Cl-O bond strength in ClO_2^-. This presumably results from the greater electronegativity of fluorine than oxygen and the increase in the electronegativity of chlorine resulting from its formal positive charge in ClF_2^+.

The splitting of the ν_2 (Eg) band of AsF_6^- and SbF_6^- and the observation of this band in the infrared of $C\ell F_2AsF_6$ as well as in the Raman spectrum indicates that the MF_6^- ion is distorted from its ideal octahedral symmetry. A similar splitting of bands and departures from the mutual-exclusion rule for molecules with a centre of symmetry has been noticed in a number of other compounds of octahedral anions such as SbF_6^- and AsF_6^- with fluorocations such as SF_3^+ and SeF_3^+ and in these cases this has been attributed to fluorine bridging between the anion and cation which reduces the octahedral symmetry of the anion (66,67), and it seems reasonable to conclude that there is also fluorine bridging in $C\ell F_2$ AsF_6. Christe and Sawodny (63) noted the occurence in the infrared spectrum of $C\ell F_2BF_4$ of a relatively strong band at 766 cm^{-1} which they attributed to the forbidden ν_1 mode. They attributed this to the BF_4^- anion having a site symmetry in the crystal lower than T_d and this lowering of the site symmetry may be reasonably attributed to fluorine bridging between BF_4^- and $C\ell F_2^+$. The small splitting of ν_1 of $C\ell F_2^+$ in $C\ell F_2SbF_6$ and $C\ell F_2AsF_6$ may be due to $C\ell^{35}$, $C\ell^{37}$ isotopic splitting, but the peak could not be satisfactorally analysed into two simple peaks of relative areas 3:1 with a Dupont curve analyser and Lorentzian line shapes. This is probably due to further crystal (ie factor-group) splitting. On dissolving the $C\ell F_2SbF_6$ compound in excess SbF_5 the bands become broad, and hence the splittings disappear. Also ν_1 and ν_3 of $C\ell F_2^+$ then appear as one broad band centred at 820 cm^{-1}.

In view of the very small difference between the symmetric and antisymmetric stretching frequencies for $C\ell F_2^+$ the molecule must be bent,

as Christe and Sawodny concluded. Using a simple valence force field, two frequencies and the bond angle are required to calculate the stretching force constant f and the bending force constant d (68). The results of such calculations are shown in Table XVIII. The frequencies ν_2 and ν_3 and assumed values of the bond angle were used to calculate values for the force constants f and d, and then these values were used to calculate ν_1. These calculated frequencies are seen to be in good agreement with the observed values for all three compounds for the values of the bond angle in the range 95 - 100°. In view of the lack of structural data for ClF_2^+, the more elaborate treatment of the spectroscopic data given by Christe and Sawodny in which they also calculate interaction constants between the bonds and between the bonds and the angle is not considered to be justified. For the angles that give the best value of the calculated frequency ν_1; the values of the stretching force constants are $ClF_2^+SbF_6^-$, 4.8 m dyne A^{-1}; $ClF_2^+AsF_6^-$, 4.7 m dyne A^{-1}; $ClF_2^+BF_4^-$, 4.6 m dyne A^{-1}. The bending force constants also show a slight decrease from 0.63 to 0.62 to 0.61 m dyne A^{-1} in the same series. Although the absolute magnitude of the force constants may be in error as much as 10% due to the crudity of the simple valence force field calculations, it is not unreasonable to assume that the small changes in the force constants reflect a slight decrease in the Cl-F bond strength in the series $ClF_2^+SbF_6^-$, $ClF_2^+AsF_6^-$ and $ClF_2^+BF_4^-$ which may be a consequence of an increased extent of interaction between anion and cation by fluorine bridging.

For comparison it may be noted that the stretching force constant of the FCℓ molecule is 4.34 m dyne A^{-1} and for the isoelectronic $C\ell O_2^-$ molecule the values of the force constants are f = 4.26 and d = 0.52 m dyne A^{-1}. (68). Christe and Sawodny obtained force constant values of f = 4.71 and d = 1.24 for a bond angle in the range 95° - 100° apparently using the frequencies they observed for $C\ell F_2^+$ AsF_6^-. Naturally the stretching force constant agrees well with the value found here but their bending force constant is twice as large, which is a consequence of the much higher frequency they assigned to the bending mode. We may note that their bending force constant is out of line with that of $C\ell O_2^-$. We may note also that the force constants for PF_3 which might be expected to be fairly close to those of $C\ell F_2^+$ have been found to be f = 5.21 and d = 0.62 m dyne A^{-1} (68).

The most reasonable structure for these $C\ell F_2^+$ compounds would appear to be one that is closely similar to that of $BrF_2^+SbF_6^-$ in which bromine achieves a distorted square planar coordination with an FBrF bond angle of 95° by forming fluorine bridges to the SbF_6^- ion (33). As has been mentioned above there is some evidence from the vibrational spectra of this and related compounds that the symmetry of the octahedral anion is reduced and this can be reasonably accounted for in terms of fluorine bridging. The proposed structure for $C\ell F_2SbF_6$ is shown diagramatically below.

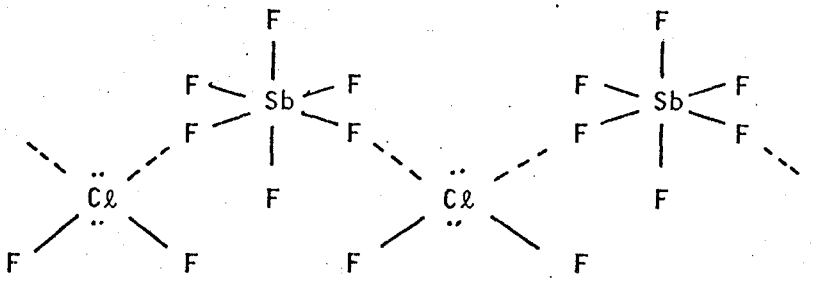

The free $C\ell F_2^+$ ion has a chlorine valency shell of eight electrons which would be expected to give an angular molecule with a bond angle of somewhat less than the tetrahedral angle. In the fluorine-bridged structure the chlorine would have a valency shell of six electron pairs and if the fluorine bridging was very strong the six electron pairs would have an approximately octahedral arrangement leading to a bond angle of approximately 90^o. However as the fluorine bridge bonds are presumably appreciably weaker than the non-bridging Cℓ-F bonds an FCℓF bond angle of rather greater than 90^o is expected. Thus the angle of 95^o-100^o obtained by the simple valence force field calculation is reasonable although it must be remembered that it could be considerably in error due to the assumptions made in such calculations. Preliminary data from the University of British Columbia (73) on the crystal structure of $C\ell F_2IrF_6$ indicate that the bond angle in $C\ell F_2^+$ is approximately 130^o, with shorter chlorine-fluorine bonds than in $C\ell F_3$, and with four other fluorine atoms at a greater distance making a highly distorted octahedral coordination around the central chlorine. This would be consistent with a degree of double bond character between chlorine and the two fluorine

atoms in ClF_2^+ in this salt, which would tend to open out the bond angle to the tetrahedral angle according to Valence Shell Electron Pair Repulsion Theory (69). The enhanced Cl-F force constants calculated for the salts studied here could be interpreted in terms of such double bond character. Single crystals of ClF_2AsF_6 have been prepared and the result of the crystal structure determination which has been undertaken by Dr. C. Davies in this laboratory will be of great interest.

2. The Cl_2F^+ cation.

In 1963 Schmeisser reported that ClF formed 1:1 adducts with Lewis acids such as AsF_5 and BF_3 which were formulated as salts of the Cl^+ cation (74). In a recent paper (39) Christe and Sawodny failed to confirm the existence of 1:1 adducts, but showed that ClF forms 2:1 adducts with AsF_5 and BF_3. Low temperature infrared spectra showed that these are salts of AsF_6^- and BF_4^-. Three frequencies common to both compounds, of 586, 529 and 293 cm^{-1} were assigned to the cation and it was concluded that the cation probably had the symmetrical $ClFCl^+$ structure as no frequency around 800 cm^{-1} expected for a -Cl-F bond was observed. Christe and Sawodny carried out detailed force constant calculations based on the three observed frequencies in which four force constants were calculated for assumed angles. They pointed out that the symmetrical FCl_2^+ cation, which they claim to have identified is unusual as it is the first known interhalogen compound in which the most electronegative atom is the central atom. The improbable structure of this cation, and the unconvincing rationalisations given (39) prompted a reinvestigation of the vibrational spectra and assignments.

The compounds AsF_5 2ClF and BF_3 2ClF were prepared exactly as described by Christe and Sawodny, and low temperature Raman spectra were run on the solids sealed under vacuum in 4 mm Kel-F tubing using 6328 A He/Ne laser excitation. The bands observed in the Raman spectra of $Cl_2F^+AsF_6^-$ and $Cl_2F^+BF_4^-$ are given in Tables XIX and XX, together with their assignments. These differ from those of Christe and Sawodny as a strong Raman band at 744 cm^{-1} was observed in both salts (Figure 14), which was not seen in the infrared. This is assigned to the Cl-F stretch in the unsymmetrical $ClClF^+$ cation. The intense Raman peaks at 516 and 540 cm^{-1} in the BF_4^- salt, and 528 and 535 cm^{-1} in the AsF_6^- salt can be assigned to the Cl-Cl stretch.

In the AsF_6^- salt, Christe and Sawodny assign the infrared bands at 586 and 593 cm^{-1} to ν_3 of FCl_2^+, whereas here they are assigned together with the corresponding Raman bands at 563 and 581 cm^{-1} to ν_2 of AsF_6^-, which is split and appears strongly in the infrared due to the removal of the degeneracy in the solid state probably as a consequence of fluorine bridging between the anion and cation. In the previous section on the vibrational spectrum of $ClF_2^+AsF_6^-$ it was shown that the Raman frequency of 544 cm^{-1} (IR 520 and 558 cm^{-1}) had been assigned incorrectly to the bending mode of the cation. In this case the Raman bands at 544 and 602 cm^{-1} were assigned to ν_2 of AsF_6^-, and the large splitting and the appearance of the bands in the infrared was attributed to removal of the degeneracy which was attributed to strong fluorine bridging. Table XXI shows how the frequency ν_1 of AsF_6^- decreases and

the splitting of ν_2 decreases in the series $Cl F_2^+ AsF_6^-$, $Cl_2F^+ AsF_6^-$ and $Cl_3^+ AsF_6^-$ (described in the next section), in which it seems reasonable to suppose that the extent of fluorine bridging decreases as the cation becomes a poorer acceptor.

In the BF_4^- salt the band at 743 cm^{-1} is again assigned to the Cl-F stretch of the cation, and the strong bands at 516 and 540 cm^{-1} to the Cl-Cl stretch, probably split by factor-group splitting. The additional weak Raman band at 874 cm^{-1} and the weak infrared band at 572 cm^{-1} may be due to the $B_2F_7^-$ anion which is stable at low temperatures (70). The infrared bands at 588 and 594 cm^{-1} assigned to ν_3 of FCl_2^+ by Christe and Sawodny are assigned here to the overtone of the 296 cm^{-1} bending frequency of Cl_2F^+.

Christe and Sawodny pointed out that the FCl_2^+ cation is isoelectronic with OCl_2. However the differences between the frequencies for this molecule (ν_3 686, ν_1 640, ν_2 300 cm^{-1}) and those of 586, 524, 293 cm^{-1} that they attribute to the FCl_2^+ cation are considerably greater than is usual for simple isoelectronic molecules. The Cl_2F^+ molecule is isoelectronic with the molecule ClClO, which Rochkind and Pimental (71) have shown to have stretching frequencies of 960 and 375 cm^{-1}. These authors estimated the frequency of the ClO molecule to be 970 ± 20 cm^{-1}, and concluded that the ClClO molecule was bent with a very weak Cl-Cl bond and a Cl-O stretching frequency little shifted from that of the diatomic molecule.

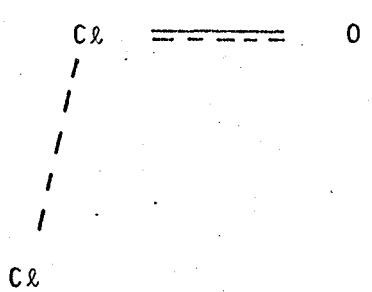

In the isoelectronic $Cl ClF^+$ cation the charge distribution may be expected to be markedly different with the positive charge spread over the chlorine atoms resulting in a stronger chlorine-chlorine bond and less double-bond character in the Cl-F bond than in the Cl-O bond. The observed frequencies are in agreement with this prediction, as the Cl-F frequency of 744 cm^{-1} is not very different from that in ClF (785 cm^{-1}) (16) , and the Cl-Cl frequency of 530 cm^{-1} lies between that of chlorine (558 cm^{-1}) (72) and that of ν_1 in Cl_3^+ (489 cm^{-1}, see later).

In view of the complete lack of structural information on Cl_2F^+ it did not seem worthwhile to attempt any force constant calculations on the basis of the observed frequencies for the molecule, as even in a simple valence force field treatment there are five undetermined parameters - three force constants, the bond angle and the bond length ratio - and only three observed frequencies.

In justification of their symmetrical structure $ClFCl^+$ for the ion, Christe and Sawodny state that as F-Cl is polar with the negative charge concentrated on the fluorine this would be expected to attract any positive ion, in this particular case the Cl^+ cation to give the symmetrical $ClFCl^+$ cation. However it does not follow that because F carries a negative charge in FCl while Cl has a positive charge that F will necessarily be a better electron donor then Cl. The positive charge on Cl is almost certainly counterbalanced by the fact that this charge can be dispersed and stabilised by the formation of multiple bonds with the ligands. This type of charge dispersal by multiple bond formation is

not possible for F^+ which is restricted by the rigid adherence of fluorine to the octet rule. Thus the bonding in $ClClF^+$ can be reasonably well described in terms of the following resonance structures:

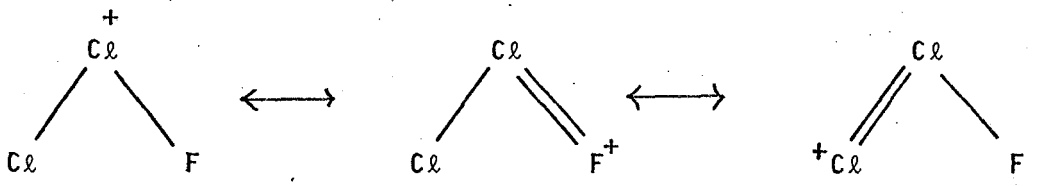

The fact that the Cl-F stretch at 744 cm^{-1} was not observed in the infrared in these salts would be accounted for by the very small dipole moment expected in the bond between the positive chlorine and the fluorine, eg Cl^+-F, resulting in only a very weak infrared absorption.

Attempts to obtain the Raman spectrum of ClF_2^+ in solution were unsuccessful as it appears that it is disproportionated even at low temperatures according to the equation

32. $2\ ClClF^+ \longrightarrow ClF_2^+ + Cl_3^+$

Thus, in a solution of ClF in excess SbF_5 and HF at -76° in addition to the rather complicated spectrum attributable to SbF_5 and $SbF_6(SbF_5)_n^-$ the only other band observed was a rather strong broad peak at 500 cm^{-1} which was assigned to ν_1 of Cl_3^+. No lines that could be attributed to $ClClF^+$ were observed. Unfortunately the spectrum of ClF_2^+ was obscured by the solvent spectrum.

3. The Cl_3^+ cation.

As it seems reasonable to regard the ClF_2^+ cation as being derived from the coordination of a ClF molecule to Cl^+, an attempt to prepare

the Cl_3^+ cation was made by displacing the ClF with chlorine. Chlorine was condensed at -76°C onto a sample of the insoluble $Cl_2F^+AsF_6^-$ salt suspended in liquid AsF_5. On pumping off all volatiles at dry ice temperature a yellow solid remained. A Raman spectrum showed that bands due to $Cl_2F^+AsF_6^-$ were still present, but in addition strong bands at 490, 225 and 508 cm^{-1} were observed, which, by comparison with the isoelectronic SCl_2 molecule (514, 208, 535 cm^{-1}) (68) seemed reasonable for the Cl_3^+ cation. Also two distinct peaks were observed in the region for ν_1 of AsF_6^-, the 685 cm^{-1} peak of $Cl_2F^+AsF_6^-$ and the peak at 674 cm^{-1} which was assigned to the anion in $Cl_3^+AsF_6^-$.

In a second experiment excess chlorine was condensed onto the Cl_2FAsF_6 salt in a Kel-F trap at -76°C, and the contents were allowed to vaporise completely on warming to just below room temperature. The contents were then cooled to dry-ice temperature and all volatiles were pumped off leaving a yellow solid. The infrared spectrum of the compound allowed to vaporise into a ten cm monel infrared gas-cell, fitted with silver chloride windows and teflon gaskets, showed only the peaks due to AsF_5, but at one third of the intensity of pure AsF_5 at the same pressure (1 cm Hg). This result was consistent with the yellow solid being $Cl_3^+AsF_6^-$ which would dissociate to a 1:1:1 mixture of AsF_5, Cl_2 and ClF; chlorine is not infrared active and the weak infrared peaks of ClF were obscured by the intense absorptions of AsF_5. The low temperature Raman spectrum of this solid, (sublimed into a Kel-F tube), shown in Figure 14 shows that in this case complete conversion to $Cl_3^+AsF_6^-$ had taken place. The Raman spectrum of this compound is given in Table XXII.

A very satisfactory assignment of the observed frequencies can be made on the basis that the compound is $Cl_3^+AsF_6^-$. The spectrum shows the Raman active frequencies of the AsF_6^- ion together with three relatively intense bands at 490 (split to 485 and 493), 225 and 508 cm^{-1}. These are assigned to ν_1, ν_2 and ν_3 respectively of the Cl_3^+ cation. No bands were observed above the band at 674 cm^{-1} (ν_1 AsF_6^-) indicating the absence of any Cl-F stretching modes. It has already been noted above that these are very close to the vibrational frequencies of the SCl_2 molecule (514, 208 and 535 cm^{-1}); this has a bond angle of 103°, and it therefore concluded that the Cl_3^+ cation has a similar structure. Using a simple valence force field two frequencies and the bond angle are required to calculate the stretching force constant f and the bending force constant d. These values can then be used to calculate ν_1. The results of these calculations are given in Table XXIII and give good agreement for a bond angle of 100° with force constants f = 0.25 m dyne A^{-1} and d = 0.36 m dyne A^{-1}. In view of the qualitative nature of such calculations, and the fact that the observed frequencies are for the solid state a more elaborate treatment is not considered to be justified.

The stretching force constant of 2.5 m dyne A^{-1} is less than that of chlorine (68). This is in contrast to the situation in ClF_2^+ (see above) for which the stretching force constant is larger than in ClF_3. This probably indicates considerable double bond character between the central chlorine and fluorine in ClF_2^+ which is not present in Cl_3^+. Similarly the broad Raman peak observed for Br_3^+ in solution at 290 cm^{-1} (Chapter IV) compared to 315 cm^{-1} for bromine indicates that the stretching

force constant in Br_3^+ is less than in bromine.

The Cl_3^+ cation has not been previously reported, although the I_3^+ is well established (23), and there has been speculation on the existence of the Br_3^+ cation previous to this work (see Chapter I). Attempts to prepare the salt $Cl_3^+BF_4^-$ by similar methods to those used for $Cl_3^+AsF_6^-$ were unsuccessful. The Raman spectra of mixtures of BF_3, ClF and Cl_2 condensed and run at -130°C showed only peaks due to the components and $Cl_2F^+BF_4^-$, even when a large excess of chlorine was used, and it is therefore concluded that $Cl_3^+BF_4^-$ is not formed under these conditions and that its stability is less that that of $Cl_2F^+BF_4^-$. The Raman spectrum of Cl_3^+ was obtained from mixtures of ClF, SbF_5 and HF at -76°C (section 2 above). However on warming to room temperature and pumping off the volatile materials the Cl_3^+ decomposed to give off chlorine. In the next section some evidence is presented for the existence of very low concentrations of the Cl_3^+ cation in the SbF_3:$3SO_3$/HSO_3F super acid system at 25°C in equilibrium with chlorine and chlorine monofluorosulphate.

As it was possible to prepare the Cl_3^+ cation by condensing ClF with Cl_2 and AsF_5 or by displacing the ClF in Cl_2F^+ by chlorine, it is predicted that it will be possible to prepare cations such as $ClBrF^+$ and $ClBrBr^+$ by displacing the ClF with BrF or Br_2. Low temperature production of molecules such as IF or BrF by fluorination in CCl_3F, followed by reaction with AsF_5 and halogens or interhalogens would be expected to produce salts of cations based on I^+ and Br^+ such as I_2F^+, IBr_2^+, $BrICl^+$, Br_2F^+, etc which could be studied in the solid state at low temperatures to prevent disproportionation. We may note

that there are a total of nineteen different halogen and interhalogen tri-atomic cations possible, (excluding F_3^+) in which the central halogen is the most electropositive, and that prior to this work the only vibrational assignments published have been for the ClF_2^+ cation in which one frequency was incorrectly assigned. The variation in force constants and structure in this series would be of great interest.

4. Chlorine Cations in the Super Acid System $SbF_5:3SO_3/HSO_3F$.

Although chlorine monofluoride is a gas at room temperature, it reacted with the super acid to give a very pale yellow solution which had a negligible vapour pressure at room temperature. As the super acid contains sulphur trioxide, the most probable explanation is that chlorine monofluorosulphate is formed according to the equation

33. $$ClF + SO_3 \longrightarrow ClSO_3F.$$

Chlorine monofluorosulphate has been prepared previously (74) by reaction of chlorine with $S_2O_6F_2$ at an elevated temperature and pressure, and is a yellow liquid with a boiling point which was estimated to be 45^oC.

The Raman spectrum of the solution obtained by reaction of ClF with the super acid is shown in Figure 15, and the seven new bands observed are listed in Table XXIV, together with the stronger Raman bands of $BrSO_3F$ (Table VIII Page 58) and the infrared bands of FSO_3F (82). By comparison with the vibrational frequencies of the Cl-O bond in $ClONO_2$, Cl_2O and HOCl also listed in Table XXIV, the strongest Raman peak 707 cm^{-1} can be assigned to the Cl-O stretching frequency in chlorine monofluorosulphate. By further comparison with the Raman spectrum of

$S_2O_5F_2$ (76), the 214 cm^{-1} band can be assigned very reasonably to the ClOS bend, and the 368 cm^{-1} band to the ClO-S stretch of $ClSO_3F$. The weak band at 1055 cm^{-1} cannot be assigned by simply considering separate stretching vibrations of any two atoms, but we may note that a similar band was observed in the infrared of FSO_3F. Other weak bands expected in the Raman spectrum of $ClSO_3F$, such as an SF stretch at around 870 cm^{-1} (76) are almost certainly masked by the solvent bands. The absence of distinct Raman peaks at 500 cm^{-1} or 225 cm^{-1} showed that the solution contained negligible concentrations of the Cl_3^+ cation, and hence that chlorine monofluorosulphate is stable to disproportionation in the super acid. An attempt was made to produce a solution of the Cl_3^+ cation in the super acid at room temperature by saturating the $ClSO_3F$ solution with a high pressure of chlorine, in the expectation that the following equilibrium would be displaced to the right hand side:

34. $ClSO_3F + Cl_2 + H_2SO_3F^+ \rightleftharpoons Cl_3^+ + 2HSO_3F.$

This experiment was performed by distilling chlorine into a solution of ClF in the super acid contained in quartz tube which was drawn out at one end to an internal diameter of 1 mm to facilitate Raman studies, and was closed at the other with a teflon-glass angle valve attached by a graded seal. Although the pressure of chlorine above the solution was increased to three atmospheres, no changes in the intensity of the $ClSO_3F$ peaks compared to those of the solvent were observed, and the only difference was a 50% increase in the relative intensity at 560 cm^{-1} which is due mainly to the solvent but also contains a contribution from

the Cℓ-Cℓ stretch of dissolved chlorine at 555 cm^{-1} (Figure 15). Therefore it is concluded that negligible concentrations of the $Cℓ_3^+$ cation, (estimated to be less than 10^{-2} molal) are produced under these conditions in the super acid, and hence, by analogy with the bromine cations it is not expected that the $Cℓ_2^+$ cation will be formed in this acid. In the bromine case it was shown that whereas the Br_3^+ cation was completely stable in the super acid, the Br_2^+ cation substantially disproportionated to $BrSO_3F$ and Br_3^+ so that under the most favourable conditions some 25% of the bromine in solution was present as the Br_2^+ cation. In fluorosulphuric acid, on the other hand, in which dilute solutions of the Br_3^+ cation were 50% dissociated to $BrSO_3F$ and Br_2, no evidence for the formation of the Br_2^+ cation was obtained, even though concentrations down to 10^{-4} molal would have been detectable by a resonance Raman spectrum.

The results of a conductivity study in which solutions of CℓF, and CℓF saturated with chlorine in the super acid were added to the super acid are listed in Table XXV and shown in Figure 16. In experiment A, additions of the concentrated CℓF solution gave an apparent γ value of 0.14, while addition of the concentrated solution containing CℓF and chlorine, in experiment B gave an apparent γ value of 0.16. These γ values should be corrected for the consumption of SO_3 by CℓF according to equation 33 which would decrease the acidity, and hence the conductivity of the super acid. Thus at a concentration of 0.10 molal CℓF the SbF_5:SO_3 ratio has been decreased from 1:2.9 to 1:2.4. Gillespie et al. have carried out conductivity studies in which the SbF_5:SO_3 ratio was varied in the range 1:2 to 1:3 at various SbF_5 concentrations (48); these results show that the conductivity of SbF_5:SO_3 solutions at this concentration

decreases by 10% when the SO_3 ratio is decreased from 2.9 to 2.4, which fully accounts for the decreased conductivity in experiment A in which the corrected γ value now becomes zero. The corrected γ value of 0.02 in experiment B is hardly significantly different from zero, but may indicate a very low concentration (2×10^{-3} molal at a 0.1 molal $Cl SO_3F$ concentration) of the Cl_3^+ cation. These results are in agreement with the conclusion from the Raman spectra, and illustrate the increased stability of the halogen monofluorosulphates on ascending Group VII. Thus whereas $Cl SO_3F$ is completely stable to disproportionation in the super acid, $BrSO_3F$ disproportionates somewhat to form bromine cations but is stable in fluorosulphuric acid: there is no evidence for ISO_3F in fluorosulphuric acid as this would be completely disproportionated (23) to I_3^+ and $I(SO_3F)_3$. The solid of composition ISO_3F which has been prepared from iodine and $S_2O_6F_2$ (75) is probably best formulated as $I_3^+ I(SO_3F)_4^-$.

5. The Evidence for the 'Cl_2^+' and 'ClF^+' cations. ESR spectra from strong acid solutions.

Raman studies of the products of the reactions between ClF, Cl_2 and SbF_5 or AsF_5 resulted in the identification of the Cl_2F^+ and Cl_3^+ cations. No evidence was found for the existence of the Cl_2^+ cation which would be expected to give a strong Raman band close to the observed gas phase frequency of 640 cm^{-1} (77). In view of these results, the compound produced by reaction of chlorine and iridium hexafluoride, which according to a private communication dated 1967 cited in reference (26) has been formulated by Bartlett as $Cl_2^+IrF_6^-$, is probably a salt of Cl_2F^+ such as $Cl_2F^+IrF_6^-$.

We may note that the structure of the first xenon compound, originally formulated as $Xe^{+}PtF_6^{-}$ (78) has also not been confirmed, but is probably a salt of the XeF^{+} cation as in the compound $XeF_2 2SbF_5$ which has the structure $XeF^{+}Sb_2F_{11}^{-}$ (79). Consideration of the thermodynamics of the formation of $Cl_2^{+}IrF_6^{-}$ also makes this structure highly unlikely, as the heat of formation comes out to be less favourable than that of the non-existent $O_2^{+}IrF_6^{-}$ salt (80). Thus although the ionisation potential of chlorine (62) is less than that of oxygen by 17 kcal, the lattice energy of $Cl_2^{+}IrF_6^{-}$ estimated from Kapustinskii's second equation (81), of 107 kcal is less than that expected for the O^{+}_2 salt (80) by 20 kcal, giving an overall heat of formation some 3kcal less favourable than that of $O_2^{+}IrF_6^{-}$, which has not been prepared. Use of PtF_6, however, with which the O_2^{+} salt has been prepared, would be expected to fluorinate the chlorine even more readily, as PtF_6 is an endothermic compound, and the resultant ClF has a bond energy D^{o} of 60kcal (16) compared to 57 kcal for chlorine. Hence the heat of reaction ΔH in a reaction such as

$$35.\quad Cl_2 + 2PtF_6 \longrightarrow 2ClF + 2PtF_5$$

would be at least -63 kcal, which is certainly more exothermic than the heat of formation of $Cl_2^{+}PtF_6^{-}$. Nor would one expect any kinetic barrier in the fluorination of chlorine via an intermediate such as Cl_2^{+} as this would certainly be strongly fluorine bridged to the anion.

The conclusion reached here that the Cl_2^{+} cation is most unlikely to be stable even in trace quantities in strong acid systems disagrees with the results of Olah and Comisarow (31,32) who claim to have identified the Cl_2^{+} and ClF^{+} cations by their ESR spectra. These authors obtained

two distinct ESR spectra from solutions of chlorine fluorides in SbF_5, HSO_3F/SbF_5 or HF/SbF_5. The first, obtained by dissolving ClF in these solvents, consisted of a seven line spectrum, g_{av}=1.998 which they attributed to the Cl_2^+ cation with hyperfine coupling constants to the chlorine atoms (spin 3/2) of 2.59 gauss for ^{35}Cl and 2.15 gauss for ^{37}Cl. With ClF_3 however, this spectrum was in equilibrium with a second more complex spectrum, g_{av}=2.006, which they attributed to the ClF^+ cation with isotropic hyperfine coupling constants of 14.75 gauss to ^{35}Cl, 12.25 gauss to ^{37}Cl and 24.0 gauss to fluorine. On warming, the relative intensity of the second spectrum increased, but it could be obtained in the absence of the first only by using ClF_5 instead of lower chlorine fluorides. Olah and Comisarow do not explain why it is necessary to use pentavalent ClF_5 to obtain the formally divalent chlorine cation in the absence of the half-valent Cl_2^+ cation. They attempt to explain the complete quenching of the spin-orbit coupling in these cations required for the observation of such well resolved spectra close to the free-spin g value by postulating very strong interaction with the solvent. Recently Symons et al. have criticised their conclusions (84) and have shown that such solvation is improbable. Instead these authors conclude that the spectrum previously attributed to the ClF^+ cation is due to the $ClOF^+$ cation, as the spin densities on chlorine and fluorine only add up to 0.62, and the ESR parameters fit in well with those of the isostructural FOO, ClOO, ClO_2 and NF_2 radicals. By analogy they suggest that the spectrum previously attributed to Cl_2^+ is due to the Cl_2O^+ cation. Although Symons et al. convincingly rule out the assignment of these ESR

spectra to the Cl_2^+ and ClF^+ cations by these and other arguments, they do not provide any further experimental evidence, such as O^{17} splitting, for these oxy-radicals, which appear to be equally improbable chemically. Moreover, they do not attempt to explain the origin of the oxygen in these radicals which can be generated by reaction of ClF_3 with SbF_5 and HF under high vacuum conditions.

Figure 17 shows the ESR spectrum of a solution of the ClF_2^+ SbF_6^- salt dissolved in SbF_5 and contained in a 4mm Kel-F tube which was sealed on the monel vacuum line. The seven line spectrum is identical to that reported by Olah and Comisarow and assigned by them to Cl_2^+, while the broader spectrum surrounding it, although unresolved due to the viscosity of the medium, appears to be due to the same species previously identified as the ClF^+ cation. After several weeks the contents of this tube turned black and it was observed that the Kel-F tube had been attacked. Samples of the dry crystalline $ClF_2^+SbF_6^-$ salt prepared by reaction of ClF_3 and SbF_5 in Kel-F on the monel vacuum line (section 1) gave no ESR spectrum. However in one experiment an attempt was made to reduce the ClF_2^+ cation by reaction of the compound dissolved in excess HF with excess chlorine; on distilling the chlorine into the solution at -76°C, a bright-green colour was observed, which disappeared when the chlorine and HF were pumped off at room temperature to leave white crystals; these gave an identical Raman spectrum as the original $ClF_2^+SbF_6^-$ salt. These crystals, which were transferred in a nitrogen atmosphere dry box to a 1 mm id quartz tube, gave the ESR spectrum shown in Figure 18, consisting of six equally spaced lines, 11 gauss apart, with perhaps two more very weak lines on each side. The

preparative conditions and the observation of attack by these compounds on Kel-F tubes over a period of time suggest that radicals may be derived from the Kel-F by abstraction of chlorine by the highly oxidising contents. We may note that Cohen and Peacock (85) reported a green colour on hydrolysis of the salt $XeF^{+}Sb_2F_{11}^{-}$, which was associated with an eight line ESR spectrum at 25°C, g=2.0057, or in one experiment a seven line spectrum, g=1.998; no splittings were given. They were tempted to correlate the green colour with a Xe(III) species. Mr. D. A. Humphreys in these laboratories has observed that solutions of XeF_2 in HF attacks Kel-F, and has observed that a six line spectrum similar to that in Figure 17 is given by the partially hydrolysed $XeF^{+}Sb_2F_{11}^{-}$ salt, which gives a bright green colour. Further experiments are planned in co-operation with Mr. D. Humphreys and Dr. E. Rotlevi to identify the species responsible for the ESR spectra observed from solutions of strong oxidising agents such as XeF_2 and $C\ell F_3$ in strong acid systems; these include addition of O^{17} water and C^{13} methyl iodide which would be oxidised in these systems. If carbon or oxygen are indeed involved in these radicals, it may be possible to observe additional characteristic splitting due to coupling of the unpaired electron to the nuclear spins of ^{13}C and ^{17}O. We may note that it is very difficult to exclude the use of fluoro- or chloro-fluoro-carbons in handling compounds such as the XeF^{+} and $C\ell F_2^{+}$ salts, and SbF_5 either as greases in glass apparatus or as containers when HF is also present. Table XXVI lists some coupling constants observed in fluoro-and chloro- carbon radicals produced by UV irradiation or γ-ray bombardment. These coupling constants should be of value in the identification of the radicals produced in strong acids,

although their values could be considerably modified when solvated in these systems.

It is concluded that there is no evidence that has not been refuted for the existence of the Cl_2^+ or ClF^+ cations in solution. Furthermore, for the reasons given in the discussion above, the existence of stable solutions of these cations in any of the systems described is considered most unlikely.

TABLE XV

Raman Spectrum of $C\ell F_2^+ SbF_6^-$

Relative* Intensity	Frequency Shift (cm^{-1})	Assignment
9	277	ν_5 SbF_6^-
13	291	
7	387	ν_2 $C\ell F_2^+$
25	532	
30	543	ν_2 SbF_6^-
5	596	
100	662	ν_1 SbF_6^-
91	805	ν_1 $C\ell F_2^+$
97	809	
63	830	ν_3 $C\ell F_2^+$

*Peak Height

TABLE XVI

Infrared and Raman Spectra of $C\ell F_2^+ AsF_6^-$

This Work			Christe and Sawodny		
Relative Intensity	Raman Frequency Shift $\Delta\nu$ cm^{-1}	Assignment	Raman Frequency Shift $\Delta\nu$ cm^{-1}	Infrared Frequency cm^{-1}	Assignment
14	373	ν_5 AsF_6^-	375 mw		ν_5 AsF_6^-
14	384	ν_2 $C\ell F_2^+$		406 m	ν_3 AsF_6^-
26	544	ν_2 AsF_6^-		520 w	
6	602		544 m	558 m	ν_2 $C\ell F_2^+$
77	693	ν_1 AsF_6^-	603 vw	609 w	ν_2 AsF_6^-
100	806	ν_1 $C\ell F_2^+$	693 s		ν_1 AsF_6^-
90	809			703 vs	ν_4 AsF_6^-
51	821	ν_3 $C\ell F_2^+$	811 vs	810 sh	ν_1 $C\ell F_2^+$
				818 s	ν_3 $C\ell F_2^+$

TABLE XVII

Infrared and Raman Spectra of $ClF_2^+ BF_4^-$

Raman - This Work			Infrared - Christe and Sawodny	
	-110°C			
Relative Intensity	Frequency cm^{-1}	Assignment	Frequency cm^{-1}	Assignment
15	63			
10	91			
15	124			
15	134			
3	355	ν_2 BF_4^-		
6	373	ν_2 ClF_2^+		
12	396			
			519 m *	ν_4 $^{10}BF_4^-$
4	526	ν_4 BF_4^-	529 sh *	ν_4 $^{11}BF_4^-$
54	762	ν_1 BF_4^-	537 ms *	ν_2 ClF_2^+
76	788	ν_1 ClF_2^+	766 m	ν_1 BF_4^-
100	798		798 s	ν_1 ClF_2^+
31	808	ν_3 ClF_2^+	813 sh	ν_3 ClF_2^+
4	930	ν_3 BF_4^-		
			978-1145	ν_3 BF_4^-

*Assigned here to ν_4 BF_4^-

TABLE XVIII

Force Constants for the ClF_2^+ Cation

$ClF_2^+SbF_6^-$	ν_1 = 807,	ν_2 = 387,		ν_3 = 830 cm^{-1}	
	Angle°	95	100	105	110
	10^{-5}f. dyne cm^{-1}	4.88	4.74	4.61	4.50
	10^{-5}d. dyne cm^{-1}	.630	.612	.593	.575
	Calculated ν_1 cm^{-1}	822	799	776	753
$ClF_2^+AsF_6^-$	ν_1 = 807,	ν_2 = 384,		ν_3 = 821 cm^{-1}	
	Angle°	95	100	105	
	10^{-5}f. dyne cm^{-1}	4.77	4.63	4.51	
	10^{-5}d. dyne cm^{-1}	.619	.601	.583	
	Calculated ν_1 cm^{-1}	813	790	768	
$ClF_2^+BF_4^-$	ν_1 = 793	ν_2 = 384		ν_3 = 808 cm^{-1}	
	Angle°	95	100	105	
	10^{-5}f. dyne cm^{-1}	4.63	4.49	4.37	
	10^{-5}d. dyne cm^{-1}	0.620	.602	.585	
	Calculated ν_1	802	778	756	

TABLE XIX

Infrared and Raman Spectra of Cl_2F^+ AsF_6^-

Infrared* cm^{-1}	Raman $\Delta\nu cm^{-1}$		Assignment Cl_2F^+	Assignment AsF_6^-
258 mw				
293 m	293	(20)+	ν_3 (bend)	
	299			
	375	(12)		ν_5
397 ms				ν_4
514 vw. sh				
520 vw				
527 mw	528	(100)	ν_2 (Cl-Cl stretch)	
535 m	535			
555 m				
569 vw	563	(16)		ν_2
586 mw	581	(12)		
593 m				
	685	(70)		ν_1
703 vs				ν_3
	744	(78)	ν_1 (Cl-F stretch)	

* Christe and Sawodny

\+ Figures in parentheses give the relative intensities (peak heights) of the observed Raman bands.

TABLE XX

Infrared and Raman Spectra of Cl_2F^+ BF_4^-

Infrared	Raman	Assignment	
cm^{-1}	$\Delta\nu$ cm^{-1}	Cl_2F^+	BF_4^-
	296 (35)	ν_3 (bend)	
	361 (10)		ν_2
511 w.sh			
519 m	516 (100)		
528 mw		ν_2 (Cl-Cl stretch)	ν_4
532 mw.sh	540 (90)		
572 mw			$B_2F_7^-$
588 w.sh			
594 m		$2\nu_3$	
	743 (90)	ν_1 (Cl-F stretch)	
770 mw	771 (17)		ν_1
	874 (8)		$B_2F_7^-$
950-1130 vs	990 (4)		ν_3

TABLE XXI

Variation of the Frequencies of ν_1 and ν_2 for The AsF_6^- ion with the nature of the cation

	AsF_5 (97)	$Cl F_2^+ AsF_6^-$	$Cl_2F^+ AsF_6^-$	$Cl_3^+ AsF_6^-$
ν_1	733	693	685	674
		544	563	571
ν_2		602	581	

TABLE XXII

Raman Spectrum of $C\ell_3^+ AsF_6^-$ -80^oC

Relative Intensity	Raman Shift	Assignment	
Peak Height	$\Delta\nu$ cm^{-1}	$C\ell_3^+$	AsF_6^-
20	170		
75	225	ν_2	
25	370		ν_5
6	394		
75	485	ν_1	
100	493		
60	508	ν_3	
18	571		ν_2
50	674		ν_1

TABLE XXIII

Force Constants for Cl_3^+ Cation in $Cl_3^+AsF_6^-$

$\nu_1 = 490$ $\nu_2 = 225$ $\nu_3 = 508$ cm^{-1}

Angle°	95	100	105
10^- f dyne cm^{-1}	2.59	2.48	2.39
10^- d dyne cm^{-1}	.369	.356	.342
Calculated ν_1 cm^{-1}	508	491	471

TABLE XXIV

Raman Spectrum of $C\ell SO_3F$, and assignments of $C\ell SO_3F$ and $BrSO_3F$ made by comparison with similar compounds.

Vibrational spectra of Halogen fluorosulphates in cm^{-1}

FSO_3F IR (82)	$C\ell SO_3F$ R. This work.	$BrSO_3F$ R. This work	Assignment $X.OSO_2F$.	
	214 w	177 m	X.O.S.	bend
	368 m	318 s	X O-S	stretch
	487 w	466 m	SO_2	bends
789*	707 s	658 s	X-O	stretch
1050	1055 w	-		
1248	1242 m	1206 m	SO_2	stretch s.
1501	1477 w		SO_2	stretch as.

$S_2O_5F_2$ (76)

157	SOS bend
323	SOS stretch s.
814	SOS stretch as.
1249, 1264	SO_2 stretch s.
1490	
1501	SO_2 stretch as.

$C\ell$-O stretching frequencies

Compound	cm^{-1}	Reference
$C\ell_2O$	640 s.	(68)
	686 as.	
$HOC\ell$	736	(68)
$C\ell ONO_2$	706	(83)

* Reassigned

TABLE XXV

Conductivities of solutions of CℓF and CℓF/Cℓ_2 in 0.184 m Super Acid

Composition of Super Acid: 244.14 g HSO_3F.

9.78 g SbF_5

10.47 g SO_3

molality of SbF_5 = 0.184

Ratio SbF_5: SO_3 = 1 = 2.94

A. Composition of concentration solution. 31.068 g Super Acid

0.574 g CℓF

Wt of Super Acid in Cell = 64.73 g

Wt Added g	10^3 m CℓF	10^4K ohm^{-1} cm^{-1}
-	-	367.1
5.3897	2.775	358.6
5.6702	5.275	349.1
5.4820	7.365	342.7
6.8316	9.610	332.5

B. Composition of concentration solution: 33.210 g Super Acid

0.650 g CℓF

0.563 g $C\ell_2$

Wt of Super Acid in Cell = 58.69 g

Wt Added g	10^3 m CℓF	10^4K ohm^{-1} cm^{-1}
-	-	367.2
5.7750	3.374	355.2
5.3372	6.010	345.1(5)
6.2270	8.630	333.8
7.6800	11.370	320.6

TABLE XXVI

ESR parameters of various Fluoro- and Chlorocarbon Radicals

Source	Assignment	Nucleus	a^*_{iso} gauss	
Teflon/γ rays.	$-CF_2.\dot{C}F.CF_2-$.	αF	86	(86)
		βF	33	
Teflon/γ rays.	$-CF_2.CF_2-O^{\cdot}$	αF	14	(86)
		βF	12.5	
C_2F_6/UV.	$^{\cdot}CF_3$	αF	144.5	(87)
Di-t-butyl Peroxide/ $CHC\ell_3$/UV.	$^{\cdot}C\ C\ell_3$	$^{35}C\ell$	6.25	(88)
Di-t-butyl Peroxide/ $CH_2C\ell_2$/UV.	$^{\cdot}CHC\ell_2$	$^{35}C\ell$	3.5	(88)

* Isotropic hyperfine coupling constant.

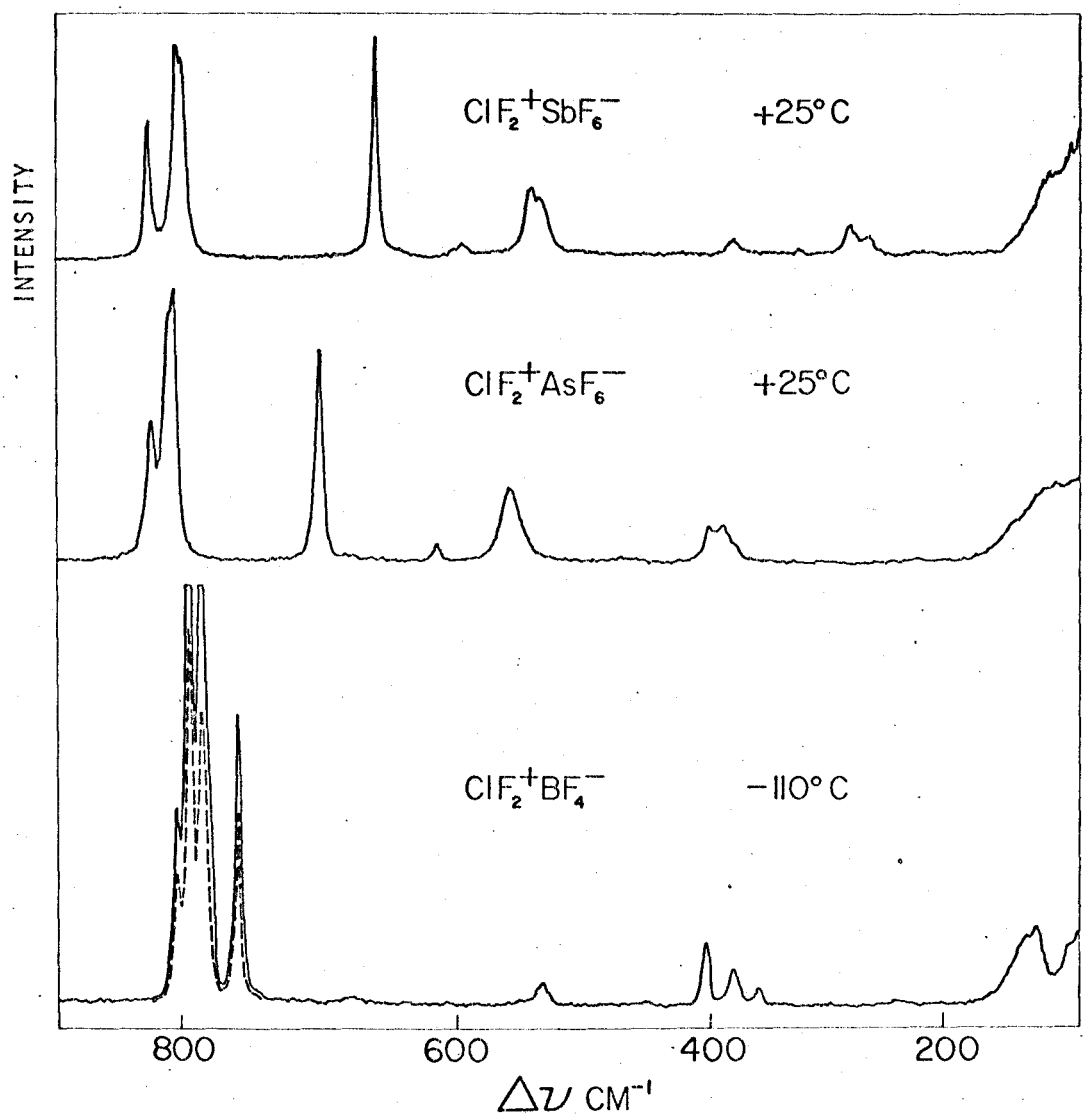

Figure 13. Raman spectra of $Cl F_2^+$ salts.

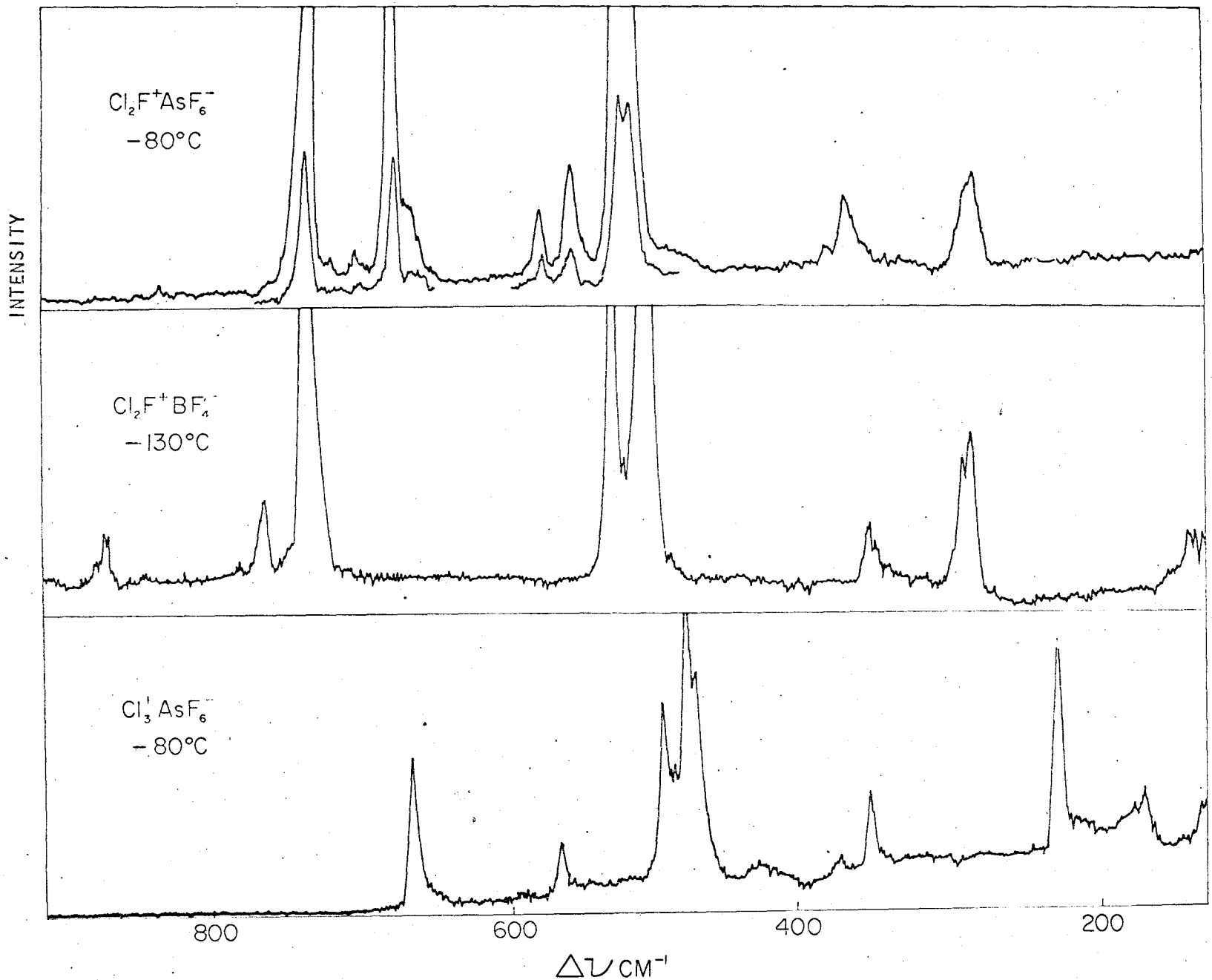

Figure 14. Raman spectra of Cl_2F^+ and Cl_3^+ salts.

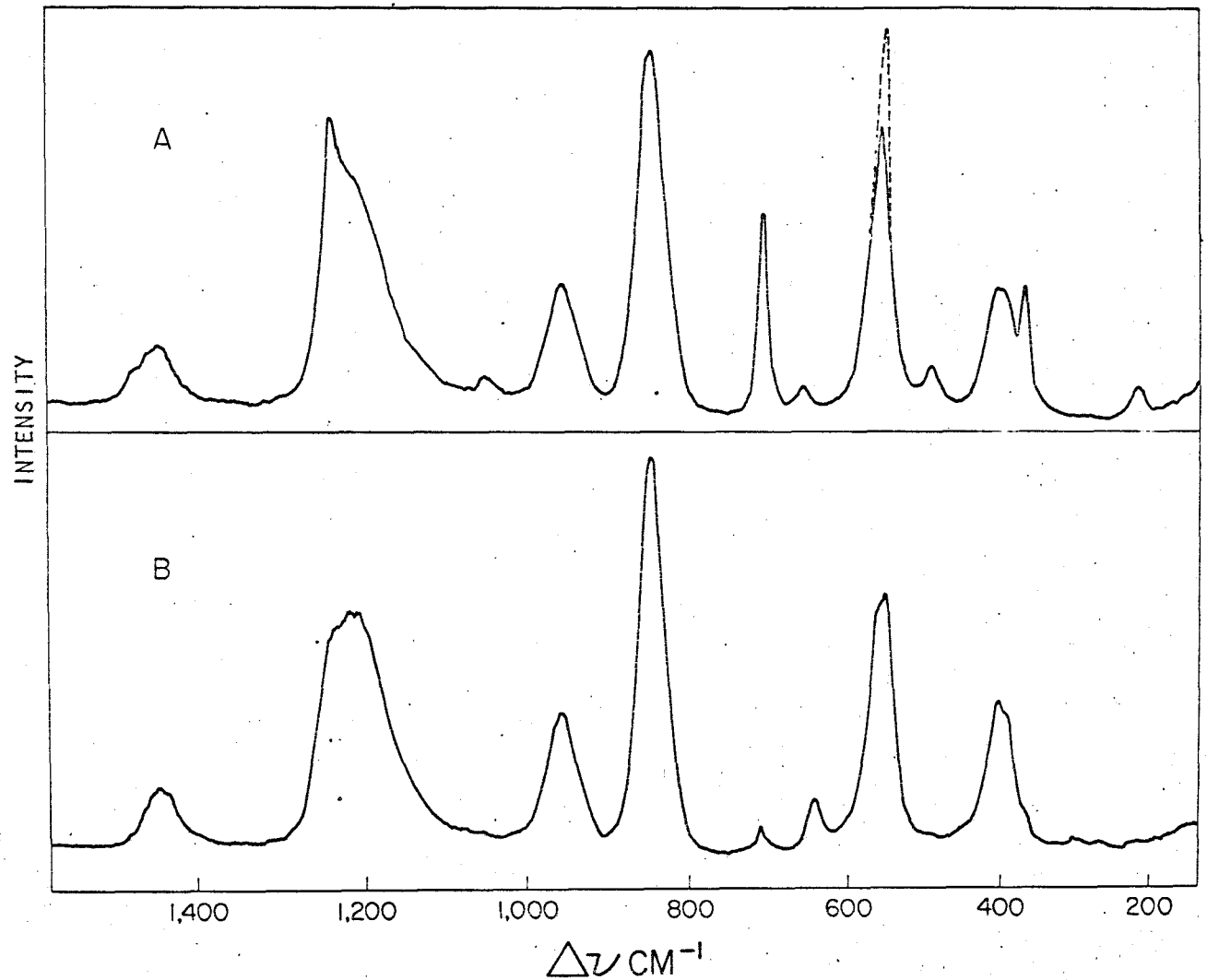

Figure 15. Raman spectra: A, ClF in super acid (---ClF/Cl_2); B, solvent.

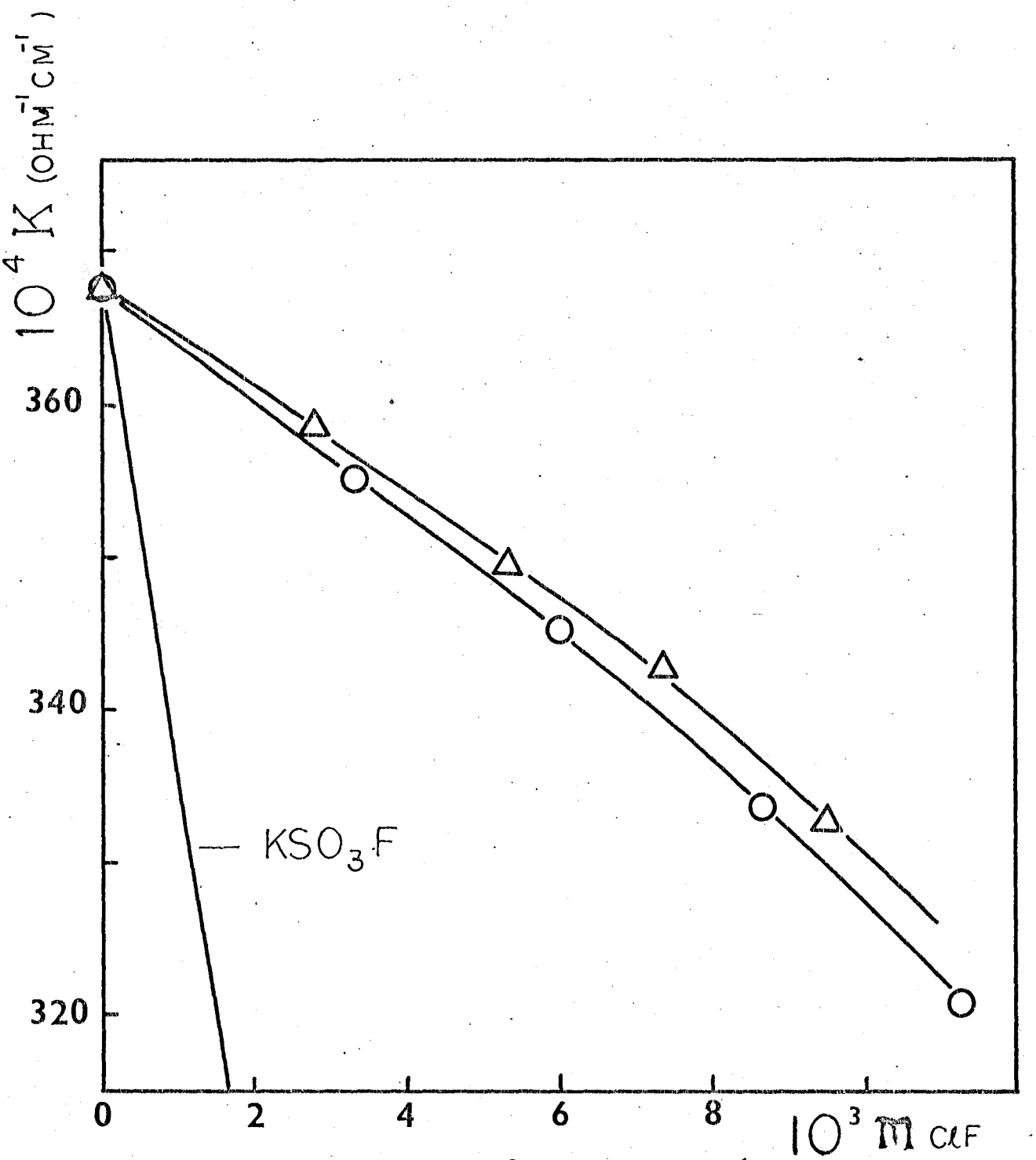

Figure 16. Conductivities at 25°C in super acid: △, ClF; ○ ClF/Cl_2.

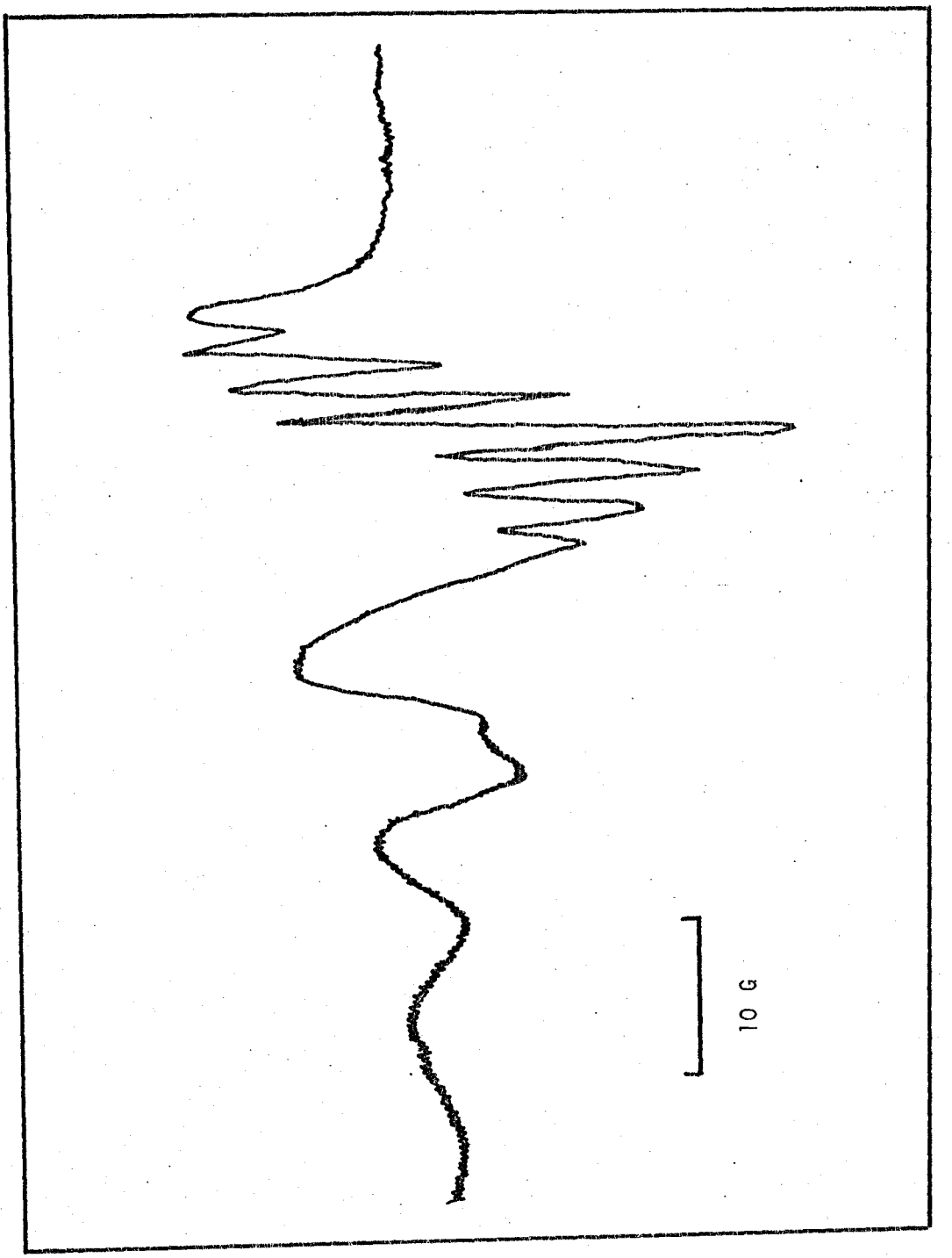

Figure 17. ESR from $C\ell F_2^+SbF_6^-/SbF_5$ in a Kel-F tube.

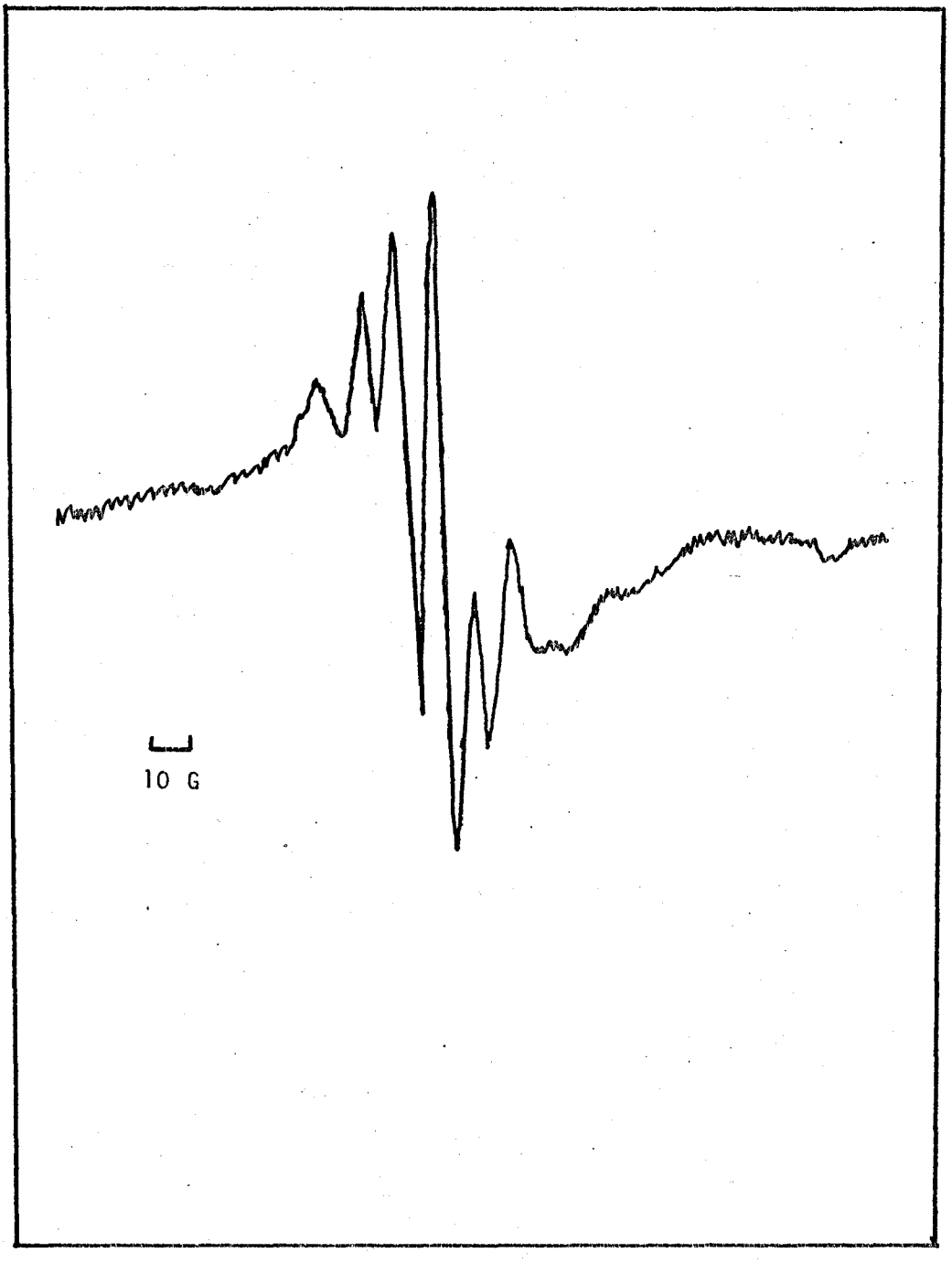

Figure 18. ESR from $Cl F_2^+SbF_6^-$ recrystallised from HF/Cl_2 in a Kel-F tube.

CHAPTER VI

Resonance Raman Spectra of Halogen Cations.

1. Introduction.

It is not normally possible to observe an ordinary Raman spectrum if the material under investigation absorbs the exciting radiation. However, if the wavelength of the exciting radiation lies underneath, and preferably close to the maximum of, an absorption band of the material it is in principle possible by careful choice of the size of the sample and the concentration of the absorbing substance to observe a resonance Raman spectrum which may have an intensity as great as 10^6 times that of an ordinary Raman spectrum (89,90).

Observed resonance Raman spectra have been reviewed by Behringer (89), together with the current theoretical approaches. These start from the quantum mechanical result for the intensity of the scattered line involving the transition $m \rightarrow n$ induced by incident radiation of frequency ν_o,

$$36. \quad I_{nm} = C(\nu_o + \nu_{nm})^4 P^2_{nm}.$$

where C is a constant, and the induced transition moment P_{nm} is given by (93)

$$37. \quad P_{nm} = 1/h \sum_r \left(\frac{M_{nr} M_{rm}}{\nu_{rn} - \nu_o} + \frac{M_{nr} M_{rm}}{\nu_{rm} + \nu_o} \right) E$$

where E is the electric vector of the incident light, and the summation is taken over the complete set of levels of the unperturbed molecule

denoted by r. The transition moments between the initial and final states and the "virtual" states denoted by r are given by M_{nr} and M_{rm}. When the term P_{nm} is approximately constant in cases where $\nu_o << \nu_{rn}$, equation 36 gives the familiar ν^4 law for the variation of Raman intensities with exciting frequency. However when this is not the case and the exciting frequency approaches that of an electronic transition certain terms in the summation for P_{nm} (equation 37) may become very large as the denominator $(\nu_{rn} - \nu_o)$ becomes small, giving rise to a resonance Raman spectrum. Application of these equations to specific experimental examples is difficult due to the complexity of the equations and the lack of knowledge of electronic energy levels and associated transition moments. The development of simplified theories has been hampered by the lack of experimental data, as until very recently the only examples studied were complex organic molecules such as nitro compounds and conjugated olefines (89), and carbon disulphide (91).

2. The Resonance Raman spectrum of the I_2^+ cation.

The spectrum shown in Figure 19 was first obtained when a dark brown solution of the I_3^+ cation in fluorosulphuric acid was irradiated with the 6328 A He/Ne laser in an attempt to obtain the Raman spectrum of the I_3^+ cation. Subsequently an identical spectrum was obtained from 10^{-2} molal solutions of the blue iodine cation I_2^+ in fluorosulphuric acid and in 65% oleum in which no I_3^+ was present. It is clear that the I_2^+ cation gives a very intense Raman spectrum and that the spectrum obtained from the brown I_3^+ solutions first studied was in fact due to

a small impurity of I_2^+, probably formed by a slight excess of the oxidising agent $S_2O_6F_2$. The I_2^+ cation has an intense broad electronic absorption band with a maximum at 6400 A and ε = 2600 (23). At the laser wavelength of 6328 A the extinction coefficient is 2580 and hence it is concluded that the very intense I_2^+ spectrum is an example of a rigorous resonance Raman spectrum (89).

The spectrum of a dilute solution of the I_2^+ cation in fluorosulphuric acid shown in Figure 19 has both stokes and anti-Stokes lines with frequency differences equal to 238 cm^{-1} within the experimental error. The frequency shifts, areas and widths of the lines in the spectrum of I_2^+ in fluorosulphuric acid are summarised in Table XXVII. It is noteworthy that there is a marked increase in line width with increasing order of the overtones.

Depolarisation measurements were made on the 10^{-2} molal solution of I_2^+ in fluorosulphuric acid contained in glass melting point tubes, id = 1.2 mm , mounted with their axis perpendicular to the laser beam (Chapter II), and the results agreed with those obtained with a larger quartz sample cell of square cross section with the beam focused very close to one corner. A depolarisation ratio of ρ = 0.30 was obtained for the fundamental, the first and second overtones and the first two anti-Stokes lines. However, due to changes in intensity of the lines caused by heating of the sample by the laser light, these results are accurate only to ± 10%. For a $\pi \rightarrow \pi^*$ transition with polarised incident light all α_{ik} except α_{xx} are expected to be zero giving ρ = 1/3 for the resonance Raman spectrum (89).

Figure 20 and Table XXVIII show the changes in the intensities of the I_2^+ peaks and those of the fluorosulphuric acid solvent with concentration of I_2^+. Due to absorption of the exciting radiation by the blue solutions, the intensities of the solvent lines decrease rapidly with increasing concentration, whereas those of the I_2^+ ion reach a maximum at 2×10^{-3}m. At 10^{-1}m no spectrum was observed at all. The intensity of a narrow parallel beam of light, with initial intensity I^o reaching a small volume in the center of the cylindrical sample tube, radius ℓ, is

38. $$I = I^o e^{-2.3\varepsilon c\ell}$$

where c is the concentration of I_2^+ which has an extinction coefficient ε. Therefore, assuming the same extinction coefficient for the scattered light, the intensity of the observed Raman emission from the small volume is proportional to $ce^{-4.6\varepsilon c\ell}$. This is a maximum when $4.6\ \varepsilon c\ell = 1$. Hence with $\varepsilon = 2600$ and $\ell = 0.06$ cm the optimum concentration of I_2^+ is $c = 1.6 \times 10^{-3}$ M or 1×10^{-3} molal, which is in reasonable agreement with the observed value.

In solutions of concentration 0.1 m or above, no Raman emission was observed at room temperature, but when the solution was cooled to approximately -80^oC a spectrum similar to that shown in Figure 19 appeared, and increased in intensity as the solution was cooled further. This indicates that the concentration of I_2^+ decreases with decreasing temperature, and is consistent with the conclusion that the blue I_2^+ cation dimerizes to the red I_4^{2+} cation at low temperatures (Chapter III). The I_4^{2+} cation has no appreciable absorption at 6400 A , and hence does not

produce a resonance Raman spectrum. The relative peak heights of the observed Raman lines of I_2^+ at 25°C and -80°C are listed in Table XXVII. The relative intensities of the anti-Stokes lines decrease at low temperatures as expected, however the temperatures within the sample tubes may have been considerably higher than the external temperatures recorded due to heating of the coloured sample by the laser beam.

Similar spectra were obtained with the 6118 A He/Ne laser wavelength, again giving a fundamental at 238 cm^{-1} from the exciting line and a strong overtone. The maximum power output that could be obtained at the sample at the 6118 A wavelength, using optimum laser optics, was only 4 mw, compared with up to 60 mw available at 6328 A . Hence the second overtone could be distinguished from noise only in the sample in which the I_2^+ concentration was at the optimum value of 2×10^{-3}m. Table XXIX gives the peak heights of the resonance Raman lines of I_2^+ relative to those of the 400 cm^{-1} fluorosulphuric acid solvent line at the two exciting wavelengths. Relative to the fluorosulphuric acid solvent in the same solution, and at similar laser power output, the I_2^+ lines were a factor of two more intense at 6328 A than at 6118 A .

If the resonance Raman intensity I is proportional to $\left[(\nu_{eg} - \nu_o)^2 + \delta_e^2\right]^{-1}$ where ν_{eg} is the electronic absorption maximum frequency, ν_o is the frequency of the exciting radiation and δ_e is an electronic damping term (89), we expect

$$39. \quad \frac{I^{6328}}{I^{6118}} = \frac{720^2 + \delta_e^2}{178^2 + \delta_e^2} = 2$$

giving $\delta_e = 640\ cm^{-1}$. It has been suggested that the electronic damping term δ_e can, in principle, be estimated from the half-value width of the vibrational structure of the electronic absorption band, $\sim 2\delta_e$ (89). Here however, the observed electronic absorption band, which has a half-width of 2,500 cm^{-1}, shows no resolvable vibrational structure. For this case Shorygin's semiclassical theory for the rigorous resonance Raman effect does not predict extensive overtones (89,90,92).

Attempts to observe the Raman spectrum of the I_2^+ cation using argon-ion laser wavelengths of 5145, 4880 and 4579 A were unsuccessful due to strong fluorescence.

3. The Resonance Raman Spectrum of the Br_2^+ cation.

The resonance Raman spectrum of the I_2^+ ion prompted a search for similar effects in other simple coloured molecules. At that time solutions of the Br_2^+ cation had just been prepared and characterised, and the strong visible absorption band at 510 mμ shown in Figure 8 was observed. By analogy with the I_2^+ cation, a resonance Raman spectrum was expected due to this band, and accordingly the Raman spectra of dilute solutions of the Br_2^+ cation were amongst samples run using the 5145 and 4880 A wavelengths of an argon-ion laser Raman instrument at the Department of Physics, University of Waterloo, by the kind persmission of Dr. A. Anderson. The observation that the Br_2^+ cation, and the Te_4^{2+} cation which also has a strong visible absorption at 510 mμ, gave resonance Raman spectra resulted in the acquisition of a Spectra Physics model 140 argon-ion laser in these laboratories.

Figure 21 shows the Raman spectrum of a solution containing a 10^{-2} molal concentration of the Br_2^+ cation excited by 5145 A wavelength radiation. In addition to solvent peaks and a weak peak due to the Br_3^+ cation also present in the solution, an intense peak at 360 cm^{-1} and five overtones are shown, due to the resonance Raman spectrum of the Br_2^+ cation. The Raman shifts, relative peak heights and half widths of the Br_2^+ bands are listed in Table XXX.

Consistent results for the relative intensities of the fundamental and overtones with different laser wavelengths were difficult to obtain due to the apparently random power fluctuations of the argon-ion laser, especially when using the weaker laser lines such as the 4579 A line. As a result the data given here may be in error up to 10%. This could be corrected by the use of a ratio recording system, which was not available at the time. A second difficulty was the sensitivity of the Br_2^+ concentrations to heating by the laser beam (Chapter VI); this was minimised by cutting down the laser output at the sample to approximately 10mw at each wavelength by the use of optical-density filters from a Cary model 14 spectrophotometer.

Table XXXI summarises the depolarisation ratios and relative intensities of the fundamental, and the relative areas of the first overtone to the fundamental, at the different exciting wavelengths available. The relative areas of the fundamental at different wavelengths were obtained by comparing the area of the fundamental with that of the double solvent peak at 400 cm^{-1} (Figure 22) at each wavelength using the same sample. Areas were measured using a Dupont 310 curve resolver and integrator; the spectra could be accurately synthesised using Lorentzian line shapes.

The resonance Raman spectrum of the Br_2^+ ion at 5145 A excitation is similar to that observed for the I_2^+ ion at 6328 A , in that the observed depolarisation ratio is 0.3 and strong overtones are observed. However the overtones are relatively stronger in the Br_2^+ case, in which the area of the first overtone was found to be equal to that of the fundamental within the experimental error of ± 10%, whereas for the I_2^+ resonance Raman spectrum the area of the first overtone was 60% that of the fundamental.

The damping constant δ_e calculated from the relative intensities of the fundamental at different wavelengths as in equation 39 was 2×10^3 cm^{-1} for the Br_2^+ cations. It is interesting that this agrees with the value estimated from the half value width ($2\delta_e$) of the total electronic absorption band, which was 4×10^{-3} cm^{-1}, rather than a smaller value expected for the damping constant of vibrational structure. No vibrational structure was observed in the visible absorption band.

It is noteworthy that whereas the depolarisation ratios and relative intensities of the fundamental reached a maximum at 5145 A excitation and then decreased with shorter wavelength, no decrease in the relative areas of the overtones to the fundamental was observed with 'post-resonance' (89) wavelengths (Table XXXI).

4. Attempts to observe the resonance Raman spectrum of the Cl_2^+ cation.

Table XXXII lists the visible absorption maxima and vibrational frequencies of the halogen molecules and their cations. By analogy with bromine and iodine the Cl_2^+ cation is expected to have a strong visible absorption band at around 400 mμ which might give rise to a resonance

Raman spectrum, with a strong fundamental close to the gas phase frequency of 645 cm^{-1}(77). At the closest available exciting wavelength of 4579 A it is expected that if Cl_2^+ does indeed give a resonance Raman spectrum it's intensity would be great enough to enable concentrations as low as 10^{-4} molal to be detected.

Raman spectra were recorded of solutions of $ClSO_3F$ and of Cl_2/$ClSO_3F$ in 0.176 m SbF_5:$3SO_3$ in HSO_3F, using 4579 A argon-ion excitation. Although excellent spectra were obtained with a signal to noise ratio of 500:1 for the 560 cm^{-1} solvent peak, no band that could be attributed to the Cl_2^+ cation was observed. This result is consistent with the conclusions reached in Chapter V that the ESR spectrum given by these solutions is not due to the Cl_2^+ cation as stated by Olah and Comisarow, and that the Cl_2^+ cation is not formed in this solvent.

5. Conclusions.

The resonance Raman spectra of the Br_2^+ and I_2^+ cations, described above, are of particular interest as, although the general theory of the effect may be reasonably well understood (89), its application to particular cases, and to predicting the intensities of fundamentals and overtones is as yet uncertain. This is largely due to the very limited experimental data available on this effect. Thus at the time the I_2^+ resonance Raman work was reported (94), the only other example of a resonance Raman study on a simple molecule of which we were aware, was a recent report on the resonance Raman spectrum of CS_2 excited by the 2537 A mercury line, in which overtones were not observed (91). Since

then Bernstein et al. have reported resonance Raman spectra of the S_2^-, S_3^-, Se_2^-, N_2^- and O_2^- ions doped in single crystals (95), and resonance Raman spectra of I_2 and Br_2 gases (96). These workers also obtained strong overtones, but the details have yet to be published. Dr. M. Booth is studying the resonance Raman spectrum of the Te_4^{2+} cation in these laboratories.

It should be noted that the relative intensities of the fundamentals and of the overtones in the resonance Raman spectra of the bromine and iodine cations reported above, have not been corrected for factors such as the variation of photomultiplyer sensitivity, the change in spectral slit widths or the effect of the visible absorption curve at different excitation wavelengths. However, such corrections do not alter the general conclusions reached, as it is estimated that their sum is not greater than the experimental error of ± 10% in the relative intensities of the fundamentals at different wavelengths, and the relative intensities of the first overtone to the fundamental at different wavelengths. An accurate reinvestigation of the resonance Raman spectra of these ions of much greater scope than that reported here, and using a wider range of exciting frequencies would be well worthwhile as these molecules are sufficiently well characterised and simple for the results to be of some use in developing the theory of the resonance Raman effect.

The low concentrations at which the resonance Raman fundamentals of the Br_2^+ and I_2^+ can be measured could make this an unusual but useful method for determining very small quantities of these elements. Thus, as Freeman and Landon(60) have shown that laser Raman spectra can be obtained from solutions in fine capillary tubes containing down to 10^{-9}

litres, and as the concentration of I_2^+ at 10^{-4} molal could probably be estimated to an accuracy of 5% or better from the relative intensities of a solvent and I_2^+ Raman line, it is in principle possible to estimate a total quantity of iodine of approximately 10^{-13} moles in this way. Iodine or iodides could very simply be oxidised to I_2^+ by 65% oleum (25).

TABLE XXVII

Frequency Shifts, Peak Heights and Widths of Lines in the Resonance Raman Spectrum of I_2^+

		Anti-Stokes			Stokes			
$\Delta\nu$ cm^{-1}.		710	474	238	-238	-476	-716	-950
Relative Peak heights*	25°	1.7	8	50	100	42	19	8
	-80°	-	3	30	100	41	18	8
Half Widths	cm^{-1}	15	10	6	6	10	15	25

* Relative height based on 100; relative area of first overtone = 60% that of fundamental.

TABLE XXVIII

Variation of I_2^+ Fundamental Intensity with Concentration.

Molality of I_2^+	Intensity of Fundamental.*
1×10^{-2}	9.6
2×10^{-3}	11.9
5×10^{-4}	8.4
2.5×10^{-4}	6.8
1×10^{-4}	2.8

* Intensity of 313 cm^{-1} line of liquid $CC\ell_4$ = 100 on this scale.

TABLE XXIX

Raman Intensity Variations with Laser Line for a 5×10^{-4} mw Solution of I_2^+

	6328 A	6118 A	Ratio
$\frac{\text{Intensity } 238 \text{ cm}^{-1}}{\text{Intensity } HSO_3F \text{ at } 400 \text{ cm}^{-1}}$	4.8	2.3	2.1
$\frac{\text{Intensity overtone at } 476 \text{ cm}^{-1}}{\text{Intensity } HSO_3F \text{ at } 400 \text{ cm}^{-1}}$	1.6	0.7	2.3
Power at sample.	5 mw	4 mw	

TABLE XXX

Frequency shifts, Peak Heights and Widths of Lines in the Resonance Raman Spectrum of a 10^{-2} m solution of Br_2^+ at 5145 A .

$-\Delta\nu$. cm^{-1}	360	716	1070	1430	1780	2130
Relative Peak heights	100	50	20	10	6	4
Half widths. cm^{-1}	10	22	30	50	-	-

TABLE XXXI

Variation of Depolarisation Ratio, and Intensities of the Raman Fundamental and Overtone of the Br_2^+ Cation with Laser Wavelength.

Laser Wavelength A	Area of Fundamental[#]	Relative Area of Overtone[*]	ρ (Areas)
6328	25	0.25	0.27
5145	100	1.0	0.30
5017	95	1.0	0.28
4965	80	1.0	0.25
4880	70	1.0	-
4765	65	1.0	0.20
4579	30	1.0	-

Concentration of Br_2^+ solutions used: 1×10^{-3} molal.
5×10^{-3} molal.
1×10^{-2} molal.

* Areas measured relative to that of fundamental at 5145 A excitation.

\# Peak area measured relative to that of the 400 cm^{-1} solvent band.

TABLE XXXII

Visible Absorption Maxima and Vibrational Frequencies of the Halogens and Halogen Molecule Cations.

	λ_{max} mμ	ν cm^{-1}
I_2	520	215
I_2^+	640	238
Br_2	410	320
Br_2^+	510	360
Cl_2	325	555
Cl_2^+ (gas)		645

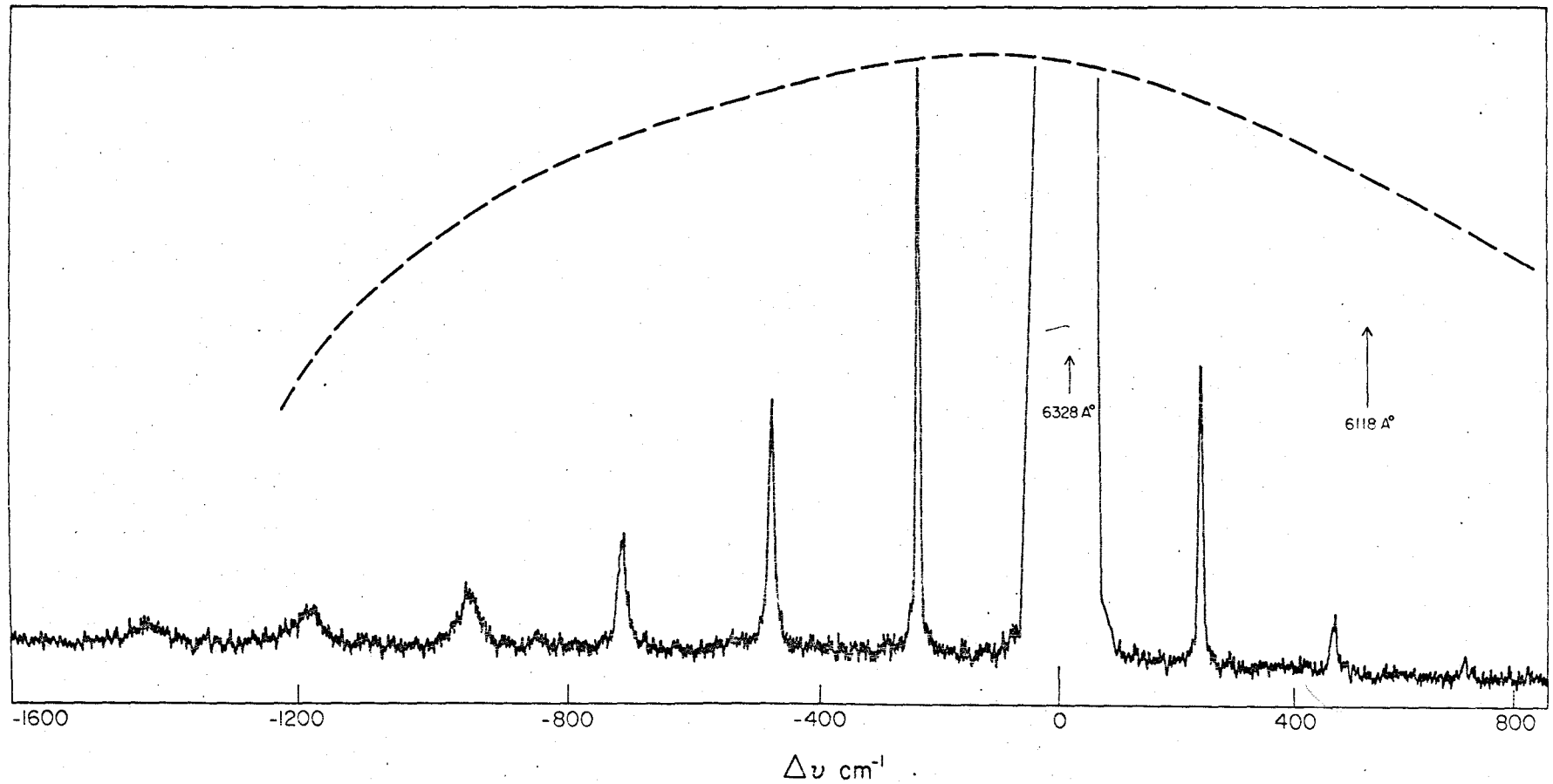

Figure 19. Resonance Raman spectrum of a 10^{-2} m solution of I_2^+ in fluorosulphuric acid: (---), contour of visible absorption band.

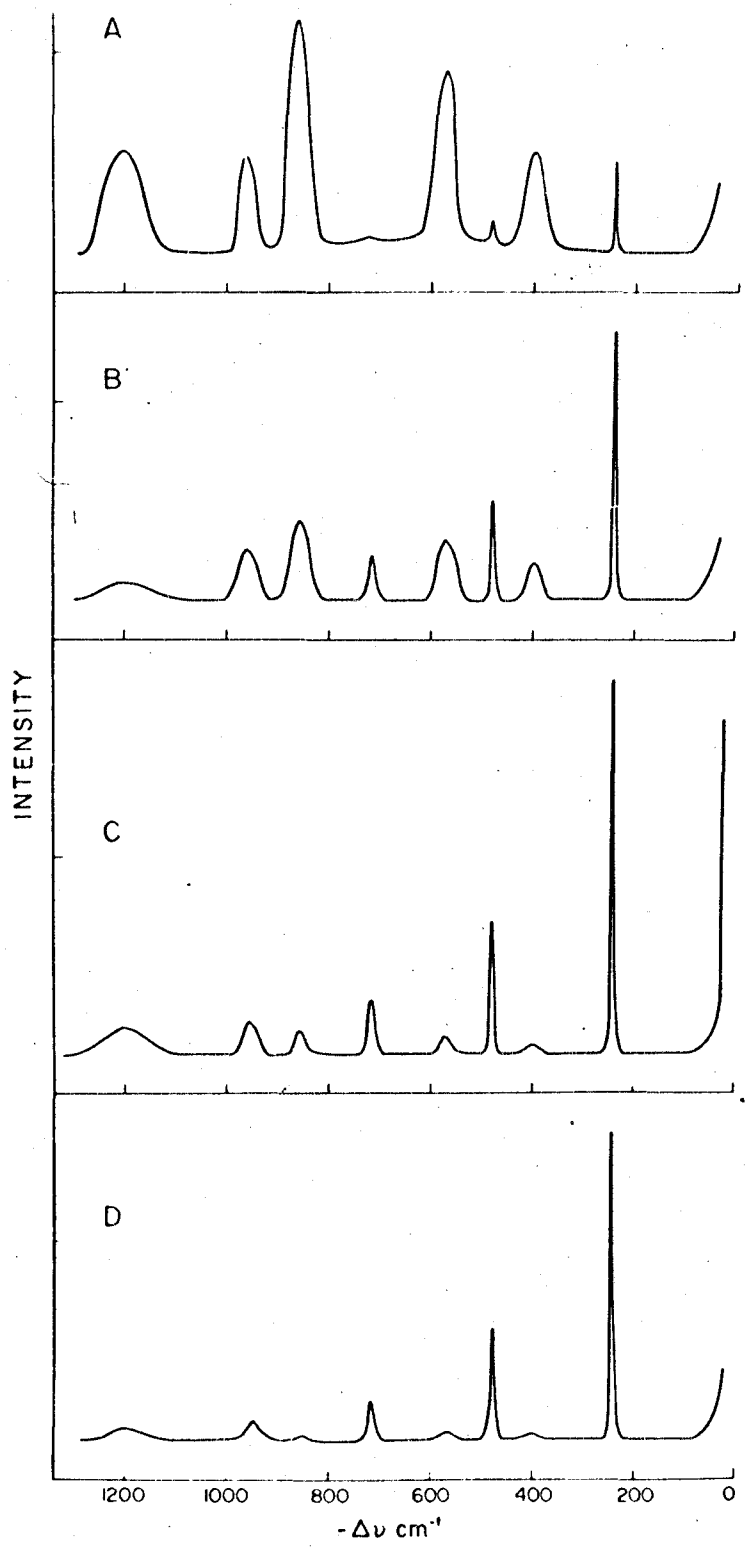

Figure 20. Resonance Raman spectra of the I_2^+ ion in solution in fluorosulphuric acid: A, 10^{-4}m; B, 5×10^{-4}m; C, 2×10^{-3}m; D, 10^{-2}m.

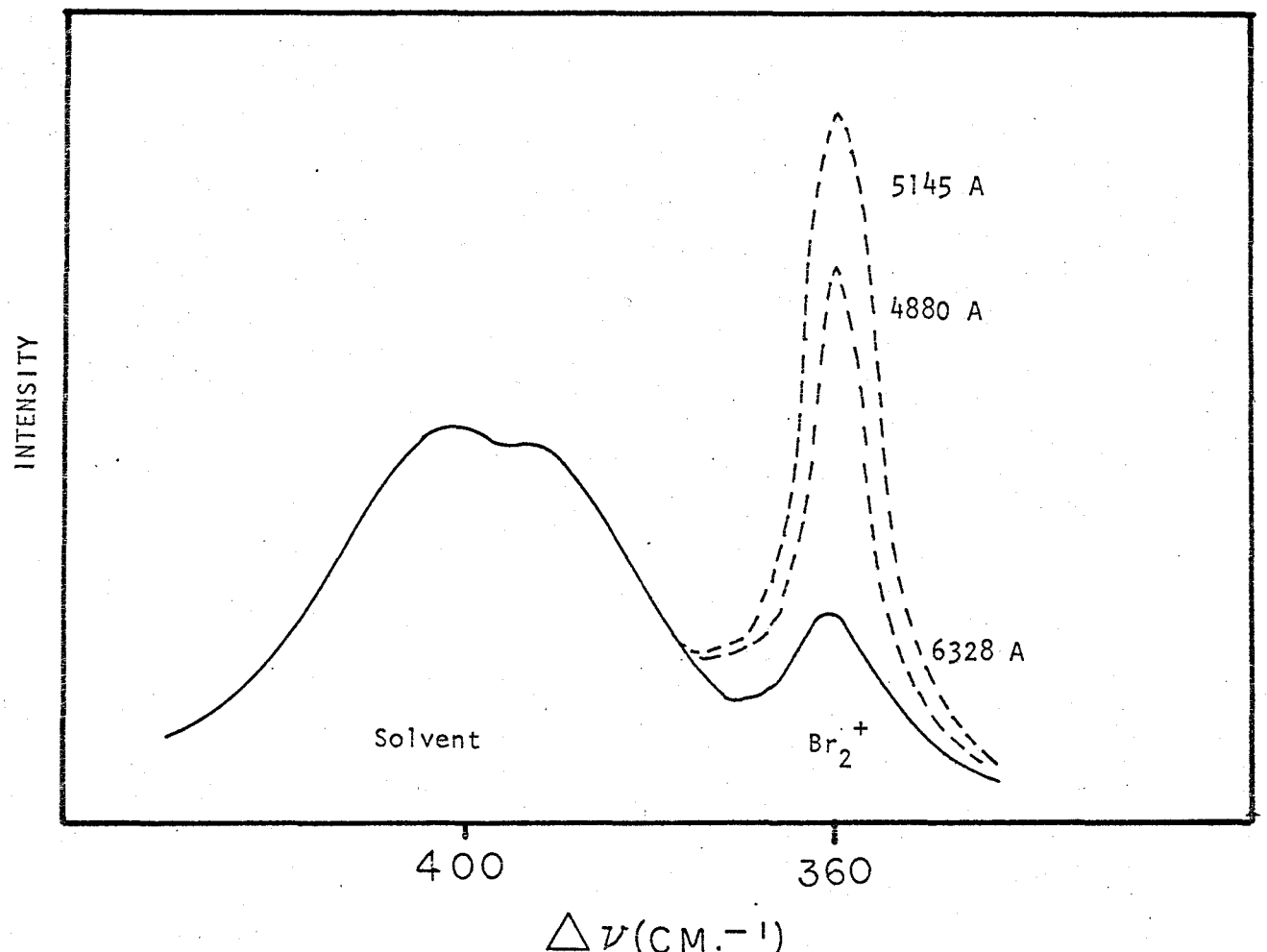

Figure 21. Resonance Raman spectrum of the Br_2^+ cation: variation with exciting wavelength.

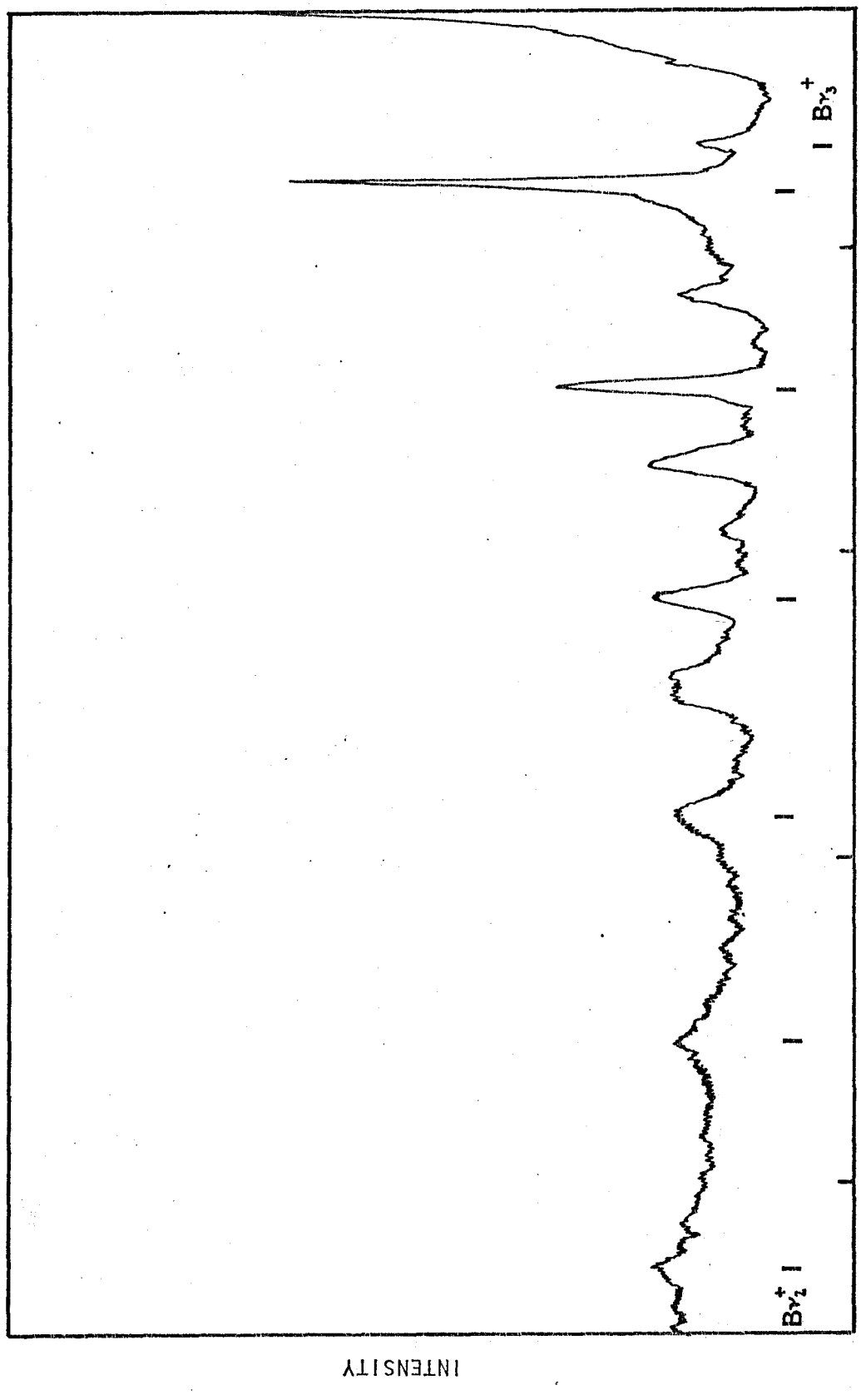

Figure 22. Resonance Raman spectrum of a 10^{-2} m solution of the Br_2^+ cation in super acid.

REFERENCES

1. J. Arotsky and M. C. R. Symons. Q. Rev. Chem. Soc. 16, 282 (1962).
2. A. Hershaft and J. D. Corbett. Inorg. Chem. 2, 979 (1963).
3. N. J. Bjerrum, C. R. Boston and G. Pedro Smith. Inorg. Chem. 6, 1162 (1967).
4. N. Bartlett and D. M. Lohman. J. Chem. Soc. 5253 (1962).
5. A. R. Young II, T. Hirata and S. I. Morrow. J. Am. Chem. Soc. 86, 20 (1964).
6. R. J. Gillespie and J. Passmore. Unpublished results.
7. J. Barr, R. J. Gillespie, R. Kapoor and K. C. Malhotra. Can. J. Chem. 46, 149 (1968).
8. J. Barr, R. J. Gillespie, R. Kapoor and G. P. Pez. J. Am. Chem. Soc. 90, 6855 (1968).
9. J. Barr, R. J. Gillespie, G. P. Pez and P. K. Ummatt. Unpublished results.
10. M. C. R. Symons. J. Chem. Soc. 475 (1957).
11. I. Masson. J. Chem. Soc. 1708 (1938).
12. J. Arotsky, H. C. Mishra and M. C. R. Symons. J. Chem. Soc. 2582 (1962).
13. R. A. Garrett, R. J. Gillespie and J. B. Senior. Inorg. Chem. 4, 563 (1965).
14. C. G. Wonk and E. H. Wiebenga. Acta Cryst. 12, 859 (1959).
15. H. Carlsohn. Angew. Chem. 45, 580 (1932).

16. V. Gutmann (Editor). 'Halogen Chemistry'. Academic Press, London and New York (1967).

17. R. P. Bell and E. Gelles. J. Chem. Soc. 2734 (1951).

18. M. C. R. Symons. J. Chem. Soc. 387 (1957).

19. M. C. R. Symons. J. Chem. Soc. 2186 (1957).

20. J. Arotsky, H. C. Mishra and M. C. R. Symons. J. Chem. Soc. 12 (1961).

21. E. E. Aynsley, N. N. Greenwood and D. H. W. Wharmby J. Chem. Soc. 5369 (1963).

22. J. B. Milne. Ph.D. Thesis, McMaster University (1965).

23. R. J. Gillespie and J. B. Milne. Inorg. Chem. 5, 1577 (1966).

24. R. J. Gillespie and J. B. Milne. Inorg. Chem. 5, 1236 (1966).

25. R. J. Gillespie and K. C. Malhotra. J. Chem. Soc. (1969).

26. R. D. W. Kemmitt, M. Murray, V. M. McRae, R. D. Peacock and M. C. R. Symons. J. Chem. Soc. 862 (1968).

27. V. M. McRae. Ph. D. Thesis, University of Melbourne (1966).

28. O. Ruff, H. Graf, W. Heller and K. Knock. Ber. 39, 4310 (1906).

29. A. J. Edwards, G. R. Jones and R. J. C. Sills. Chem. Comm. 1527 (1968).

30. R. J. Gillespie and M. J. Morton. Chem. Comm. 1565 (1968).

31. G. A. Olah and M. B. Comisarow. J. Am. Chem. Soc. 90, 5033 (1968).

32. G. A. Olah and M. B. Comisarow. J. Am. Chem. Soc. 91, 2172 (1969).

33. A. J. Edwards and G. R. Jones. J. Chem. Soc. 1467 (1969).

34. M. Schmeisser, W. Ludovici, D. Naumann, P. Sartori and E. Scharf. Ber. 101, 4214 (1968).

35. A. A. Woolf. J. Chem. Soc. 3678 (1950).

36. F. Seel and O. Detmar. Angew. Chem. 70, 163 (1958). Z. Anorg. Allgem. Chem. 301, 113 (1959).

37. A. A. Woolf and H. J. Emeleus. J. Chem. Soc. 2865 (1949).

38. K. O. Christe and D. Pilipovich. Inorg. Chem. 8, 391 (1969).

39. K. O. Christe and W. Sawodny. Inorg. Chem. 8, 212 (1969).

40. D. H. Brown, K. R. Dixon and D. W. A. Sharp. Chem. Comm. 654 (1966).

41. R. A. Garrett, R. J. Gillespie and J. B. Senior. Inorg. Chem. 4, 563 (1965).

42. Y. A. Fialkov and I. L. Abarbachuk. Ukr. Chem. J. 15, 116 (1949).

43. Y. A. Fialkov and A. A. Kuz'menko. Zh. Obs. Khim. 21, 433 (1951).

44. A. A. Woolf. J. Chem. Soc. 433 (1955).

45. J. Bacon, P. A. W. Dean and R. J. Gillespie. Can. J. Chem. 47, 1655 (1969).

46. R. C. Thompson. Ph.D. Thesis, McMaster University (1962).

47. J. Barr, R. J. Gillespie and R. C. Thompson. Inorg. Chem. 3, 1149 (1964).

48. R. C. Thompson, J. Barr, R. J. Gillespie, J. B. Milne and R. A. Rothenbury. Inorg. Chem. 4, 1641 (1965).

49. R. J. Gillespie, J. B. Milne and R. C. Thompson. Inorg. Chem. 5, 468 (1966).

50. R. J. Gillespie, J. B. Milne and J. B. Senior. Inorg. Chem. 5, 1233 (1966).

51. R. J. Gillespie. Accounts of Chemical Research. July (1968).

52. F. B. Dudley and G. H. Cady. J. Am. Chem. Soc. 79, 513 (1957).

53. R. E. Dodd and P. L. Robinson. 'Experimental Inorganic Chemistry'. Elsevier (1954).

54. G. Jones and D. M. Bollinger. J. Am. Chem. Soc. 57, 280 (1935).

55. G. Jones and B. C. Bradshaw. J. Am. Chem. Soc. 55, 1780 (1933).

56. G. W. Haupt. J. Opt. Soc. Am. 42, 441 (1952).

57. A. Earnshaw, Department of Chemistry, Leeds University, Private Communication.

58. A. Guest. Ph.D. Thesis, McMaster University (1969).

59. B. N. Figgis and J. Lewis in J. Lewis and R. G. Wilkins (Editors), "Modern Coordination Chemistry". Interscience Publishers. New York (1960).

60. S. K. Freeman and D. O. Landon. The Spex Speaker VIII no. 4 (1968).

61. F. Aubke and R. J. Gillespie. Inorg. Chem. 7, 599 (1968).

62. D. C. Frost, C. A. McDowell and D. A. Vroom. J. Chem. Phys. 46, 4255 (1967).

63. K. O. Christe and W. Sawodny. Inorg. Chem. 6, 313 (1967).

64. K. O. Christe and A. E. Pavlath. Z. Anorg. Allgem. Chem. 335, 210 (1965).

65. G. M. Begun and A. C. Rutenburg. Inorg. Chem. 6, 2212 (1967).

66. M. Azeem, M. Brownstein and R. J. Gillespie. Can. J. Chem. In Press.

67, R. J. Gillespie and A. Whitla. Can. J. Chem. In Press.

68. H. Siebert. 'Anwendungen der Swingungsspektroscopie in der Anorganishen Chemie'. Spring-Verlag, Berlin (1966).

69. R. J. Gillespie. Angew. Chem. (Internat. Edit.) 6, No. 10, 819 (1967).

70. S. Brownstein. Can. J. Chem. 45, 2403 (1967).

71. M. M. Rochkind and G. C. Pimentel J. Chem. Phys. 46, 4481 (1967).

72. H. Stammreich and R. Forneiss. Spectrochimica Acta 17, 775 (1961).

73. J. Passmore Private communication (1969).

74. W. P. Gilbreath and G. H. Cady. Inorg. Chem. 2, 496 (1963).

75. F. Aubke and G. H. Cady. Inorg. Chem. 4, 269 (1965).

76. F. J. Gillespie and E. A. Robinson. Can. J. Chem. 39, 2179 (1961).

77. G. Herzberg. 'Molecular Spectra and Molecular Structure' Vol. 1. Van Nostrand, Princeton, New Jersey (1960).

78. N. Bartlett. Proc. Chem. Soc. 218 (1962).

79. V. M. McRae, R. D. Peacock and D. R. Russel. Chem. Comm. 62 (1969).

80. N. Bartlett, S. P. Beaton and N. K. Jha. Chem. Comm. 168 (1966).

81. A. F. Kapustinskii. Q. Rev. Chem. Soc. 10, 284 (1956).

82. F. B. Dudley, G. H. Cady and D. F. Eggers Jr. J. Am. Chem. Soc. 78, 290 (1956).

83. K. Brandle, M. Schmeisser and W. Luttke. Ber. 93, 2300 (1960).

84. R. S. Eachus, T. P. Sleight and M. C. R. Symons. Nature 222, 769 (1969).

85. B. Cohen and R. D. Peacock. J. Inorg. Nuc. Chem. 28, 3056 (1966).

86. M. Iwasaki, K. Toriyama, T. Sawaki and M. Inoue. J. Chem. Phys. 47, 554 (1967).

87. R. W. Fessendon and R. H. Schuler. J. Chem. Phys. 43, 2704 (1965).

88. A. Hudson and H. A. Hussain. Mol. Phys. 16, 199 (1969).

89. J. Behringer in, H. A. Szymanski (Editor) 'Raman Spectroscopy' Plenum Press, New York (1967).

90. P. P. Shorygin. Pure Appl. Chem. 4, 87 (1966).

91. L. Bernard and R. Dupeyrat. J. Chim. Phys. 65, 410 (1968).

92. P. P. Shorygin and L. L. Krushinskii. Opt. i. Spek. 17, 551 (1964).

93. G. Placzek in E. Marx (Editor), 'Handbuch der Radiologie' Vol. 6, Part 2. Akademische Verlagsgesellshaft, Leipzig (1934).

94. R. J. Gillespie and M. J. Morton. J. Mol. Spec. 30, 178 (1969).

95. H. J. Bernstein, W. Holzer and W. F. Murphy. Paper presented at 23rd symposium on Molecular Structure and Spectroscopy. Ohio State University. September 1968.

96. H. J. Bernstein, W. Holzer and W. F. Murphy. Paper presented at the International Conference on Raman Spectroscopy. Carleton University, Ottawa. August 1969.

97. L. C. Hoskins and R. C. Lord. J. Chem. Phys. 46, 2402 (1967).